



TECHNICAL REPORT 99-07

Grimsel Test Site
Investigation Phase V (1997-2002)

Conclusions of the Tunnel Near-Field Programme (CTN)

September 1999

P. Marschall, E. Fein, H. Kull, W. Lanyon
L. Liedtke, I. Müller-Lyda, H. Shao

TECHNICAL REPORT 99-07

Grimsel Test Site Investigation Phase V (1997-2002) **Conclusions of the Tunnel Near-Field Programme (CTN)**

September 1999

P. Marschall¹⁾, E. Fein²⁾, H. Kull²⁾, W. Lanyon³⁾
L. Liedtke⁴⁾, I. Müller-Lyda²⁾, H. Shao³⁾

¹⁾ NAGRA, National Cooperative for the Disposal of Radioactive Waste,
Wettingen, Switzerland

²⁾ GRS, Society for Plant and Reactor Safety, Braunschweig, Germany

³⁾ GeoScience Limited, Falmouth, United Kingdom

⁴⁾ BGR, Federal Institute for Geoscience and Natural Resources,
Hannover, Germany

This report was prepared on behalf of Nagra. The viewpoints presented and conclusions reached are those of the author(s) and do not necessarily represent those of Nagra.

ISSN 1015-2636

"Copyright © 1999 by Nagra, Wettingen (Switzerland) / All rights reserved.

All parts of this work are protected by copyright. Any utilisation outwith the remit of the copyright law is unlawful and liable to prosecution. This applies in particular to translations, storage and processing in electronic systems and programs, microfilms, reproductions, etc."

GTS Phase V



NAGRA National Cooperative for the Disposal of Radioactive Waste



ANDRA Agence nationale pour la gestion des déchets radioactifs



BMWi Bundesministerium für Wirtschaft und Technologie

BGR Bundesanstalt für Geowissenschaften und Rohstoffe

FZK/INE Forschungszentrum Karlsruhe, Institut für Nukleare Entsorgungstechnik

GRS Gesellschaft für Anlagen- und Reaktorsicherheit



DOE/CAO Department of Energy, Carlsbad Area Office

SNL Sandia National Laboratories



ENRESA Empresa Nacional de Residuos Radioactivos



ERL/ITRI Energy and Resources Laboratories / Industrial Technology Research Institute



JNC Japan Nuclear Cycle Development Institute

Obayashi Obayashi Corporation

RWMC Radioactive Waste Management Center



RAWRA Radioactive Waste Repository Authority



SKB Svensk Kärnbränslehantering AB



EC European Community

Foreword

Concepts for the disposal of radioactive waste in geological formations depend crucially on a thorough knowledge of relevant processes in the host rock and on an understanding of the whole repository system, comprising both engineered and geological barriers. The Grimsel Test Site (GTS) is a first-generation underground rock laboratory which is used to investigate many of these processes in hard, fractured rocks. It has been operated since 1984 by the Swiss National Cooperative for the Disposal of Radioactive Waste (NAGRA).

The laboratory is located in the crystalline rock of the Central Aar Massif, 450 m below the eastern flank of the Juchlistock at an altitude of 1730 m. It is reached via a 1200 m horizontal access tunnel, operated by the hydropower plant KWO. The layout of the tunnels that comprise the GTS allowed the establishment of a radiation controlled zone (IAEA type B/C) in 1990 in which experiments with radioactive tracers are carried out. With increasing experience in the implementation of in-situ experiments, improved process understanding and more advanced repository concepts, the experimental programmes at the GTS have gradually become more complex and more directly related to open questions defined by performance assessors or by regulatory bodies. Demonstration of disposal concepts by performing large- or full-scale, long-term experiments has also become a key aspect of investigations in the rock laboratory.

The current investigation phase (Phase V; 1997 - 2002) was initiated in 1997 in close cooperation with international partner organisations. Seven experimental programmes and projects are included in Phase V, covering a broad spectrum of investigations.

This report documents the results of the project Conclusions of the Tunnel Near-Field (CTN). The project was aimed at deriving a state-of-the-art approach for geoscientific characterisation and conceptualisation of the zone of rock around tunnels and caverns of a radioactive waste repository, driven by the requirements of PA. The project was initiated in 1997 on the basis of the experimental work performed within GTS Phase IV (1994 to 1996) by BGR, GRS and NAGRA, and on the basis of the collaboration agreement with BMWi/BGR/GRS. USDOE, represented by Sandia National Laboratories, and ERL/ITRI formally joined the programme in 1998 as full partners.

GTS Phase V



NAGRA National Cooperative for the Disposal of Radioactive Waste



ANDRA Agence nationale pour la gestion des déchets radioactifs



BMWi Bundesministerium für Wirtschaft und Technologie

BGR Bundesanstalt für Geowissenschaften und Rohstoffe

FZK/INE Forschungszentrum Karlsruhe, Institut für Nukleare Entsorgungstechnik

GRS Gesellschaft für Anlagen- und Reaktorsicherheit



DOE/CAO Department of Energy, Carlsbad Area Office

SNL Sandia National Laboratories



ENRESA Empresa Nacional de Residuos Radioactivos



ERL/ITRI Energy and Resources Laboratories / Industrial Technology Research Institute



JNC Japan Nuclear Cycle Development Institute

Obayashi Obayashi Corporation

RWMC Radioactive Waste Management Center



RAWRA Radioactive Waste Repository Authority



SKB Svensk Kärnbränslehantering AB



EC European Community

Vorwort

Bei der Entsorgung radioaktiver Abfälle wird aus Sicherheitsüberlegungen die Endlagerung in geologischen Formationen vorgesehen. Dafür sind Kenntnis über das Wirtgestein sowie ein vertieftes Verständnis der technischen Sicherheitsbarrieren von entscheidender Bedeutung.

Seit 1984 betreibt die Nagra (Nationale Genossenschaft für die Lagerung radioaktiver Abfälle) ein standortunabhängiges Felslabor im Grimselgebiet (FLG), in den granitischen Gesteinen des Zentralen Aar Massivs.

Das FLG liegt 450 m unter der Ostflanke des Juchlistocks auf einer Höhe von 1730 m ü.M. und kann durch einen 1200 m langen horizontalen Zugangstollen der Kraftwerke Oberhasli AG (KWO) erreicht werden. Im Jahr 1990 wurde in einem der Stollenabschnitte des FLG's eine kontrollierte Zone (IAEA Typ B/C) für Versuche mit radioaktiven Tracern eingerichtet.

Mit zunehmender Erfahrung in der Durchführung von Feldversuchen, verbessertem Systemverständnis der geologischen und technischen Barrieren sowie der weiterentwickelten Lagerkonzepte, verlagerten sich die Programm-Schwerpunkte zu komplexen, direkt auf die Anforderungen der Sicherheitsanalyse ausgerichteten Versuche. Langzeitdemonstrationsversuche gewannen in den letzten Jahren immer mehr an Bedeutung.

Die Untersuchungsphase V (1997 - 2002) wurde in enger Zusammenarbeit mit den Partnerorganisationen geplant. Sie beteiligen sich wesentlich bei der Durchführung der insgesamt 7 Versuchsprogramme, die ein breites Spektrum wissenschaftlicher und technischer Fragestellungen abdecken.

Der vorliegende Bericht "Conclusions of the Tunnel Near-Field" (CTN) ist eine Synthese – aus dem Blickwinkel der Sicherheitsanalyse – die den aktuellen Stand der Technik/Methodik zur Charakterisierung und Konzeptualisierung des Stollennahfelds zusammenfasst. Basis des Syntheseberichts bilden die Versuchsergebnisse, die von BGR, GRS und Nagra zwischen 1994 und 1996 erarbeitet wurden. Durch den Zusammenarbeitsvertrag mit BMWi/BGR/GRS wurde das CTN Projekt 1997 initialisiert. Seit 1998 sind neben den oben erwähnten Partnern das US-DOE/Sandia National Laboratories und ERL/ITRI beteiligt.

GTS Phase V



NAGRA National Cooperative for the Disposal of Radioactive Waste



ANDRA Agence nationale pour la gestion des déchets radioactifs



BMWi Bundesministerium für Wirtschaft und Technologie

BGR Bundesanstalt für Geowissenschaften und Rohstoffe

FZK/INE Forschungszentrum Karlsruhe, Institut für Nukleare Entsorgungstechnik

GRS Gesellschaft für Anlagen- und Reaktorsicherheit



DOE/CAO Department of Energy, Carlsbad Area Office

SNL Sandia National Laboratories



ENRESA Empresa Nacional de Residuos Radioactivos



ERL/ITRI Energy and Resources Laboratories / Industrial Technology Research Institute



JNC Japan Nuclear Cycle Development Institute

Obayashi Obayashi Corporation

RWMC Radioactive Waste Management Center



RAWRA Radioactive Waste Repository Authority



SKB Svensk Kärnbränslehantering AB



EC European Community

Préface

Le stockage définitif des déchets radioactifs est prévu, pour des questions de sécurité, dans des formations géologiques. La connaissance détaillée des roches d'accueil et une compréhension approfondie des processus se déroulant dans la roche et dans les barrières techniques de sécurité sont d'une importance décisive.

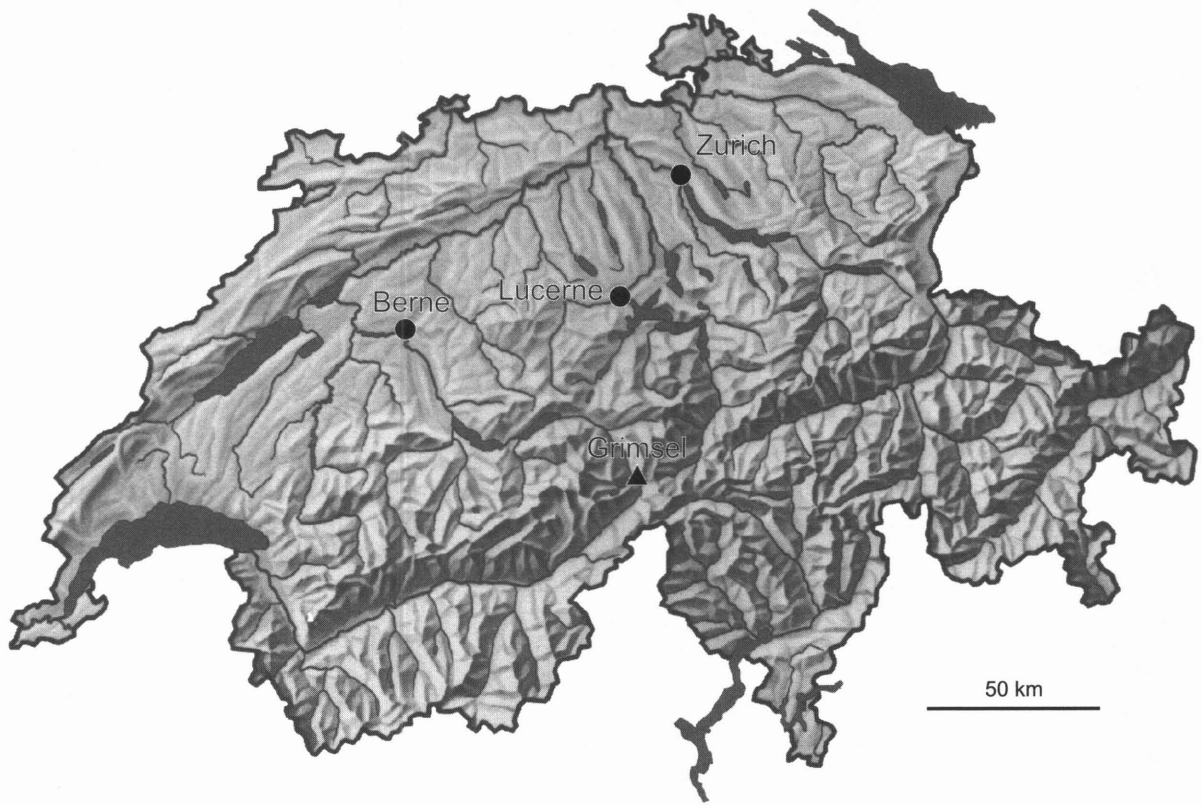
Le laboratoire souterrain du Grimsel (LSG) est un laboratoire de première génération en fonction depuis 1984, exploité par la Société coopérative nationale pour l'entreposage de déchets radioactifs (CEDRA).

Le laboratoire est situé à une altitude de 1730 m dans les roches granitiques du Massif Central de l'Aar, à 450 m de profondeur sous le flanc est du Juchlistock. On l'atteint par un tunnel d'accès horizontal exploité par la centrale électrique Oberhasli AG de la société KWO. En 1990, on a aménagé dans le LSG une zone de radiation contrôlée (type B/C de l'AIEA) pour des essais avec traceurs radioactifs.

Avec l'expérience croissante dans la conduite d'essais in-situ, une meilleure compréhension des barrières géologiques et techniques, le programme de recherche s'est orienté vers des essais toujours plus complexes liés aux exigences des analyses de sécurité. La démonstration de faisabilité de concepts de dépôt à grande échelle et sur de longues durées est devenue l'un des points forts des recherches dans le laboratoire souterrain.

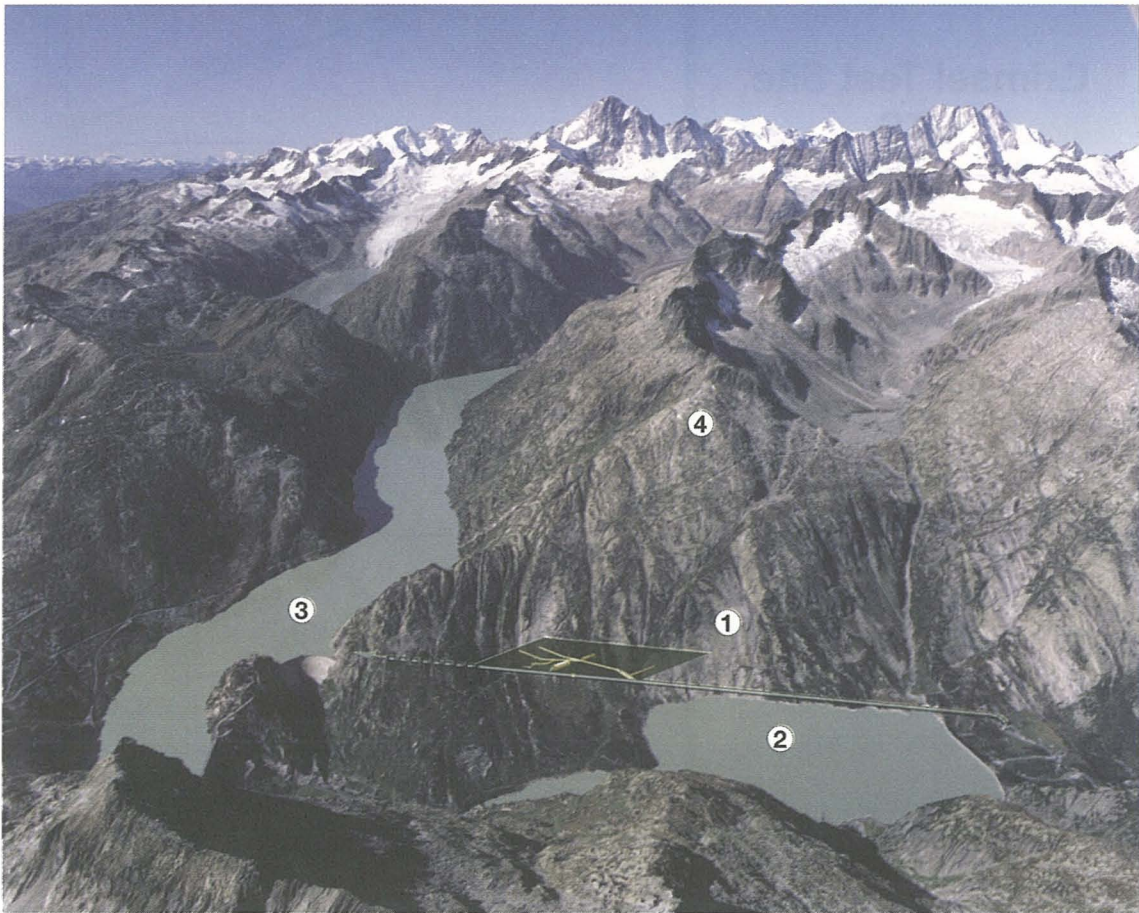
La phase de recherche actuelle (phase V 1997 - 2002) a été planifiée en concertation étroite avec des partenaires internationaux. Elle comprend sept projets et programmes d'essais couvrant un large spectre de questions scientifiques et techniques.

Le présent rapport sur les conclusions liées au champ proche du tunnel (CTN, Conclusions of the Tunnel Near-Field) apporte une synthèse, du point de vue de l'analyse de sécurité, de l'état actuel des connaissances techniques et méthodologiques sur la caractérisation et la conceptualisation du champ rocheux proche d'une galerie ou d'une caverne de dépôt radioactif. Le projet CTN a débuté en 1997 à la suite des travaux réalisés par le BGR, le GRS et la CEDRA au cours de la phase IV du LSG (1994 à 1996), et sur la base d'un contrat de collaboration avec le groupe BMWi/BGR/GRS. Depuis 1998 l'US-DOE, représenté par les Sandia National Laboratories, ainsi que l'ERL/ITRI, ont rejoint formellement le groupe des partenaires à part entière.



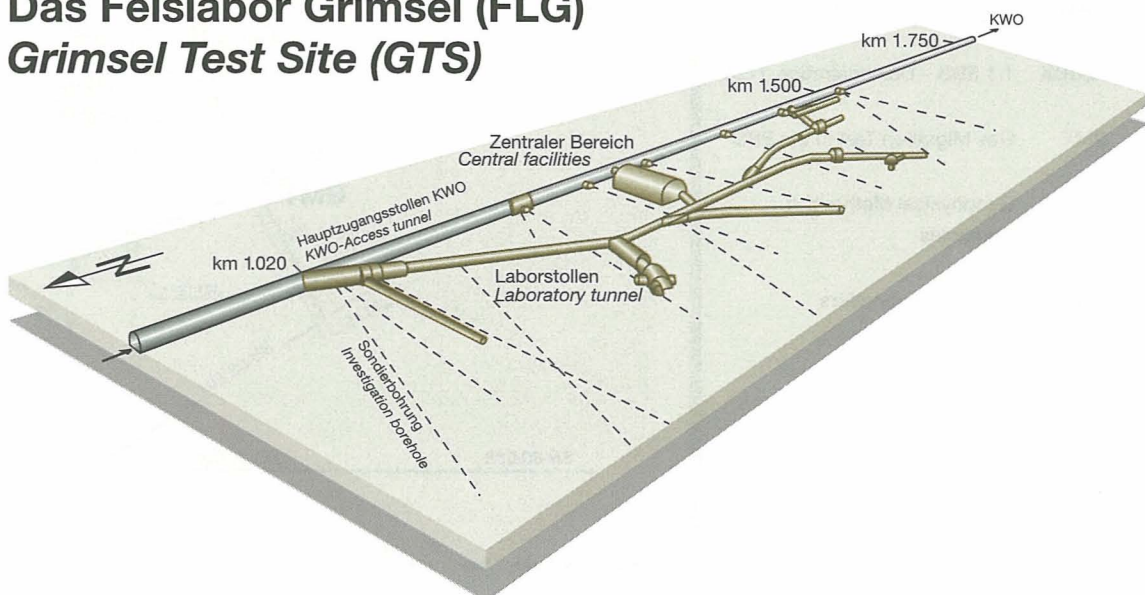
Location of Nagra's underground test facility at the Grimsel Pass in the Central Alps (Bernese Alps) of Switzerland

Grimsel-Gebiet (Blick nach Westen) / **Grimsel area** (view to the west)



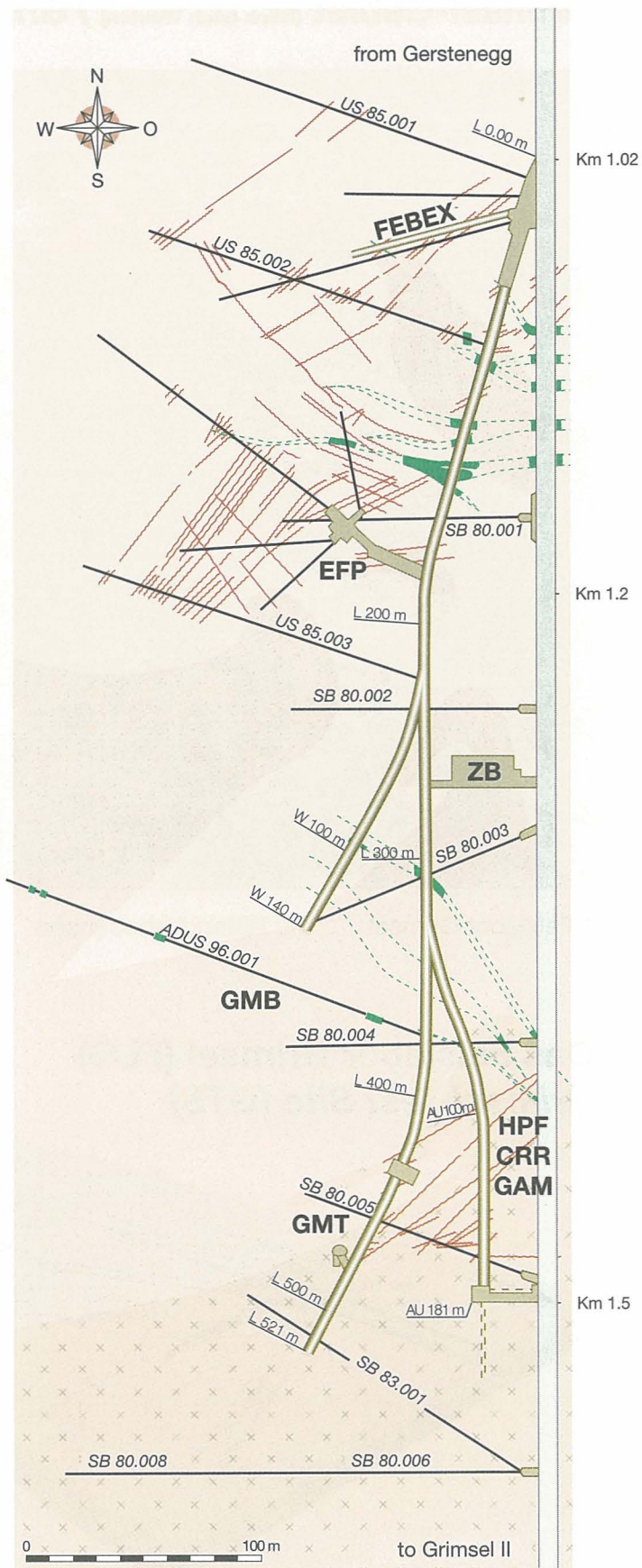
1 Felslabor Grimsel 2 Räterichsbodensee 3 Grimselfsee 4 Juchlistock

Das Felslabor Grimsel (FLG)
Grimsel Test Site (GTS)



Grimsel Test Site GTS

-  KWO-Access tunnel
-  Laboratory tunnel
-  Central Aaregranite (CAGR)
High biotite content CAGR
-  Grimsel-Granodiorite
-  Shear zone
-  Lamprophyre
-  **SB** Investigation borehole
-  **ZB** Central facilities
- GTS Phase V 1997-2002**
-  **HPF** Hyperalkaline Plume
-  **CRR** Colloid and Radionuclide Retardation
-  **GAM** Gastransport in the Geosphere
-  **FEBEX** 1:1 EBS - Demonstration (HLW)
-  **GMT** Gas Migration Test in the EBS
-  **GMB** Geophysical Methods in Boreholes
-  **EFP** Effective Parameters



SUMMARY

The project "Conclusions of the Tunnel Near-Field Programme" provides a synthesis of the achievements of the "Tunnel Near-Field Programme" of the GTS Investigation Phase IV (1994 - 1996). The synthesis is aimed, in the light of performance assessment requirements, at deriving a state-of-the-art approach for geoscientific characterisation and conceptualisation of the zone of rock around tunnels and caverns of a radioactive waste repository. The impact of the tunnel near-field on repository performance depends strongly on the type of host rock being assessed. The investigations addressed in this report are largely based on experience from the Grimsel Test Site and, therefore, are representative for crystalline rock or - in a broader sense - for fractured hard rock formations. Particular emphasis is given to the following issues:

- What is the role of the tunnel near-field in the assessment of repository performance? The particular processes addressed are migration of waste-generated gas, resaturation of the tunnel near-field after repository closure and the effect of the excavation disturbed zone on groundwater flow.
- How to convert geoscientific field data into valuable deliverables for performance assessment? A systematic and traceable approach is proposed, aimed at identification of the key processes of the synthesis procedure and at definition of a data exchange format adapted to the needs of performance assessment.
- With the focus on tunnel near-field characterisation, what are the determining factors in planning an underground site exploration programme? The choice of the site characterisation technique for a given exploration programme must respect the geological conditions as well as economic and time constraints. This report gives an overview of suitable exploration methods with special focus on equipment development within the framework of the Tunnel Near-Field Programme.
- How to establish quantitative models for gas migration and post-closure repository resaturation? For modelling two-phase flow processes in fractured hard rock, equivalent porous medium approaches have been shown to be an appropriate conceptualisation. Parametric models of capillary pressure and relative permeability, as well as two-phase flow parameter values, are compiled for matrix zones and shear zones of the GTS. An upscaling procedure for two-phase flow parameters is proposed, which respects the complexity of the fracture systems in a fractured hard rock. Finally, experimental evidence is given for the evolution of an unsaturated zone around underground excavations. The relevance of the unsaturated zone in terms of repository performance is assessed by numerical scoping calculations.
- How to establish quantitative models for estimating axial flow along sealed tunnel sections and how to estimate groundwater flow enhancement along emplacement caverns? Based on the fracture network approach, a conceptualisation of the excavation disturbed zone around underground openings is given. The hydraulic properties of the EDZ around TBM drilled and blasted tunnel sections at the GTS are compiled. Finally, a conceptual framework for estimation of axial flow around seal zones is given. A numerical sensitivity study of axial flow with generic field data is presented.

Complementary to the investigations at the GTS, this report presents a survey of tunnel near-field studies in other hard rock laboratories worldwide and a review of numerical tools for modelling groundwater flow and two-phase flow processes in the tunnel near-field.

ZUSAMMENFASSUNG

Das Projekt "Conclusions of the Tunnel Near-Field Programme" stellt eine Synthese der Untersuchungsergebnisse dar, die im "Programm Stollennahfeld" im Verlauf der FLG Untersuchungsphase IV (1994 - 1996) erarbeitet wurden. Ziel der Synthese ist die Bereitstellung einer Methodik zur geowissenschaftlichen Charakterisierung des Gebirges in der unmittelbaren Umgebung eines Endlagers für radioaktive Abfälle ("Stollennahfeld") sowie die Konzeptualisierung des Stollennahfeldes in einer Form, die den Bedürfnissen der Sicherheitsanalyse Rechnung trägt. Die Bedeutung des Stollennahfeldes für die Sicherheit eines Endlagers hängt wesentlich von den Eigenschaften des Wirtgesteins ab. Die im vorliegenden Bericht behandelten Arbeiten beziehen sich hauptsächlich auf kristalline Gesteine und - im weiteren Sinne - auf geklüftete Festgesteine. Der Schwerpunkt der Synthese liegt auf folgenden Fragestellungen:

- Welche Rolle spielt das Stollennahfeld für die Sicherheit eines Endlagers? Insbesondere werden hierbei die Ausbreitung von endlagergenerierten Gasen, die Wiederaufsättigung des Stollennahfelds nach dem Verschluss des Endlagers sowie der Einfluss des Stollennahfelds auf die natürlichen Grundwasserfließsysteme angesprochen.
- Wie können geowissenschaftliche Felddaten in verwertbare Informationen für die Sicherheitsanalyse aufgearbeitet werden? Es wird eine systematische und nachvollziehbare Methodik für die Synthese der Felddaten vorgeschlagen. Die Schlüsselprozesse des Synthesevorgangs werden identifiziert und im Rahmen eines generischen Beispiels wird ein strukturierter Datensatz für die Sicherheitsanalyse erstellt.
- Welche Faktoren beeinflussen massgeblich die Planung eines Untertage-Explorationsprogramms zur Charakterisierung des Stollennahfelds? Bei der Auswahl der Untersuchungstechniken müssen geologische, ökonomische und vortriebstechnische Randbedingungen berücksichtigt werden. Der vorliegende Bericht gibt einen Überblick über geeignete Untersuchungstechniken unter besonderer Berücksichtigung der im Programm Stollennahfeld durchgeführten Methodenentwicklungen.
- Wie werden quantitative Modelle zur Gasausbreitung in der Geosphäre bzw. zur Wiederaufsättigung des Stollennahfelds erstellt? Poroelastische Kontinuum-Ansätze wurden in der Vergangenheit erfolgreich für die Modellierung von Zweiphasenflussprozessen eingesetzt. Basierend auf diesen Ansätzen werden für Matrixbereiche und Scherzonen des Felslabors Grimsel Parametermodelle der relativen Permeabilität sowie der Kapillardruck-Sättigungsbeziehung abgeleitet und typische Wertebereiche der Zweiphasenflussparameter angegeben. Eine Methode zur Ermittlung äquivalenter Zweiphasenflussparameter wird vorgeschlagen, welche der Komplexität der Kluftnetzwerke im kristallinen Festgestein Rechnung trägt. Schliesslich wird die Ausbildung einer ungesättigten Zone in belüfteten Untertagebauwerken experimentell belegt. Die Bedeutung dieser Zone für die Sicherheitsanalyse wird durch numerische Modellrechnungen überprüft.
- Wie kann mit quantitativen Modellen der Einfluss des Stollennahfelds auf die Grundwasserzirkulation in der Umgebung eines Endlagers abgeschätzt werden? Auf der Grundlage eines Kluftnetzwerk-Ansatzes wird ein konzeptuelles Modell der in der Umgebung von Untertagebauwerken auftretenden Auflockerungszone gegeben. Die geometrischen und hydraulischen Eigenschaften der im Felslabor Grimsel angetroffenen Auflockerungszone werden zusammengestellt; dies gilt sowohl für gesprengte Stollenabschnitte als auch für solche Abschnitte, die im TBM-Vortrieb

erstellt wurden. Schliesslich wird ein numerisches Modell zur Abschätzung des axialen Flusses entlang von Versiegelungsstrecken aufgebaut. Mit Hilfe von generischen Daten werden Sensitivitätsrechnungen zum axialen Fluss durchgeführt.

Als Ergänzung zu den Untersuchungen am Felslabor Grimsel wird am Ende des Berichts eine Übersicht über Stollennahfelduntersuchungen in anderen Felslabors gegeben. Ausserdem wird eine Zusammenschau von numerischen Werkzeugen für hydraulische Klufnetzwerkmodellierungen und Zweiphasenflussmodellierungen erstellt.

RESUME

Le projet intitulé "Conclusions du programme sur le champ proche de la galerie" offre une synthèse de ce qui a été réalisé dans le cadre de ce programme faisant partie de la phase IV des recherches au laboratoire souterrain du Grimsel (1994 - 1996). La synthèse a pour but de donner, à la lumière des analyses de sécurité et en l'état actuel des connaissances, une approche pour la caractérisation géoscientifique et la conceptualisation du milieu rocheux autour des galeries et cavernes d'un dépôt pour déchets radioactifs. L'impact du champ proche de la galerie sur la sûreté du dépôt dépend fortement du type de roche d'accueil analysé. Les recherches présentées dans ce rapport se basent largement sur les expériences réalisées au laboratoire souterrain du Grimsel (LSG) et sont donc représentatives de la roche cristalline voire d'autres formations de roches dures fracturées. On accorde une importance particulière aux résultats suivants:

- Quel est le rôle du champ proche de la galerie dans les analyses de sécurité du dépôt? Les processus particuliers étudiés sont la migration du gaz généré par les déchets, la resaturation du champ proche de la galerie après scellement du dépôt et l'effet de la zone de décompression sur la circulation des eaux souterraines.
- Comment convertir des données de terrain géoscientifiques en informations servant aux analyses de sécurité. On propose une approche simple et systématique visant à identifier les processus clés de la synthèse et à définir un format d'échange des données adapté aux besoins de l'analyse de sécurité.
- Si on se concentre sur la caractérisation du champ proche de la galerie, quels sont les facteurs déterminants pour planifier un programme de recherche en laboratoire souterrain? Le choix de la technique de caractérisation de site pour un programme de recherche souterraine donné doit tenir compte tant des conditions géologiques en présence que des impératifs économiques et de temps. Ce rapport offre une vue d'ensemble exhaustive des méthodes de recherches adéquates, une attention particulière étant accordée au développement de l'équipement dans le cadre du programme sur le champ proche de la galerie.
- Comment établir des modèles quantitatifs pour la migration du gaz et la resaturation du dépôt après scellement? Pour modéliser des processus d'écoulement biphasique en roche diaclasée, des approches en milieu poreux équivalent se sont avérées une conceptualisation adéquate. On a dressé des modèles paramétriques de la pression capillaire et de la perméabilité relative, et recueilli des valeurs paramétriques de l'écoulement biphasique pour les zones de la matrice rocheuse et les zones de cisaillement du LSG. On propose une procédure pour des paramètres d'écoulement biphasique, que tiendra compte de la complexité des systèmes diaclasés dans la roche diaclasée. On a la preuve expérimentale de l'évolution d'une zone insaturée autour des excavations souterraines. De vastes calculs numériques évaluent l'importance de la zone insaturée en perspective de la sûreté du dépôt.
- Comment établir des modèles quantitatifs pour estimer l'écoulement axial le long de sections de galerie scellées et comment estimer l'augmentation de l'écoulement souterrain le long des cavernes? Basée sur l'approche en réseaux diaclasés, une conceptualisation de la zone de décompression autour des brèches souterraines est donnée. Les propriétés hydrauliques de la zone de décompression autour des sections de galeries forées ou creusées à l'explosif au LSG sont connues. On fixe un cadre conceptuel pour estimer l'écoulement axial autour des zones scellées.

Une étude de sensibilité numérique sur l'écoulement axial avec données de terrain génériques est présentée.

En plus des recherches au LSG, ce rapport offre une vue d'ensemble des études réalisées dans le champ proche des galeries d'autres laboratoires souterrains du monde ainsi qu'une revue des instruments numériques utilisés pour modéliser l'écoulement des eaux souterraines et les processus d'écoulement biphasique dans le champ proche de la galerie.

CONTENT

Summary	I
Zusammenfassung	II
Resumé	IV
Content	VI
List of Figures	IX
List of Tables.....	XII
Abbreviations	XIII
1 Introduction.....	1
1.1 Background and scope.....	1
1.2 Objectives.....	4
1.3 Project organisation and responsibilities	5
2 The role of the tunnel near-field in repository performance	7
2.1 Some words on terminology	7
2.2 Importance of the tunnel near-field in performance assessment.....	7
2.3 Synthesis of site characterisation data as input for performance assessment	9
3 Geoscientific characterisation of the tunnel near-field	13
3.1 Exploration strategy.....	13
3.2 Equipment and methodology developments - overview	14
3.2.1 Surface packer	15
3.2.2 Combined short interval packer system	17
3.2.3 Modular mini packer system (MMPS).....	17
3.2.4 Slim hole piezometer systems.....	18
3.2.5 Time domain reflectometry (TDR)	21
3.2.6 Thermography	22
3.2.7 DC geoelectric surveys.....	24
3.2.8 Mini sonic probe	25
3.2.9 Sampling of shear zone cores.....	27
3.3 Equipment and methodology developments	27
3.4 Applicability of equipment developments to other rock formations.....	30
3.5 Comprehensive overview of field methods for tunnel near-field characterisation	31

4	Gas release and the unsaturated zone	33
4.1	Modelling two-phase flow processes in fractured hard rock.....	33
4.1.1	The continuum approach.....	33
4.1.2	Parametric models of two-phase flow properties.....	35
4.1.3	Empirical relationship between transmissivity and gas entry pressure	37
4.2	Compilation of a GTS database on two-phase flow properties	38
4.2.1	Geological background.....	39
4.2.2	Structural and hydraulic properties of the rock.....	41
4.2.3	Two-phase flow parameters	45
4.3	System models for modelling gas migration through fractured hard rock.....	47
4.3.1	Relevant processes and gas flowpaths	48
4.3.2	Structural models for gas migration at the GTS	49
4.3.3	Effective two-phase flow parameters (upscaling approach)	50
4.3.4	Issues for future investigation.....	53
4.4	Resaturation of the tunnel near-field	54
4.4.1	Two-phase flow processes in the matrix	54
4.4.2	Experimental verification	58
4.4.3	Quantitative assessment of resaturation scenarios.....	62
4.4.4	Concluding remarks.....	66
5	Excavation Disturbed Zone	67
5.1	Importance of the EDZ for repository performance	68
5.1.1	The disturbed zone around repository seals	68
5.1.2	The disturbed zone around emplacement caverns	68
5.1.3	Evolution of the disturbed zone	69
5.1.4	Performance assessment.....	70
5.2	EDZ investigations at the GTS	70
5.2.1	Rock matrix in the disturbed zone	75
5.2.2	Fractures in the disturbed zone	78
5.3	Conceptual model of flow in the excavation disturbed zone.....	81
5.3.1	Conceptual model of the EDZ around the ZPK / BK site.....	82
5.3.2	Conceptual model of the EDZ around the EDZ site	83
5.3.3	Description of the disturbed zone for performance assessment	84
5.3.4	Numerical modelling of effective permeability around the tunnel	84
5.4	Issues for further investigation.....	92

6	Complementary studies	95
6.1	Numerical models for hydrogeological tunnel near-field investigations.....	95
6.1.1	Continuum two-phase flow simulators.....	96
6.1.2	Fracture network and coupled rock mechanical/hydraulic codes	101
6.2	Underground rock laboratories	102
7	Conclusions of the Tunnel Near-Field Programme	108
8	References	113

LIST OF FIGURES

Fig. 1.1:	Organisation of the Grimsel Test Site Programme - Phase IV (1994 - 1996)	2
Fig. 1.2:	Research topics and projects in the GTS Phase IV Tunnel Near-Field Programme.....	3
Fig. 1.3:	Locations of the experimental sites of the Tunnel Near-Field Programme at the GTS	4
Fig. 2.1:	Synthesis procedure for derivation of a tunnel near-field database for performance assessment	12
Fig. 3.1:	Surface packer system, side view	16
Fig. 3.2:	Combined installation of short interval packer and surface packer	18
Fig. 3.3:	The modular minipacker system (MMPS)	19
Fig. 3.4:	Slim hole piezometer system: (a) schematic and (b) test configuration at the ZPM site.....	20
Fig. 3.5:	TDR probes for water content measurements in boreholes, (a) packer TDR and (b) permanent TDR installation	21
Fig. 3.6:	Thermography system: (a) test set-up and (b) temperature distribution at the tunnel surface at the ZPM site	23
Fig. 3.7:	Calibration curves for DC resistivity measurements. Electrical conductivity of a total of eight core samples (Central Aare granite) is measured as a function of water saturation.....	25
Fig. 3.8:	The mini sonic probe: (a) photograph of the probe and (b) principle sketch	26
Fig. 3.9:	Recovery of undisturbed shear zone core samples	28
Fig. 4.1:	Geological overview of the GTS	40
Fig. 4.2:	Structural characterisation of core samples of shear zone material (from MARSCHALL & CROISÉ 1999): (a) bitmap of a core section and (b) aperture distribution of 10 core samples	42
Fig. 4.3:	Thin section of a typical granodiorite-granitic rock matrix. Pore spaces are yellow coloured (G) by fluorescent resin. Small intergranular pores between the grain boundaries are expected to be the main pathways of the matrix.....	44
Fig. 4.4:	Multistep constant head gas injection tests for determination of gas entry pressure in matrix zones at the ZPM site. Piezometers located at 0.3 and 2.4 m from the tunnel wall	47
Fig. 4.5:	Model variants for gas flow through a fractured host rock formation: (a) the water-conducting features form a complex network and (b) the water-conducting features are highly variable in transmissivity, but do not intersect each other	50
Fig. 4.6:	Derivation of simplified fracture network models for two-phase flow simulations, which are consistent with the original hydraulic models: (a) original hydraulic model with colour-coded log transmissivities of	

	the water-conducting features, (b) identification of the major pathways by particle tracking and (c) discarding of all minor flowpaths	52
Fig. 4.7:	Determination of synthetic relationships for relative permeability / capillary pressure and liquid saturation by numerical simulations of two-phase flow processes through the simplified fracture network	53
Fig. 4.8:	Conceptualisation of two-phase flow conditions in the rock matrix: (a) due to the very small pore sizes of the inter- and transgranular pore channels formation of a continuous (and mobile) gas phase is restricted to the condition of very low water saturation (wetting phase); (b) thin section of a typical quartz matrix and nanometre-size intergranular pores spaces	55
Fig. 4.9:	Movement of a desaturation front into the rock matrix: the balance between evaporation and advective flow of the liquid phase determines the extent of the unsaturated zone	56
Fig. 4.10:	Two-phase flow conditions in the rock matrix due to degassing. Spontaneous degassing is observed when the hydraulic pressure of the liquid phase is lowered below the bubble pressure of the dissolved gas component	56
Fig. 4.11:	The ZPM experimental site in the dead end section of the VE drift: (a) vertical section of hydraulic pressure monitoring system and (b) electrode array for electrical resistivity measurements at the tunnel face	57
Fig. 4.12:	Ventilation steps to induce the movement of an unsaturated zone into rock	58
Fig. 4.13:	Pressure profiles in the tunnel near-field during different ventilation phases	59
Fig. 4.14:	Effective permeability distribution in the tunnel near-field during steps I and II	60
Fig. 4.15:	The change in resistivity distribution was measured 0.25 and 2.5 m from the surface of the tunnel and sections between the borehole electrodes (edges of the 3D pictures): (a) at the beginning of step II; (b) after 3 months of ventilation	61
Fig. 4.16:	Model Region for the 1D desaturation simulations	62
Fig. 4.17:	Evolution of water pressure profiles after start of ventilation for (a) case 1 representing conditions of strong tunnel ventilation and (b) case 2 with tunnel ventilation at a minimum	63
Fig. 4.18:	Evolution of water saturation after start of ventilation for (a) case 1 and (b) case 2	64
Fig. 4.19:	Water mass flux density along the model axis for case 1 at a very early time (15 h) and at almost steady-state after 130 days	65
Fig. 4.20:	Air mass flux density along the model axis for case 1 at a very early time (15 h) and at almost steady-state after 20 years	66
Fig. 5.1:	Schematic illustration of excavation damage and disturbed zones	67
Fig. 5.2:	GTS Map showing the two ZPK and the EDZ experimental sites	72

Fig. 5.3:	Geological map of the EDZ site showing the breakout zone	73
Fig. 5.4:	Stresses around the EDZ/WT and ZPK/BK tunnels: (a) stress invariant for EDZ / WT area tunnel calculated from analytical solution for continuum homogeneous linear elastic material and (b) stress invariant for ZPK area tunnel calculated using the Adina finite element system.	74
Fig. 5.6:	Interval transmissibility with distance from tunnel.....	80
Fig. 5.7:	Conceptual model of permeability distribution in the EDZ around the BK site	82
Fig. 5.8:	Model variants used in axial flow calculations and field data from the GTS: (a) variant 1 - high transmissibility intervals are damaged zone features, (b) variant 2 - high transmissibility intervals are channels in natural fractures and (c) hydraulic conductivity profiles measured in the EDZ / WT area.....	85
Fig. 5.9:	Sample realisation from different models of fracture system around tunnel at EDZ site: natural fracture network (a) without damage zone and (b) with stress induced damage zone.....	86
Fig. 5.10:	Methodology for calculating total and effective stress around an excavation	87
Fig. 5.11:	Total and effective minimum stress for the operational and post-closure phases	88
Fig. 5.12:	Simplified factor model geometry as might be used in repository scale groundwater flow models.....	91
Fig. 5.13:	Experimental set-up for Connected Permeability Experiment in the Mine-By Tunnel at AECL Underground Research Laboratory from FROST & EVERITT (1997).	93

LIST OF TABLES

Table 2.1: Geodata on "Groundwater and gas flow through the tunnel near-field" as input for performance assessment. The table shows a possible format for structured delivery of geoscientific data. The definition of deliverables depends on the particular repository concept and on site specific characteristics of the host rock formation	11
Table 3.1: Overview of methodology developments in GTS Phase IV	15
Table 3.2: Specifications of the BGR packer systems: surface packer (cf. Figure 3.1) / combined packer system (cf. Figure 3.2)	17
Table 3.3: Field data and expected deliverables from tunnel near-field investigations.....	28
Table 3.5: Proposed field methods for tunnel near-field characterisation	32
Table 4.1: Parametric models for capillary pressure and relative permeability	36
Table 4.2: Hydraulic classification of discontinuities at the BK site (762 fractures) based on an approach by PAHL et al. (1992)	41
Table 4.3: Two-phase flow properties of the FRI shear zone	46
Table 4.4: Two-phase flow properties of matrix zones at the VE site.....	47
Table 5.1: Interpretation of stresses at the ZPK / BK and EDZ / WT sites	75
Table 5.2: Matrix intrinsic permeability measurements at the EDZ sites.....	77
Table 5.3: Fracture transmissibility	80
Table 5.4: Effective axial permeability averaged over different annuli around tunnel.....	90
Table 5.5: Factor model fits to simulate effective permeability for model variant 1	92
Table 6.1: Comparison of areas of application of various two-phase flow codes	99
Table 6.2: Comparison of the numerics, input, output and preprocessing features of various two-phase flow codes	100
Table 6.3: Comparison of underground laboratories in hard rock formation	106

ABBREVIATIONS

BGR	- Bundesanstalt für Geowissenschaften und Rohstoffe, Hannover - Germany
BK	- Bohrlochkranzversuch / fracture system flow test (GTS experimental site)
BMFT	- Bundesministerium für Forschung und Technologie, Bonn - Germany
BOS	- Borehole Sealing Experiment (GTS experimental site)
CP	- Connected Porosities (GTS experimental site)
CTN	- Conclusions of the Tunnel Near-Field (GTS Phase V project)
DC	- Direct current
EDZ	- Excavation Disturbed Zone (GTS experimental site)
ENRESA	- Empresa Nacional de Residuos Radiactivos SA, Madrid - Spain
EPM	- Equivalent porous medium
ERL/ITRI	- Energy and Resources Laboratories / Industrial Technology Research Institute Taiwan
FEBEX	- Full-scale Engineered Barriers Experiment (GTS experimental site)
FEP	- Features, Events and Processes
FZK	- Forschungszentrum Karlsruhe - Germany
GRS	- Gesellschaft für Anlagen- und Reaktorsicherheit
GTS	- Grimsel Test Site
HLW	- High-level waste
HRL	- Hard rock laboratory
ISCO	- International Steering Committee of the GTS Investigation Phase V
LL/ILW	- Low / intermediate-level waste
MMPS	- Modular mini packer system
NAGRA	- Nationale Genossenschaft für die Lagerung radioaktiver Abfälle / National Cooperative for the Disposal of Radioactive Waste, Wetingen - Switzerland
NEA	- Nuclear Energy Agency, Paris - France

PA	- Performance assessment
PNC	- Power Reactor and Nuclear Fuel Development Corporation (now JNC) Japan
RRP	- Radionuclide Retardation Project (GTS experimental site)
SNL	- Sandia National Laboratories, Albuquerque - USA
US-DOE	- US - Department of Energy, Washington
SKB	- Svensk Kärnbränslehantering AB, Stockholm - Sweden
TBM	- Tunnel boring machine
TDR	- Time-domain reflectometry
TOM	- Tomography (GTS experimental site)
TPF	- Two-Phase Flow in Shear Zones (GTS experimental site)
UZ	- Unsaturated Zone (GTS experimental site)
VE	- Ventilation Test (GTS experimental site)
WCF	- Water-conducting feature
WT	- Wärmetest / Heater Test (GTS experimental site)
ZPK	- Zweiphasenfluss in Klüften / Two-Phase Flow in Fractures (GTS experimental site)
ZPM	- Zweiphasenfluss in Matrixzonen / Two-Phase Flow in Matrix (GTS experimental site)

1 INTRODUCTION

1.1 Background and scope

Motivation

In a future repository for L/ILW or HLW, particular significance will be attached to the zone of rock immediately surrounding the tunnels and caverns, which represents the transition from the repository installations to the geosphere. It is characterised by specific hydraulic and rock mechanical properties that have a significant influence on water and gas flow and, consequently, on potential transport of radionuclides to the biosphere. In the context of performance assessment, the following key issues are directly associated with the tunnel "near-field":

- The excavation disturbed zone (EDZ) around tunnels and caverns leads to an increased effective hydraulic conductivity in the immediate vicinity of the repository. Hence, natural groundwater flow at the site will be affected by this enhanced conductivity.
- The hydraulic properties of the EDZ significantly influence potential axial water flow. These properties can impact the technical feasibility and ultimate quality of tunnel sealing.
- The release of gas through the geosphere after closure of the repository is strongly influenced by the two-phase flow properties of the tunnel near-field. If the gas cannot escape through the rock, then overpressures could build up in the caverns. This, in turn, may result in a decrease in the barrier effect of the rock formation.
- The resaturation of the tunnels and caverns of a repository in the post-operational phase is determined by the flow of groundwater towards the underground facilities. Desaturation of the tunnel near-field during the operational phase due to tunnel ventilation can cause considerable reduction of water inflow and, consequently, extend the pressure recovery phase after closure of the repository.

The impact of the tunnel near-field on repository performance depends strongly on the type of host rock being assessed. The tunnel near-field investigations addressed in this report are largely based on experience from the Grimsel Test Site (GTS), Nagra's rock laboratory situated in a crystalline rock environment in the central Swiss Alps. Hence, findings and conclusions presented here are more representative for crystalline rock or - generally speaking - fractured hard rock formations rather than argillaceous media.

The Tunnel Near-Field Programme (GTS Phase IV)

The emphasis of the GTS Investigation phase IV (1994 – 1996) was on conducting projects of a practically oriented nature in the areas of underground site investigation methodologies, geoscientific databases for performance assessment and emplacement technologies. In total, eight experiments were initiated within the framework of an international cooperation programme. The experiments included (McKINLEY & SPRECHER 1996, cf. Figure 1.1):

- Seismic Tomography (TOM), aimed at clarifying the potential of this method for remote identification of structures in the rock. This project was conducted by Nagra.
- Borehole Sealing (BOS), with the emphasis on testing sealing technologies for long, subhorizontal boreholes. The experiment was conducted by Nagra.

- Radionuclide Retardation Project (RRP), focusing on validation of sorption and matrix diffusion models. RRP was a joint experiment with PNC (Power Reactor and Nuclear Fuel Development Corporation).
- Full-scale Engineered Barriers Experiment (FEBEX) under the lead of Enresa (Empresa Nacional de Residuos Radiactivos SA), aimed at demonstrating waste emplacement technologies for high-level waste.
- Tunnel Near-Field Programme.

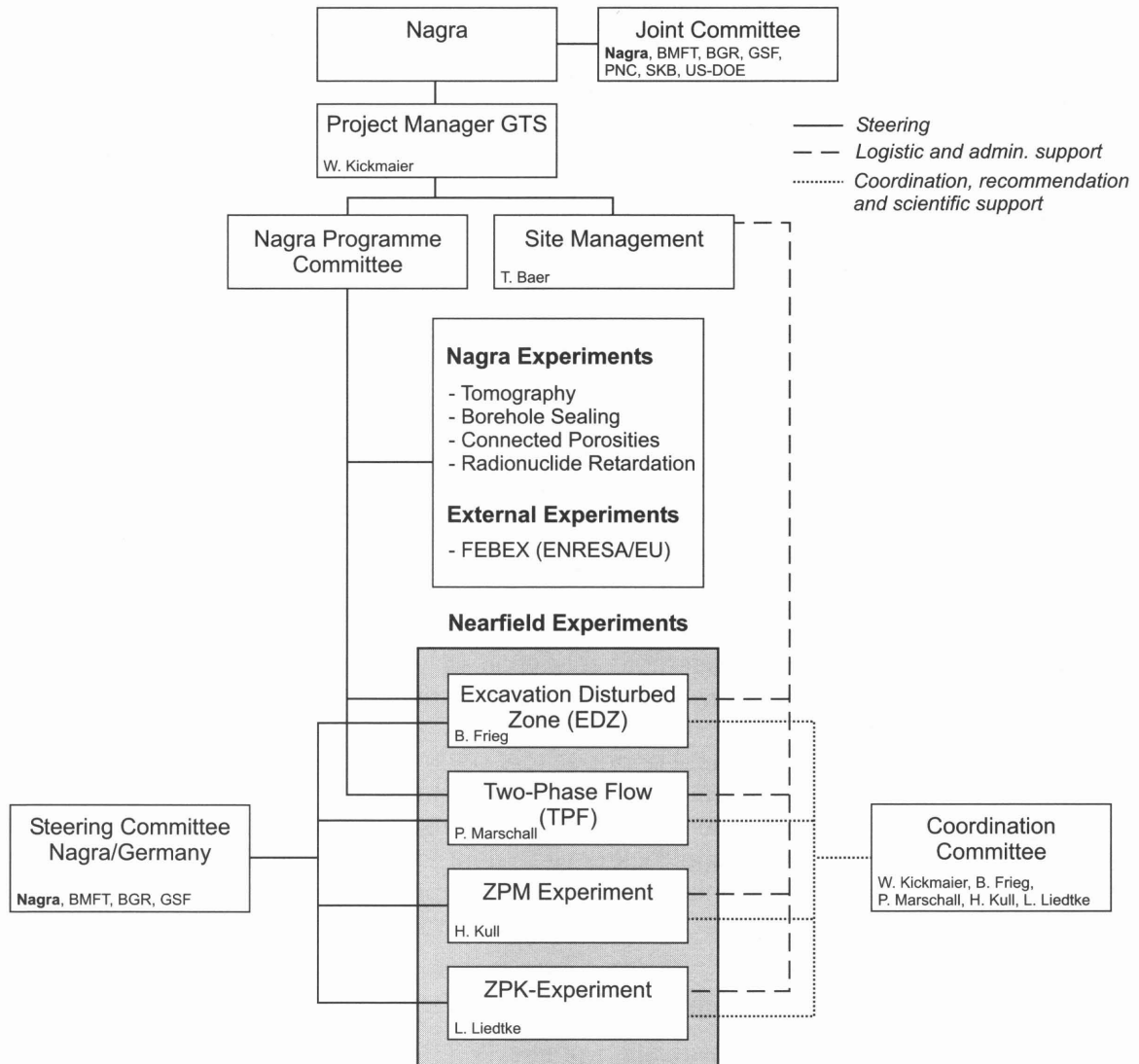


Fig. 1.1: Organisation of the Grimsel Test Site Programme - Phase IV (1994 - 1996)

The Tunnel Near-Field Programme was conducted by Nagra and its German partners BGR ("Bundesanstalt für Geowissenschaften und Rohstoffe") and GRS ("Gesellschaft für Anlagen- und Reaktorsicherheit") to study, for a crystalline rock environment, the relevance of the tunnel near-field as a key issue for performance assessment (FRIEG et al. 1996). The programme consisted of four more or less independent experiments, namely EDZ (Excavation Disturbed Zone, Nagra), ZPK (Zweiphasenfluss in Klüften, BGR), ZPM (Zweiphasenfluss in der Matrix, GRS) and TPF (Two-Phase Flow in Shear

Zones, Nagra). Figure 1.1 gives an overview of the organisation of the Tunnel Near-Field Programme as part of the GTS Investigation Phase IV.

The progress of the Tunnel Near-Field Programme was reviewed by a Steering Committee, consisting of members of the participating organisations BGR, BMBF ("Bundesministerium für Bildung, Wissenschaft, Forschung und Technologie", Germany), GRS and Nagra. In addition, a Coordination Committee was established to ensure information exchange between the projects.

The focal points of the Tunnel Near-Field Programme were (cf. Figure 1.2):

- Development and testing of techniques which are widely applicable in hydraulics, geophysics and rock mechanics for characterising the near-field of tunnels and caverns.
- Development and application of in-situ methods for investigating the two-phase flow properties of fracture / shear zones and matrix zones in the near-field of tunnels and caverns.
- Development of conceptual and numerical models of the rock mechanical and hydraulic behaviour of the EDZ around tunnels and caverns.
- Development of conceptual and numerical models for the simulation of two-phase flow processes in fracture and matrix zones in the tunnel near-field.

Projects in the Near-Field Programme

EDZ Excavation disturbed zone

TPF Two-Phase Flow

ZPK Two-Phase Flow in Fracture Networks

ZPM Two-Phase Flow in Rock Matrix

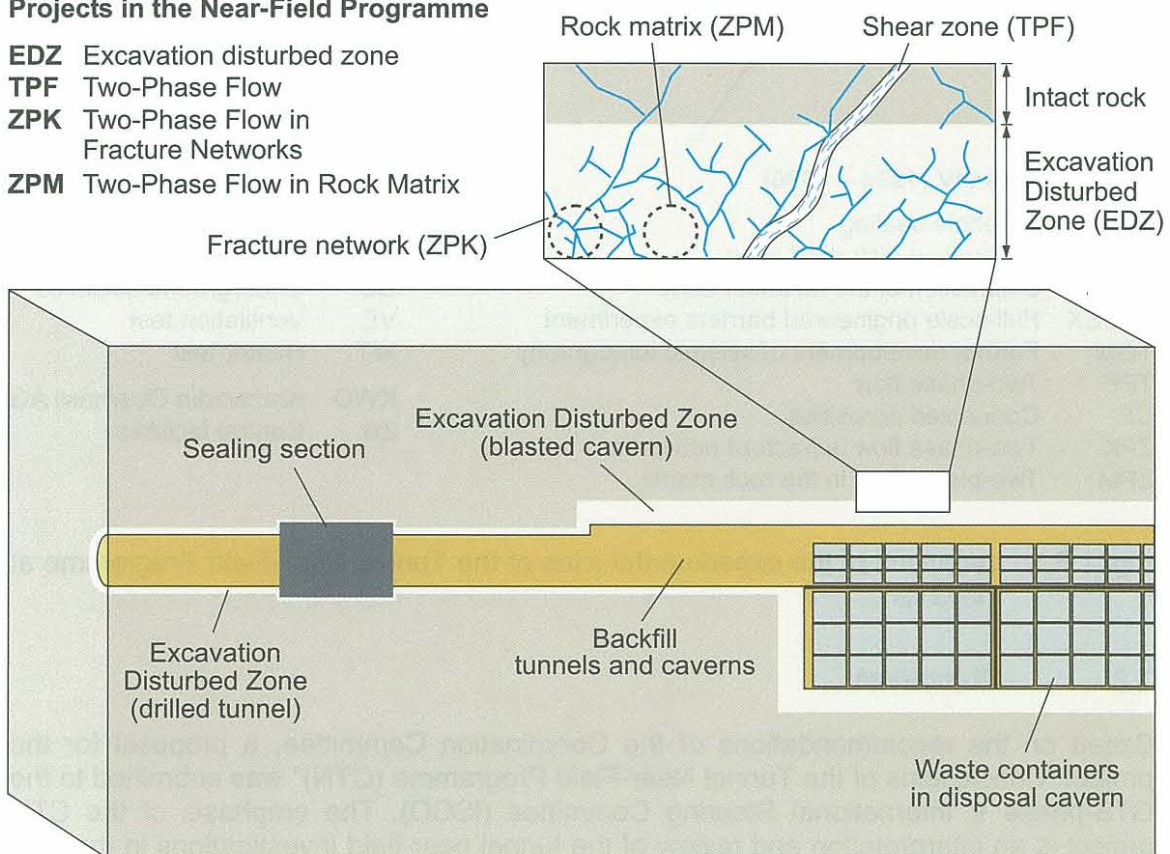
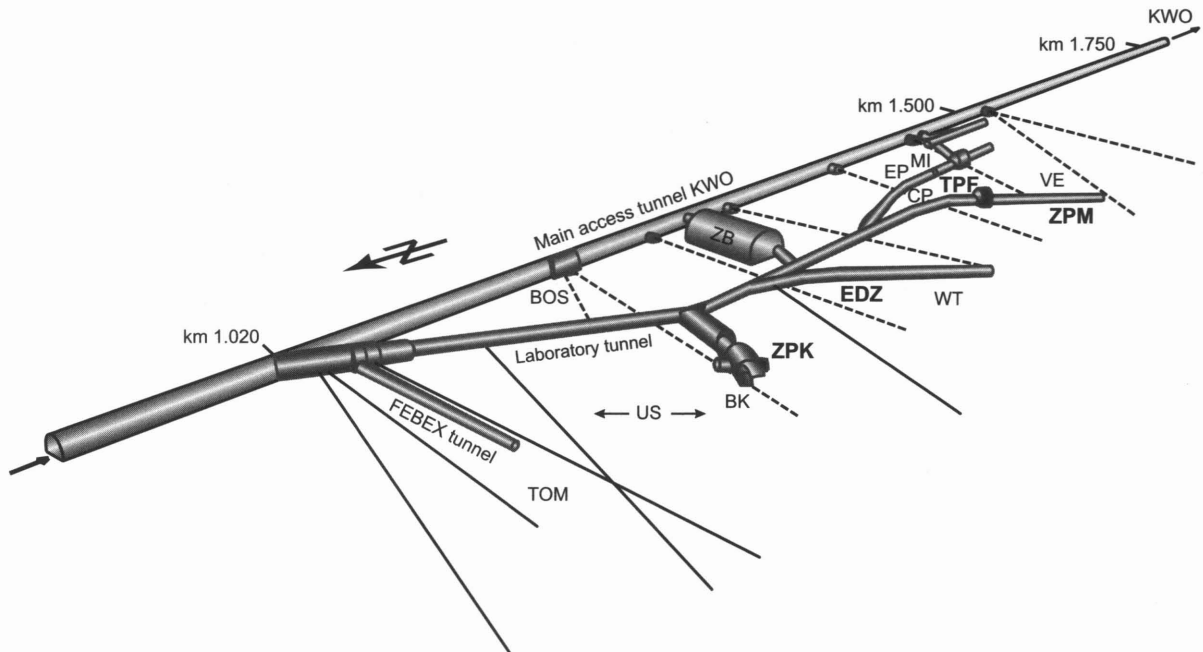


Fig. 1.2: Research topics and projects in the GTS Phase IV Tunnel Near-Field Programme

The projects EDZ (FRIEG & BLASER 1999) and ZPK (LIEDTKE et al. 1999) were aimed at investigating the excavation disturbed zone around tunnel sections excavated either with a tunnel boring machine (EDZ) or by drill and blast methods (ZPK). The ZPM experiment (KULL et al. 1999) focused on two-phase flow processes in the rock matrix. Finally, the TPF experiment (MARSCHALL & CROISÉ 1999) was aimed at developing in-situ techniques for determination of two-phase flow properties within Nagra's L/ILW site investigation programme. The locations of the experiments at the GTS are given in Figure 1.3.



Tests in Phase IV (1994 – 1996)

BOS	Borehole sealing
EDZ	Excavation disturbed zone
EP	Excavation of the MI shear zone
FEBEX	Full-scale engineered barriers experiment
TOM	Further development of seismic tomography
TPF	Two-phase flow
CP	Connected porosities
ZPK	Two-phase flow in fracture networks
ZPM	Two-phase flow in the rock matrix

Test areas

BK	Fracture system flow test
MI	Migration experiment
US	Underground seismics
VE	Ventilation test
WT	Heater test
KWO	Kraftwerke Oberhasli AG
ZB	Central facilities

Fig. 1.3: Locations of the experimental sites of the Tunnel Near-Field Programme at the GTS

1.2 Objectives

Based on the recommendations of the Coordination Committee, a proposal for the project "Conclusions of the Tunnel Near-Field Programme (CTN)" was submitted to the GTS-phase V International Steering Committee (ISCO). The emphasis of the CTN project is an interpretation and review of the tunnel near-field investigations in the light of performance assessment requirements, integrating the complementary research issues of the different projects which formed part of the Tunnel Near-Field Programme

of GTS Phase IV. Experience from the first three phases of Grimsel investigations (e.g. Ventilation Experiment / VE, Unsaturated Zone / UZ) is also considered when synthesising these results (cf. chapter 4).

This synthesis is aimed at presenting a state-of-the-art approach for the geoscientific characterisation and conceptualisation of the tunnel near-field in a crystalline environment in the perspective of performance assessment, including the issues of site characterisation methodologies, data analysis, conceptualisation and, finally, input of conceptual models and effective parameters to PA. Specific focus will be on the following objectives:

- to evaluate the achievements in equipment and methodology development, both for the characterisation of an EDZ and the estimation of two-phase flow parameters
- to develop a methodological framework for the derivation of effective two-phase flow parameters on the site scale
- to infer the extension and shape of an EDZ around drilled and blasted tunnel sections, depending on the stress conditions and rock mechanical properties of the formation
- to evaluate the numerical codes which have been applied to quantify enhanced axial water flow and gas transport in the tunnel near-field.

1.3 Project organisation and responsibilities

The CTN project was initiated in the framework of the GTS Investigation Phase V (1997 – 2002). Project partners are Nagra (project leader), the German partners BGR and GRS under sponsorship of BMBF, ERL-ITRI (Energy and Resources Laboratories-Industrial Technology Research Institute, Taiwan) and SNL (Sandia National Laboratories), funded by US-DOE (Department of Energy). The CTN project team consisted of representatives of the partners BGR (L. Liedtke, H. Shao), GRS (H. Kull, E. Fein, I. Müller-Lyda) and Nagra (P. Marschall). W. Lanyon (Geoscience / UK) joined the project team as external support. The role of ERL-ITRI (S.Ouyang, C. Lin) and SNL (K. Knowles) was to carefully review the project report.

The CTN project was subdivided into 4 different tasks:

- Task 1: Overview and evaluation of equipment and methodology developments which have been accomplished in support of detailed characterisation of the tunnel near-field.
- Task 2: Assessment of the most critical two-phase flow processes affecting migration of repository gas through the host rock and resaturation of a repository in the post-closure period and compilation of two-phase flow properties of fractured rock.
- Task 3: Assessment of the evolution of an EDZ around an excavation and compilation of its hydraulic and geomechanical properties.
- Task 4: Desk study on near-field investigations in other hard rock laboratories and comparison with the results from the GTS. This task also includes an assessment of numerical tools available for the simulation of hydraulic and two-phase flow processes in the tunnel near-field.

The responsible subtask leaders were L. Liedtke (Task 1), P. Marschall (Task 2 / gas migration), H. Kull (Task 2 / resaturation), W. Lanyon (Task 3) and E. Fein (Task 4).

The main part of the CTN synthesis work was accomplished in the course of 1998. A draft version of the CTN report was distributed to all ISCO members by December 1998. Subsequently, a review meeting was held at Nagra's offices on January 19, 1999. In addition to the input of the above mentioned reviewers, valuable comments were given W. Bechtholt (FZK - Forschungszentrum Karlsruhe), W. Brewitz (GRS) and L. Stenberg (SKB - Svensk Kärnbränslehantering AB, Sweden). The present report incorporates comments and suggestions provided by the review team.

2 THE ROLE OF THE TUNNEL NEAR-FIELD IN REPOSITORY PERFORMANCE

2.1 Some words on terminology

In crystalline rock formations, groundwater (and gas) flow is linked largely to brittle structures such as shear zones or tensile fractures (joints). In certain tectonic environments like at the GTS, these brittle structures are found in rock masses which have been subjected to strong ductile deformation (e.g. cleavage zones, ductile shear zones) or at the interface of different rock types with significant competence contrast (e.g. intrusions, lamprophyres). From the viewpoint of hydrogeological assessment, all these discontinuities can be referred to in a broad sense as *water-conducting features (WCF)*.

The most important characteristic of water-conducting features in a crystalline formation is their structural complexity. Water-conducting features may vary in type (e.g. shear zones, tensile fractures, hydrothermally altered fractures containing vein mineralisations), orientation, spatial distribution, size and hydraulic properties. Different types of features with variable orientation may intersect each other, forming a complex interconnected fracture network. Hence, the main challenge of any site investigation programme in crystalline rock consists of comprehensive characterisation and classification of the water-conducting features as a prerequisite for construction of a structural model of the host rock.

Rock masses between major faults are expected to exhibit low fracture intensity. When minor fractures are observed, they tend to be only weakly connected and would not form major groundwater flowpaths. Hydrogeologically, such weakly deformed zones are termed (unfractured) *rock matrix*.

Normally, the porosity of the matrix of crystalline rock is made up of very small pores (cf. section 4.2). The contribution of the rock matrix to groundwater flow is generally small. Nevertheless, in a host rock with relatively low fracture intensity, the fraction of groundwater flow through the matrix can not be ignored when compared to flow through the network of fractures. Similarly, at large depth, the transmissivity of the water conducting features may be reduced due to lithostatic load (closure of subhorizontal fractures) and thus matrix permeability may govern groundwater flow. The structural and hydraulic properties of the unfractured rock matrix are generally characterised by low spatial variability. Within the framework of site investigations, only limited databases are required for hydrogeological characterisation of the rock matrix.

2.2 Importance of the tunnel near-field in performance assessment

The essential outcome of the calculations performed within performance assessments (e.g. NAGRA 1994, NIREX 1997) is quantitative estimates of radionuclide transport into the biosphere and the resulting radiation doses or risks for the various scenarios. Assessment of long-term safety of radioactive waste repositories requires geoscientific data as input for scenario analyses (cf. SKB 1995). Systematic databases - so-called FEP lists - have been compiled by the Nuclear Energy Agency (NEA) and national organisations for various host rock and waste types, summarising the Features, Events and Processes that influence repository performance now or in the future (NEA 1998). In these FEP lists, the tunnel near-field plays an important role, because it represents

the transition from the repository installations to the geosphere. Any type of repository-induced perturbations, and in particular their evolution with time, will be strongly affected by the rock properties and hydraulic state conditions in the immediate vicinity of the excavations. In this report, particular emphasis is placed on the issues of gas migration, resaturation of the tunnel near-field after repository closure and the effect of the excavation disturbed zone on groundwater flow.

Gas migration

Once the caverns in a repository for L/ILW have been sealed, it is expected that gas (e.g. hydrogen, methane, CO₂) will be generated by anaerobic corrosion of metals and by chemical and microbial degradation of organic substances. Gas generation may cause unacceptable pressure build-up in the emplacement caverns, resulting in failure of either the barrier function of the tunnel sealing or the geosphere. In addition, an enhanced outflow of contaminated groundwater from the disposal area into the geosphere is expected when the repository is overpressurised with respect to the geosphere.

Gas production in the repository depends on various factors such as resaturation time and waste inventory. During the resaturation period the gas generation rate is limited by the availability of water and pressure build-up is moderate due to the high compressibility of the air-filled void space in the emplacement caverns. Therefore, from the viewpoint of performance assessment, the scenario of gas generation after resaturation of the repository is the relevant one. The issue to be addressed here is whether waste-generated gas can migrate through the fractured host rock without causing unacceptable release of radionuclides from the emplacement tunnels of the repository into the biosphere. In the ideal situation, gas would be transported away from the repository in solution by advection / dispersion (including diffusion) in the groundwater. However, if gas production exceeds a certain rate, a distinct gas phase will form in the near-field and the near-field gas pressure will rise until the total flux of fluids (gas phase and groundwater) out of the emplacement tunnels is equal to the gas generation rate. Possible gas pathways from the emplacement tunnels to the biosphere that have to be considered are not only through the geosphere, but also through seals and along backfilled access tunnels and shafts. The two-phase-flow properties of the tunnel near-field are, therefore, critical to the assessment of the issue of gas migration.

Resaturation of underground facilities after repository closure

Basically, a long resaturation and pressure recovery period after closure of the disposal facilities is a beneficial aspect for the long-term performance of a repository. This is because groundwater flow is directed towards the repository during the pressure recovery phase and will thus, prolong the residence times of radionuclides in the emplacement caverns. In addition, as long as the emplacement caverns are not fully saturated, reduced gas generation rates may be expected due to limited availability of water and the pressure build-up in the caverns will be moderate due to the high compressibility of gas filled pore spaces in the cavern backfill.

Resaturation of the repository can be affected by the formation of an unsaturated zone around the excavations, because the two-phase flow conditions may considerably reduce the inflow of groundwater towards the backfilled underground facilities. During the operational phase, two-phase flow conditions in the tunnel near-field can originate from the following processes:

- desaturation of the tunnel near-field caused by tunnel ventilation,
- degassing of gas-saturated groundwater, when the hydraulic pressure of the groundwater is lowered below the bubble point of dissolved gas components due to the pressure decline around the excavation.

The disturbed zone around underground excavations (EDZ)

The existence of a zone of altered rock properties around repository excavations may be an important control on fluid flowpaths through the repository and hence on transport paths for radionuclides (e.g. BENGTTSSON et al. 1991). There are two ways in which the EDZ may have an impact on the overall repository performance. Essentially these are both aspects of the potential difference in permeability between the EDZ and the host rock and the effect of this on groundwater flowpaths. However, they will be considered separately here:

- In low permeability rocks, the shafts and tunnels associated with the repository may form a preferential path for fluid migration unless adequate seals exist to limit groundwater flow. Such seals may be compromised by the existence of a highly permeable EDZ around the excavation.
- The existence of a permeable EDZ may also focus flow from the host rock through the EDZ. Depending on the relative permeabilities of host rock, EDZ and backfill / waste, increased flow may also occur around the waste packages.

2.3 Synthesis of site characterisation data as input for performance assessment

Planning of site investigations in support of performance assessment (PA) requires a clear and traceable procedure for the synthesis of the geological databases acquired. It is desirable to establish the concept for the synthesis in an early phase of the site investigation programme in order to optimise the efforts within the field projects.

Within the framework of its surface investigation programme for a L/ILW repository at the Wellenberg site, Nagra developed a systematic approach for the synthesis of geological data (NAGRA 1997). The heart of the approach, used as a steering mechanism for the entire synthesis procedure, was the formal definition of PA requirements, the so-called "Geodata Set Wellenberg". The *geodata set* consisted of a number of tables, aimed at compiling the relevant geoscientific information for PA. Each table was dedicated to a specific PA issue (e.g. geological site model, groundwater flow in the host rock) and contained (i) a brief assessment of important processes and basic assumptions, (ii) the most likely conceptual models and alternative ones and (iii) the range and most likely effective parameters. In addition, a *data flow analysis* was conducted. The deliverable of this system analysis was a data flow chart "Synthesis of geoscientific field data", which linked data from field investigations to the corresponding PA deliverables.

It is believed, that a similar approach could also apply for a future programme of underground site investigations, aimed at compilation of a tunnel near-field database for PA. The following section gives an outline of the structure of such a tunnel near-field geodata set and the corresponding data flow chart.

Geodata set "Groundwater and gas flow in the tunnel near-field"

In a PA programme for a real repository the issues to be addressed will depend on numerous factors such as repository design, waste inventory and the particular geological conditions at the site. It is the purpose of this section to develop a pragmatic *methodology* for establishing a tunnel near-field database, rather than to compile a complete "Tunnel Near-Field" geodata set, which would be restricted to a particular repository design and the specific geological conditions at the GTS. Special emphasis placed on establishing the geodata set in a structured format which is compatible with the structure of the geological input data used in PA analysis.

Geodata as input for PA are of both qualitative and quantitative nature; they may be grouped into the following categories (cf. Table 2.1):

- conceptual assumptions,
- geometry of the tunnel near-field and relevant structural elements,
- relevant processes and repository induced perturbations.

Characterisation of processes and repository induced perturbations consists of determination of rock properties (parameters) and state conditions of interest as input for qualitative / quantitative process models (e.g. axial groundwater flow around seals, gas migration through the geosphere). It also includes estimation of the ranges of uncertainty of parameters, assessment of the spectrum of conceptual models considered and, finally, evaluation of numerical tools for modelling of composite system behaviour.

Table 2.1 presents a reasonable format for a template containing relevant geodata on "Groundwater and gas flow through the tunnel near-field". As mentioned before, the table is not aimed at providing qualitative and quantitative input for a particular PA concept, because these data would be valid only for a particular repository concept and for the site-specific characteristics of the rock formations at the GTS. For instance, although not mentioned in Table 2.1, thermal load may play an important role in a HLW repository concept, inducing rock mechanical and hydraulic disturbances in the tunnel near-field. Furthermore, hydro chemical coupling (e.g. self-healing of fractures by swelling or precipitation, osmotic potentials) may no longer be a second order effect, if the fractures are filled with clay-rich material. In the case of a LL/ILW repository, geochemical alteration caused by concrete porewater (high pH plume) may strongly alter the EDZ properties at a certain time during repository evolution. In the context of the methodology of geodata sets, all these repository induced perturbations would be addressed in separate templates.

Table 2.1: Geodata on "Groundwater and gas flow through the tunnel near-field" as input for performance assessment. The table shows a possible format for structured delivery of geoscientific data. The definition of deliverables depends on the particular repository concept and on site specific characteristics of the host rock formation

Groundwater and gas flow in the tunnel near-field	
Category of PA-Input	Deliverable to PA (qualitative / quantitative) *
Conceptual assumptions	<ul style="list-style-type: none"> - groundwater flow takes place along discrete water-conducting features - the contribution of the matrix is (almost) negligible (note: this assumption is valid for the GTS environment, but not necessarily for other sites) - geochemical effects on groundwater flow are negligible (note: geochemistry is not negligible in radionuclide transport processes!)
Geometry of tunnel near-field (zonation) and structural elements	<ul style="list-style-type: none"> - classification and nature of the main structural elements (e.g. natural / excavation-induced / reactivated fractures; deterministic / stochastic description) - quantitative description of the fracture network (cf. section 3.3)
Repository-induced perturbations / processes, parameters and state conditions	<ul style="list-style-type: none"> - evaluation of relevant pathways for water / gas - microstructural properties, hydraulic and two-phase flow properties of fractures and matrix; rock mechanical properties (cf. sections 4.2 and 5.2)
(a) migration of repository gas	<ul style="list-style-type: none"> - state conditions / boundary conditions (hydraulic head, dissolved / free gas content, rock mechanical stress) - upscaling procedures (methodology, numerical tools) and effective parameters (cf. sections 4.3 and 5.3) - spectrum of conceptual models and parameter ranges (cf. chapter 6)
(b) resaturation of the tunnel near-field	
(c) axial flow along sealed zones / caverns	
* Deliverables to PA may depend on repository concept and site-specific characteristics of the host rock	

Data flow analysis "Ground water and gas flow through the tunnel near-field"

Assuming that the deliverables to PA have been defined ("geodata set"), the data flow analysis is a technique for structuring the overall synthesis procedure. The objectives of data flow analysis are to determine the main elements (processes) of the interpretation and synthesis procedure and to identify how the field data feed in. Data flow analysis allows the particular relevance of the different sets of field data for the overall procedure to be assessed and may therefore be applied to refine the site investigation programme and adapt it to the specific needs of PA. Data flow analysis is presented in so-called data flow charts, containing the input data (field data), the deliverables (geodata set) and a sequence of processes (interpretation / synthesis steps).

The synthesis procedure can be divided into different levels of maturity:

- *interpretation of field data*: the main structural elements of the site (e.g. geological units, classification of water conducting features) and the key hydrogeological processes (e.g. groundwater flow along discrete features) are identified. Point values for rock properties are determined (fracture statistics, hydraulic and rock mechanical properties)
- *derivation of structural / process models*: conceptual models of the main structural elements (e.g. fracture network model) and the key processes (e.g. two-phase flow parametric models, hydromechanical coupling) are established.
- *development of system models for process simulation*: quantitative / numerical models are established which (i) incorporate the relevant structural / process models and (ii) account for correct representation of site-specific boundary and initial conditions.

Each level consists of a number of key processes, relevant for the specific PA issue under investigation. Assuming "groundwater and gas flow in the tunnel near-field" is considered as an important PA issue, Figure 2.1 gives a sensible representation of the interpretation / synthesis levels and some of the key processes. It is worth noticing that selection of key processes is related to the assessed host rock formation and its site specific characteristics.

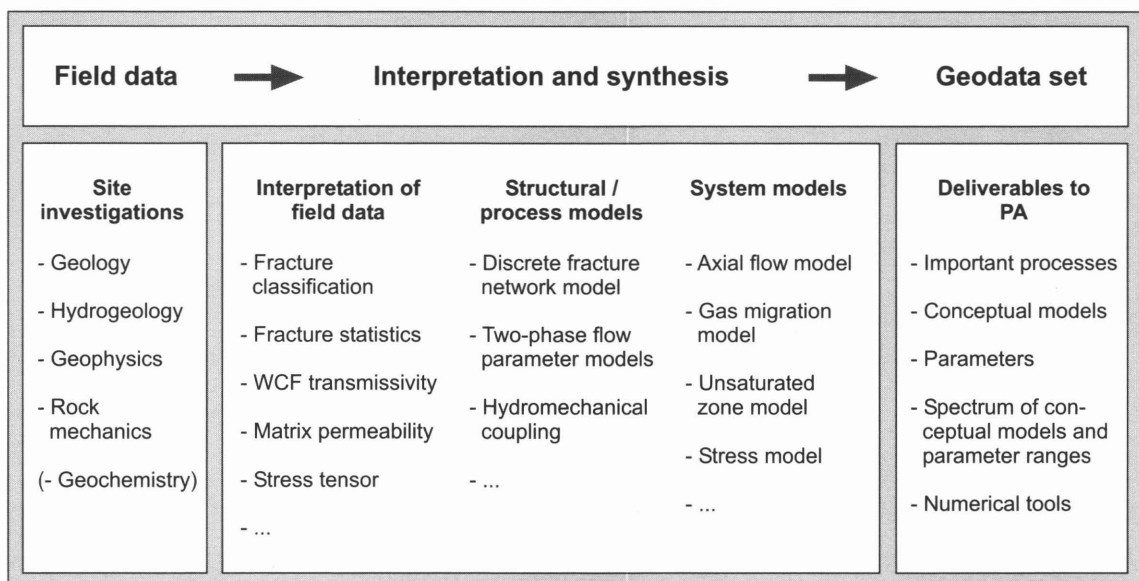


Fig. 2.1: Synthesis procedure for derivation of a tunnel near-field database for performance assessment

3 GEOSCIENTIFIC CHARACTERISATION OF THE TUNNEL NEAR-FIELD

The geological, hydrogeological and rock mechanical data base required for geoscientific characterisation of the host rock in the tunnel near-field is gained mostly from underground investigations. The exploration strategy and the field methods applied, will be determined not only by scientific needs, but also by large a number of other project restrictions. This chapter outlines the planning and schedule of an underground site investigation programme. Chapter 3.1 focuses on the exploration strategy. Chapter 3.2 highlights the equipment and methodology developments which have been accomplished as part of the Tunnel Near-Field Programme. The value of the new methods for characterisation of a crystalline host rock environment will be assessed and their applicability to other host rock formations (e.g. sediments) will be discussed (chapters 3.3 and 3.4). Finally, a comprehensive overview of existing and novel methods recommended for the investigation of the tunnel near-field in an underground facility will be compiled, with special emphasis on assessing the suitability of the available investigation methods for a real underground exploration programme (chapter 3.5).

3.1 Exploration strategy

When planning the underground exploration of a candidate host rock formation as part of a site investigation programme, the exploration concept will be determined not only by the specific geological conditions of the site, but also by economic constraints, waste disposal concept, excavation techniques applied, time schedule for waste emplacement and many other factors. Thus, the exploration procedure will greatly depend on the specific needs of the particular disposal programme. Based on practical considerations with respect to excavation progress and the specific aims to be achieved, the exploration procedure can be divided into the following phases:

- investigations during the excavation phase,
- test phases,
- long-term monitoring phases.

Investigations during the excavation phase

Investigations during the excavation phase are aimed at collecting those data which cannot be acquired during later phases. For example, geological mapping of the tunnel wall is much easier during the excavation phase because it is not yet complicated by safety arrangements (shotcrete, anchors, safety nets). Observation of transient hydraulic or rockmechanical effects (convergence of the tunnel profile, acoustic emissions, hydraulic head decline in the tunnel near-field, inflow rates to the tunnel) may allow inference of the geomechanical and geohydraulic state parameters of the formation under undisturbed conditions. As a disadvantage, geoscientific investigations could be disturbed by the excavation procedure. In addition, the access to the tunnel will be complicated by the presence of excavation equipment in the tunnel (e.g. TBM). Site investigations during the excavation phase are generally associated with tight time constraints.

Test phases of limited duration

Test phases are carried out to characterise the formation properties in greater detail under well defined test conditions and with minor time restrictions. Such field cam-

paings can be realised during major breaks in the excavation procedure or as part of an investigation programme in an underground rock laboratory. Typical measurements in a test phase are petrophysical logging in boreholes, geophysical surveys and hydraulic packer tests. In addition, geophysical surveys and core sampling campaigns can be realised within these test phases.

Long-term monitoring phases

Long-term monitoring is essentially carried out to record long-term development of state variables such as the hydraulic head, groundwater inflow into the tunnel or the convergence of the tunnel surface. In addition, irregular events or unexpected behaviour of the host rock formation can be surveyed. When selecting an experimental site for long-term monitoring, care must be taken to ensure that the location is not disturbed by major operational activities or by other experiments.

Another issue to be considered when detailed planning of a site exploration programme is initiated is the specification of the efforts required for preparation of the experimental location (e.g. drilling of boreholes, blasting of niches, treatment of the tunnel wall). From this perspective, the tunnel near-field investigations can be grouped into categories related to their exposure:

- investigations at the tunnel surface,
- investigations in underground boreholes,
- laboratory tests with drillcore samples.

Both aspects - subdivision of the exploration procedure into phases and the test location - are important criteria for selection of the appropriate exploration techniques.

3.2 Equipment and methodology developments - overview

As part of the Tunnel Near-Field Programme, various equipment developments have been accomplished in terms of geological, hydrogeological and rock mechanical characterisation of the tunnel near-field in underground facilities. In Table 3.1 an overview of these developments is given, describing the expected deliverables of the methods, addressing the suggested framework of application and specifying the required experimental environment. The methods are described in more detail in sections 3.2.1 – 3.2.9.

Table 3.1: Overview of methodology developments in GTS Phase IV

Methodology	Purpose / deliverables	Exposure	Exploration Phase
I. Surface packer	<ul style="list-style-type: none"> - Trace length of water conducting features (WCF) - Transmissivity and gas entry pressure of WCF (incl. variability along WCF) - Hydraulic conductivity of matrix 	Tunnel surface	Test phase
II. Short interval packer / combined packer system	<ul style="list-style-type: none"> - See above - Conductivity profiling in the tunnel near-field - Transmissivity and gas entry pressure of WCF 	Short boreholes in the tunnel near-field	Test phase
III. MMPS system	<ul style="list-style-type: none"> - Conductivity profiling in the tunnel near-field - Transmissivity and gas entry pressure of WCF - Long-term monitoring of hydraulic head 	Short boreholes	Test phase & long-term monitoring
IV. Slim Hole Piezometer Systems	<ul style="list-style-type: none"> - Long-term monitoring of hydraulic head - Gas entry pressure of matrix 	Short boreholes	Long-term monitoring
V. Time-Domain Reflectometer	<ul style="list-style-type: none"> - Location of inflow points in boreholes - Water content profiles in matrix 	Short boreholes	Test phase & long-term monitoring
VI. Thermography	<ul style="list-style-type: none"> - Mapping of inflow points towards the tunnel 	Tunnel surface	Excavation phase, test phase
VII. Geoelectric surveys	<ul style="list-style-type: none"> - Spatial distribution of water content in 3D (matrix zones) 	Tunnel surface	Test phase
VIII. Mini-Sonic Probe	<ul style="list-style-type: none"> - Location of WCFs in boreholes - Determination of the extent of the EDZ - Determination of phase conditions in WCF 	Tunnel surface, short boreholes	Test phase
IX. Core sampling of shear zone material	<ul style="list-style-type: none"> - Test samples of brittle structures for laboratory investigations (structural, hydraulic, two-phase flow, rock mechanical) 	Short boreholes	Test phase

3.2.1 Surface packer

Excavation-induced fractures may enhance the local hydraulic conductivity in the immediate vicinity of the tunnel by orders of magnitude. However, it is the hydraulic connectivity of the induced and pre-existing fractures which essentially determines the effects of the EDZ on groundwater flow. The BGR surface packer system (LIEDTKE et al. 1999) was developed to characterise the hydraulic connectivity of fracture networks in the tunnel near-field and to determine the transmissivity distribution along excavation

induced / natural fractures which intersect the tunnel (internal heterogeneity of fracture zones).

The device consists of a metal cylinder (130 mm in diameter) closed at one end and pressed against a metal ring attached to the tunnel wall (Figure 3.1) or, when used in the laboratory, to a test sample. An overview of the technical specifications of the system is given in Table 3.2. To ensure a good seal, there is an O-ring between the cylinder and the metal ring, which is bonded to the rock with a two-component adhesive. The packer has ports for the injection line and for temperature and pressure gauges.

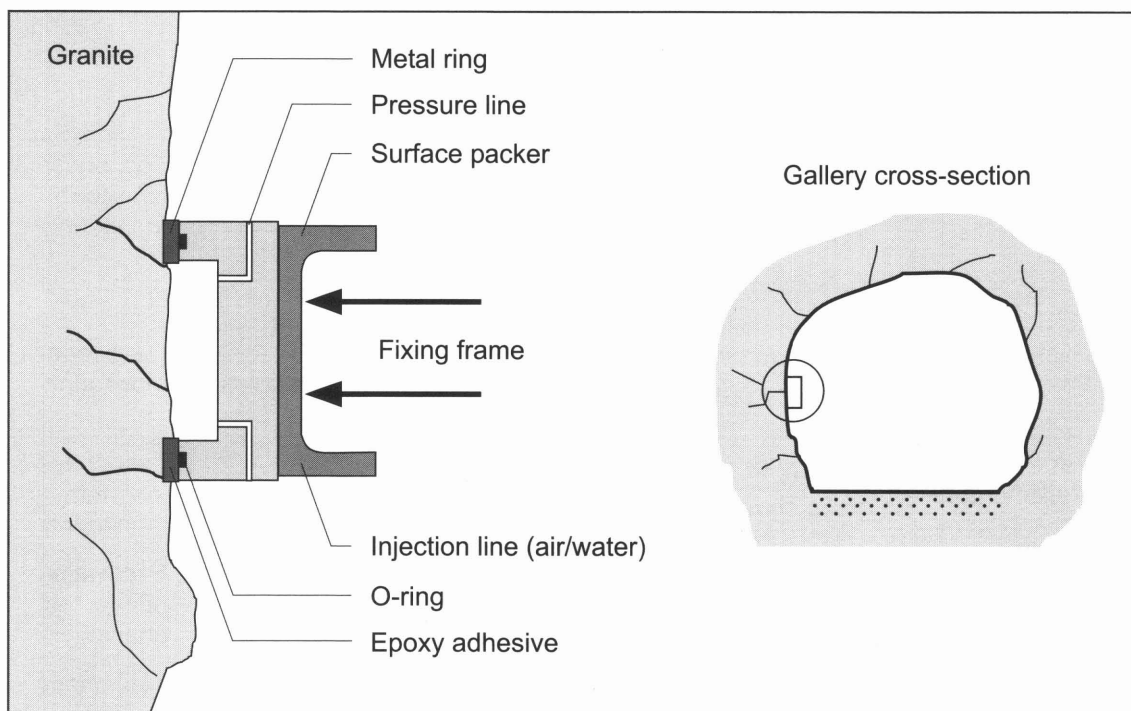


Fig. 3.1: Surface packer system, side view

The surface packer system was tested extensively at the GTS in the galleries of the BK site. In a tunnel section which had been geologically mapped, the surface packer was installed subsequently at various locations on the tunnel surface. After installation, gas is injected through the packer into the rock. Injection pressures up to 15 bar were applied. The injected gas propagated through the fracture systems of the tunnel near-field. Locations where the gas flowed into the tunnel were detected by applying a special leak spray to the tunnel surface. The gas inflow locations were marked on a geological map. The further test procedure consisted of a water injection sequence, followed by another gas injection phase. This procedure permits both single-phase flow of gas and water and two-phase flow to be examined. The flow experiments were simulated using numerical models. An iterative procedure was used to calculate the hydraulic properties of the test zone.

In addition to the tests at the GTS, the surface packer system has been applied in the laboratory to determine the permeability of rock samples. The device was applicable for permeabilities as low as $E-21 \text{ m}^2$ (LIEDTKE et al. 1999).

Table 3.2: Specifications of the BGR packer systems: surface packer (cf. Figure 3.1) / combined packer system (cf. Figure 3.2)

	Surface packer	Combined packer system
Packers	Metallic injection cell	Surface packer + 2 mechanical packers
Interval length	(Diameter: 130 mm)	Test interval I2: 100 mm Intervals I1 & I3: variable length
Interval volume	< 0.2 l	Test interval I2: < 0.6 l
Diameter of the BH	-	86 mm
Max. working pressure	20 bar	20 bar
Max. injected flow rate	10 l/min	10 l/min
Test fluids	Water / gas	Water /gas

3.2.2 Combined short interval packer system

Profiling of hydraulic properties along radial boreholes is a key requirement for any EDZ investigation programme. The combined short interval packer system developed by BGR (LIEDTKE et al. 1999) is aimed at determining continuous profiles of hydraulic conductivity starting immediately at the tunnel surface (Figure 3.2 / Table 3.2). The tool consists of a short interval double packer system combined with the above-described surface packer system. The double packer consists of two rubber sleeves with a diameter of 82 mm mounted on a steel tube. The test interval (interval 2) between the two rubber sleeves is 100 mm long and the packer length is 85 mm. The packers are inflated hydraulically by an inflation line. Two control lines for water injection and pressure monitoring, respectively, are passed through the steel tube into the test interval. A third control line is connected to the bottom hole interval (interval 3). The steel tube of the double packer system is passed through the surface packer and sealed with O-rings. This allows positioning of the test interval at any location of the borehole between 0.1 and 1.5 m along hole and monitoring of pressure response in the adjacent intervals (interval 1 and 3). The upper interval (interval 1) can also be used for water injection tests.

The combined short interval packer system was used to determine profiles of hydraulic conductivity along radial boreholes at the ZPK / BK site of the GTS. Characterisation of the EDZ (cf. chapter 5) was carried out with water and gas. Numerical models were used to analyse the hydrotests performed.

3.2.3 Modular mini packer system (MMPS)

The modular mini packer system (MMPS) was developed for detailed hydraulic characterisation of the EDZ around tunnels (FRIEG & BLASER 1999). A modular test assembly was designed that allows up to 6 individual packer modules to be coupled in a variety of configurations. The standard configuration consists of a series of 5 packer modules with 100 mm packer length and a test interval of 100 mm between the packer seals, followed by a 1 m guard packer (Fig. 3.3). Each packer module is a stand-alone unit with a packer inflation line and two control lines (Fig. 3.3). The diameter of the de-

flated packers is 48 mm, the maximum working diameter of the 100 mm packer elements is approximately 55 mm. The maximum working pressure (i.e. interval pressure) is 15 bar. The water injection / withdrawal rates are limited to about 50 ml/min. The total test interval volume is 45 ml and test system compressibility stabilises at a value of $7E-8 \text{ Pa}^{-1}$ at inflation pressures above 10 bar.

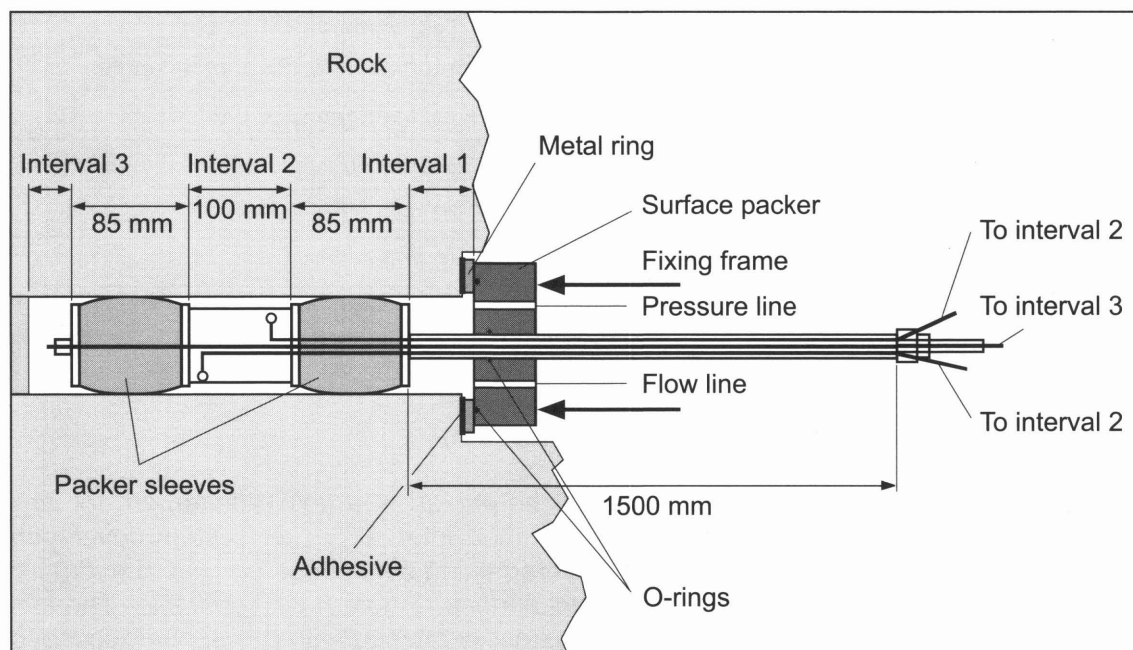


Fig. 3.2: Combined installation of short interval packer and surface packer

The MMPS is aimed at determining profiles of hydraulic head and hydraulic conductivity along radial boreholes around tunnels. In each test interval, hydrotests can be performed, consisting of any sequence of test events (constant rate, constant head, slug, pulse). In addition, the response in the adjacent intervals to a pressure disturbance in the test interval can be observed. For the purpose of characterising the hydraulic connectivity along the EDZ in the axial direction, hydraulic crosshole tests can be designed by inserting additional MMPS systems in nearby boreholes.

The MMPS has been applied successfully in the fractured hard rock environment at the GTS as well as in the Opalinus Clay at the Mont Terri Rock Laboratory. As part of the EDZ experiment at the GTS, the hydraulic conductivity profiles determined with the MMPS were used to condition fracture network models of the tunnel near-field.

3.2.4 Slim hole piezometer systems

As part of the ZPM experiment, small-diameter piezometers were designed by GRS for hydraulic head measurements in the unsaturated zone of the tunnel near-field. The piezometers had to meet the following requirements: (i) diameter of the piezometer boreholes less than 20 mm to minimise disturbances of the pore pressure distribution by the presence of the boreholes, (ii) small monitoring intervals to ensure quick equilibration of the measured pressures to changing pressure and saturation conditions in the low permeability rock matrix of the tunnel near-field and, finally, (iii) no metallic

material in the piezometer boreholes which might disturb the geoelectric measurements applied for monitoring the water content distribution in the tunnel near-field. The piezometers were not only used for monitoring the pore water pressure in the tunnel near-field but also to determine hydraulic and two-phase flow properties of the low permeability rock matrix on the small scale.

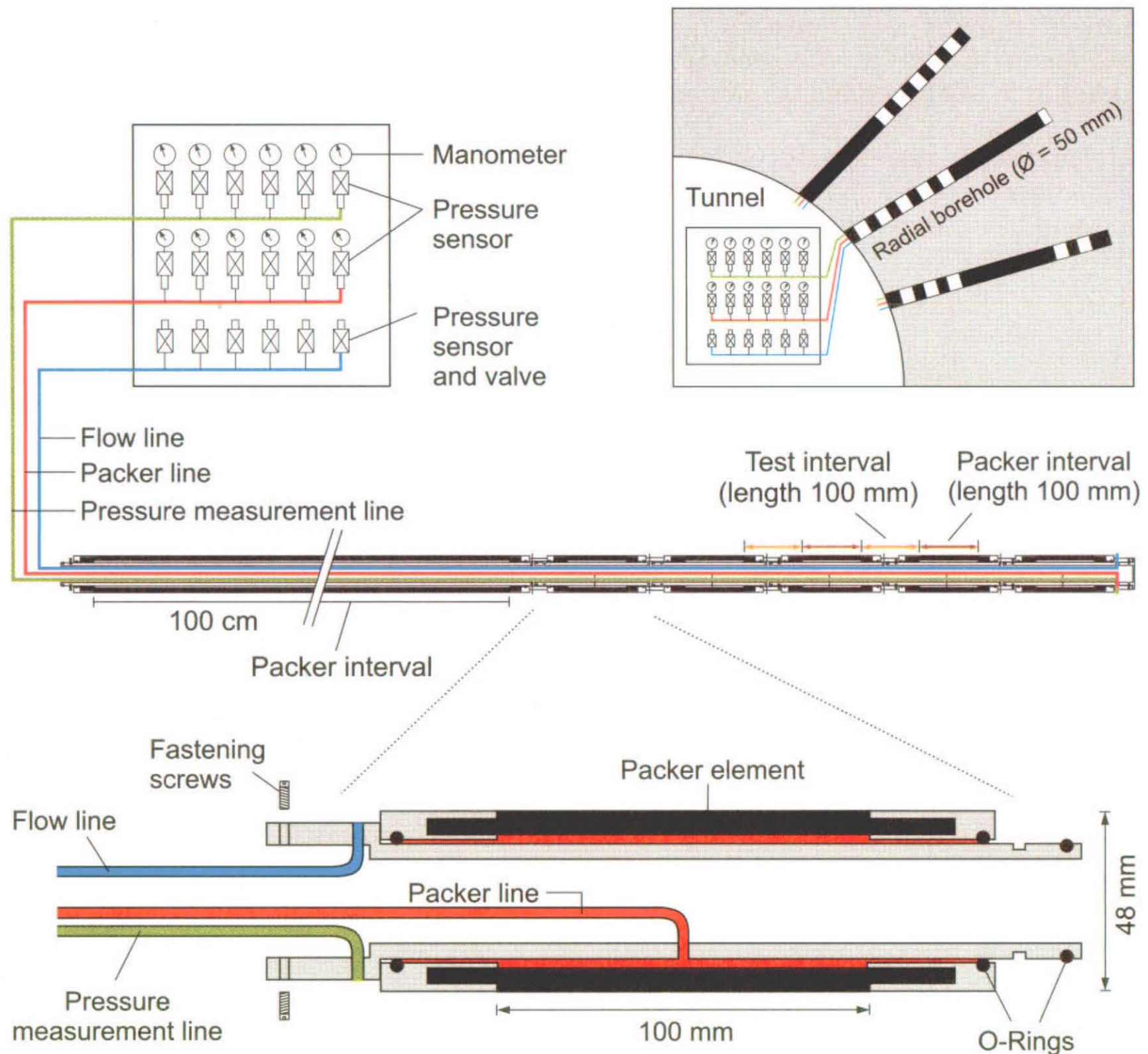


Fig. 3.3: The modular minipacker system (MMPS)

The slim hole piezometer system (Figure 3.4) consists of a non-metallic mechanical minipacker system (length of the rubber sleeves 10 mm, diameter 15 mm) and, at the bottom end of the borehole, a small cavity (length $< 10 \text{ mm}$) for pore pressure measurements. Two control lines for water / gas injection and pressure monitoring (inner diameter 3 and 1 mm) are passed through the minipacker system. The upper part of the piezometer borehole on top of the minipacker system is sealed with a water activated resin. The piezometer is equipped with a pressure transducer, an injection manifold for active testing and a data acquisition system outside the borehole. Slim hole piezometers with a maximum length of 2.5 m were installed at the GTS.

At the GTS, pore pressure measurements with slim hole piezometers were carried out in a tunnel section of the VE drift characterised by low density fracturing. Investigations were focused on groundwater flow processes in the unsaturated zone of the tunnel near-field. Long-term pressure transients were monitored. They were correlated with operational activities at the GTS and aperiodic events such as changes of the ventilation rate. The results indicate that pore pressure changes in matrix areas depend on tunnel ventilation. Capillary forces lead to sub-atmospheric pressure zones. The desaturation of the rock, however, is limited to the first centimetres to decimetres behind the tunnel surface (cf. chapter 4). Gas entry pressures were determined as well as changes in effective transmissivities.

A slim hole piezometer configuration was recently installed as part of a two-phase flow experiment at the Äspö HRL. The layout and the instrumentation concept used to determine long-term hydraulic pressure effects in matrix and fracture zones are similar to those at the GTS.

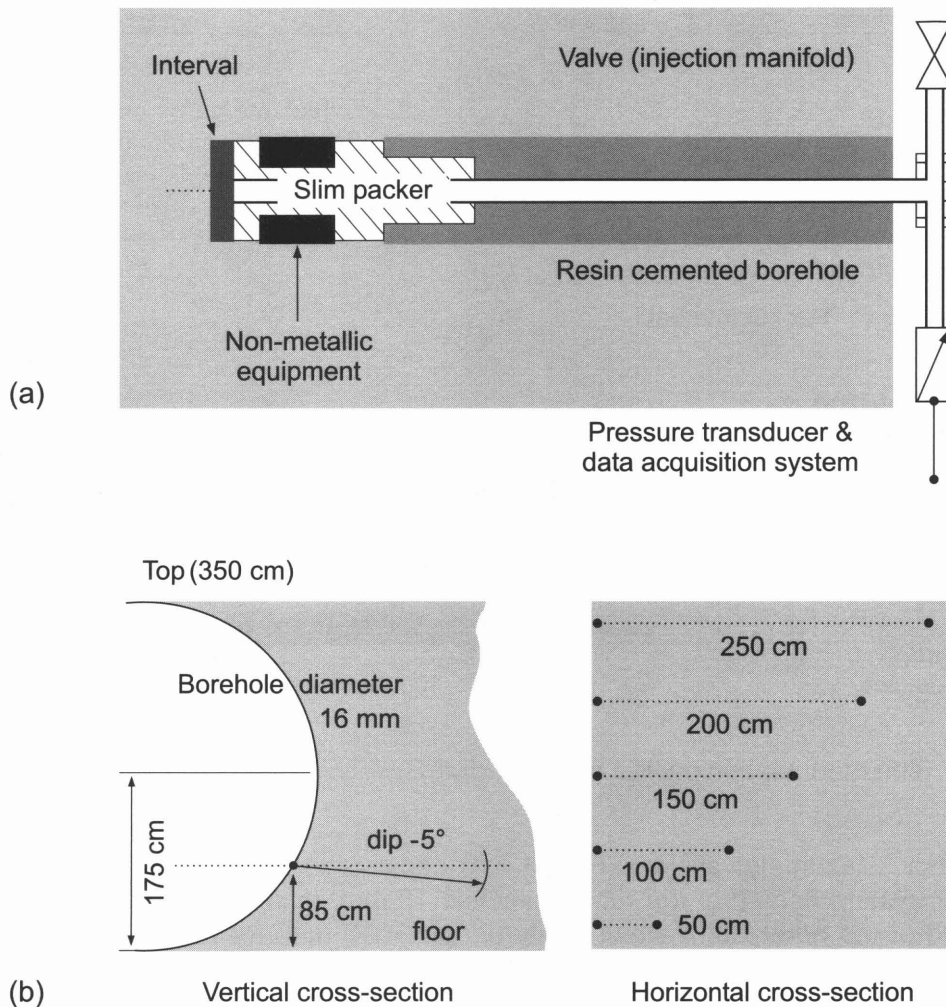


Fig. 3.4: Slim hole piezometer system: (a) schematic and (b) test configuration at the ZPM site

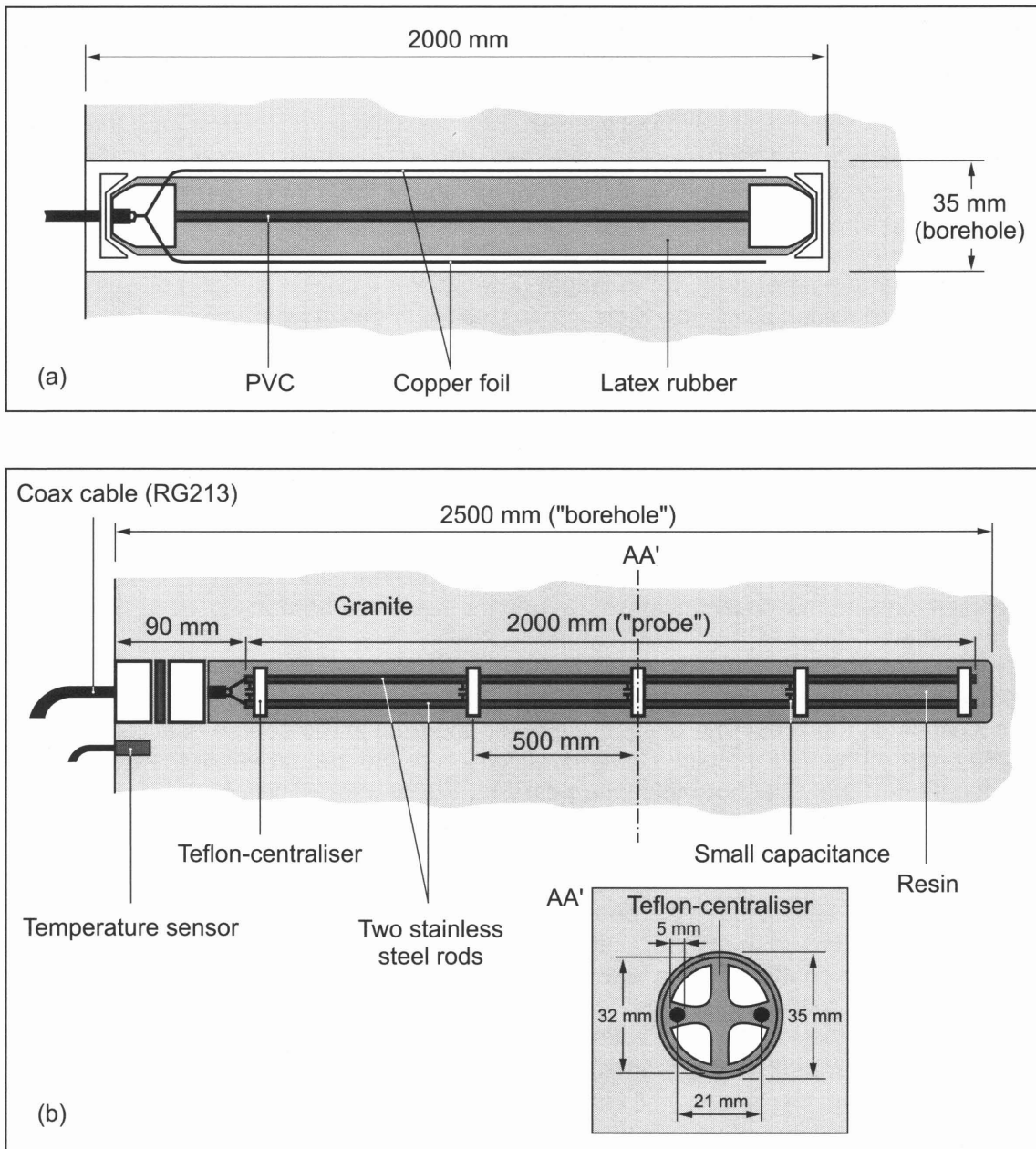


Fig. 3.5: TDR probes for water content measurements in boreholes, (a) packer TDR and (b) permanent TDR installation

3.2.5 Time domain reflectometry (TDR)

Time-domain reflectometry is a well-known technique for determining water content in unconsolidated soils which exhibit a high porosity (typically > 10%). The TDR measuring system consists of an electromagnetic pulse generator and a waveguide system (measuring probe), emplaced in the soil material. The propagation velocity of the pulse depends critically on water content of the soil and can be measured with high accuracy. During previous investigation phases at the GTS, Nagra developed novel TDR systems which can determine the water content in rocks with porosities as low as 0.1% (FRIEG & VOMVORIS 1994). A further extension of the TDR methodology was developed as

part of the TPF experiment (MARSCHALL & CROISÉ 1999): a single-rod TDR probe was designed which allows determination of the profiles of water content along a borehole. This feature is of key importance in localising the hydraulically active part of water-conducting features in fractured media.

Two different types of TDR probes were developed: (i) a mobile packer TDR system which is aimed at determining water content profiles in the course of a hydro / gas test (Figure 3.5a) and (ii) a permanent TDR probe which is used for long-term monitoring of water content profiles (Fig. 3.5b). The packer TDR probe consists of a pneumatic packer, 33 mm in diameter and 2 m in length. The packer element is made of a latex rubber, which is a material with low dielectric losses. Two thin copper foils are fixed on the opposite sides of the rubber along the packer element, acting as a waveguide for high frequency electromagnetic signals. The packer can be inflated to a maximum pressure of 10 bar.

The permanent TDR probe consists of two parallel steel rods with a total length of 2 m, fixed by centraliser elements. The diameter of the centralisers is 32 mm. Small capacitors are fixed between the two steel rods at a spacing of 0.5 m. These capacitors act as markers which simplify the interpretation of the TDR reflectograms. The TDR probe is inserted into a 35 mm borehole. After installation, the borehole is filled with a special resin with low dielectric losses. When the resin has hardened, the TDR is ready for operation.

Both systems, the mobile packer TDR and the permanent probe, have been tested successfully at the GTS. The packer TDR was operated in the course of a gas injection test as part of the TPF project. Clear identification of the first arrival of the gas front at the location of the TDR borehole was possible. Furthermore, the zones of preferential gas flow could be distinguished. The packer TDR probe is still under development; in particular the robustness under field conditions will be improved.

The permanent TDR probe has been tested at the FEBEX site (MARSCHALL et al. 1996). It is being used to monitor potential changes in water content in the tunnel near-field. Only minor changes in the water content have been observed during the last two years; the TDR system worked reliably and without any drifting of data. With both types of TDR probes, the resolution in water content is in the range of 0.2% (note: porosity of the granodiorite matrix $\approx 1\%$, fault gouge porosity 10 - 30 %; cf. chapter 4). The spatial resolution is in the cm range (2 - 5 cm).

3.2.6 Thermography

The infrared radiation scanning method can be used to determine the surface temperature of a rock body with high accuracy at almost any scale. Temperature differences at the tunnel surface are measured when cooling effects, caused by evaporation and water flow in fractures, change the normal background temperature of the rock mass. Water-bearing structures can be detected in dry rock masses. The thermography technique is applicable for mapping water-bearing structures in tunnels, caverns, shafts, faults and geotechnical barriers. As part of the ZPM experiment (KULL et al. 1999), the efficiency of this technique for characterisation was tested.

The temperature distribution of underground objects is scanned areawise using a mobile AGEMA Thermovision 900 including a lithium-detector scanner and a controller unit with OS9 data processing software (cf. Figure 3.6 a). A PC-unit and a videoprinter are used for visualisation of data in the field. Size of area and data resolution depend

on the distance between system and object. With respect to temperature information, areas of 1 to 4 m² are preferred. By changing the position of the system, measurements are adapted to local requirements, e.g. geometry of the tunnel surface or orientation of structures. During data processing raw data are filtered, boundary effects are corrected and temperature anomalies are located. The actual temperature distribution is documented as a coloured print. Further information can be obtained by scanning areas of interest in spot, profile and area measurements (Figure 3.6 b). Using statistical means such as histograms and isotherms, changes in the temperature distribution are quantified.

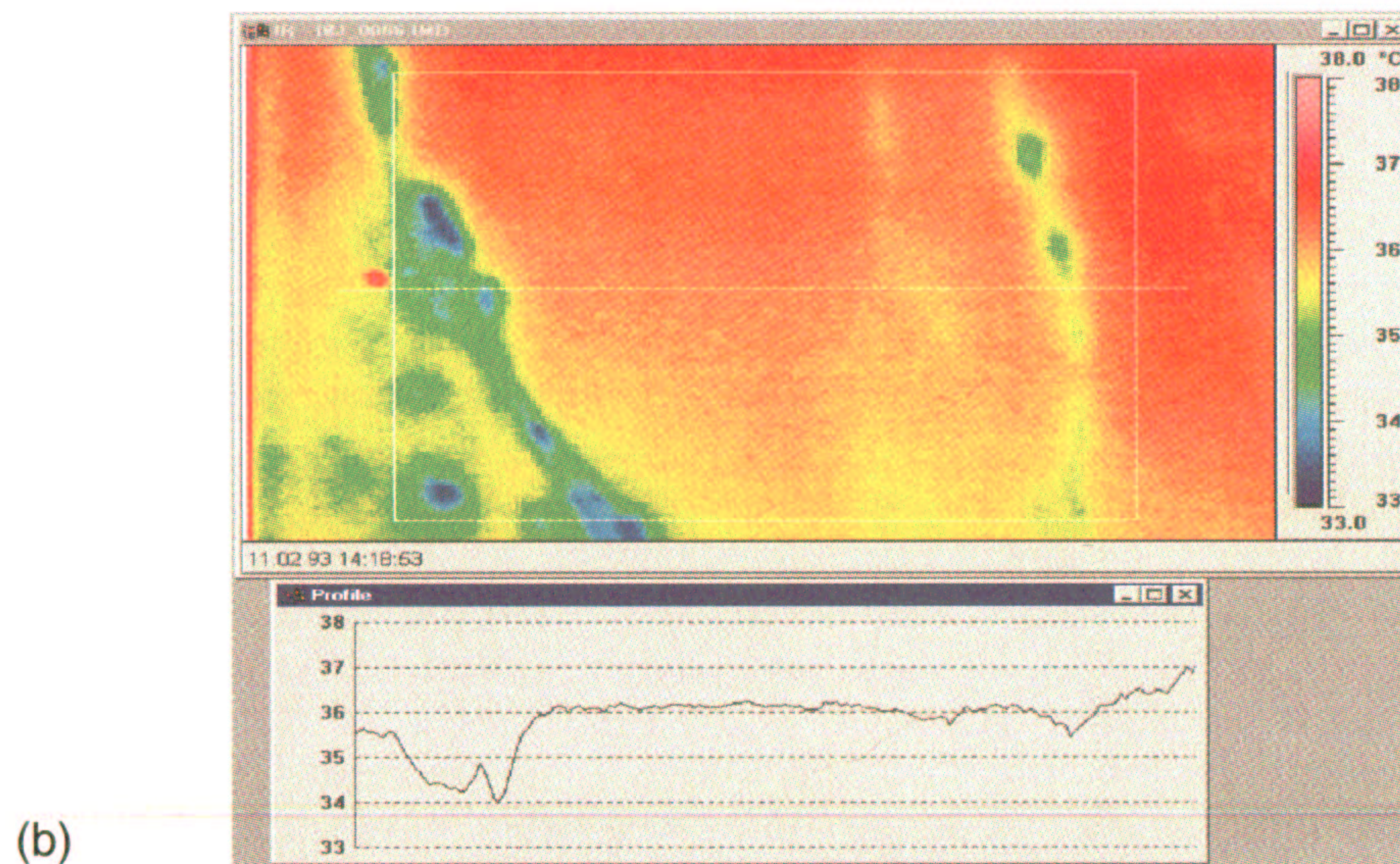
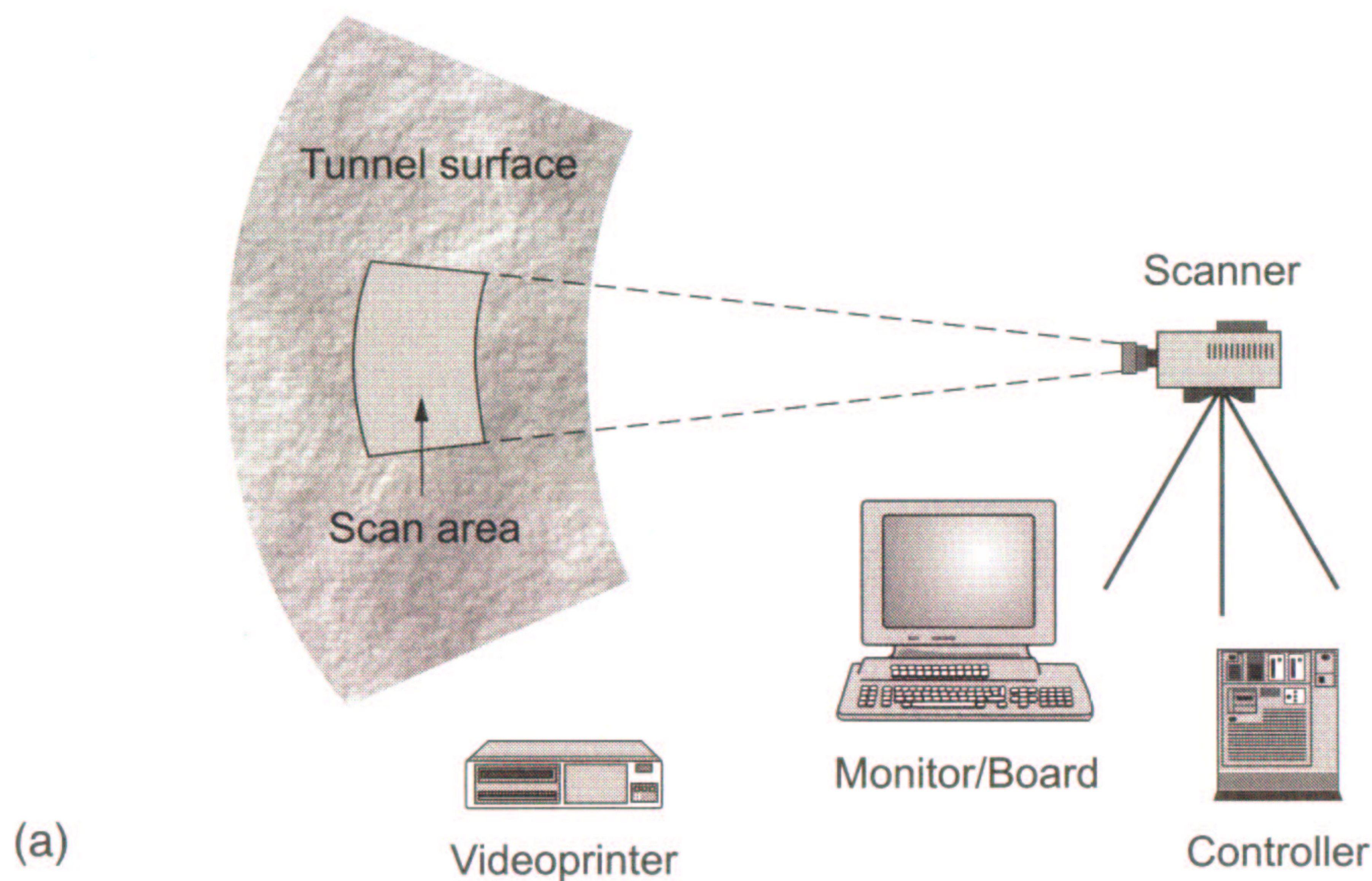


Fig. 3.6: Thermography system: (a) test set-up and (b) temperature distribution at the tunnel surface at the ZPM site

At the GTS, thermography measurements were applied to locate fractures in homogeneous matrix areas of the VE drift. Aerial temperature distribution was measured for different ventilation conditions (low and high relative humidity), when cooling effects, caused by water evaporation and water flow in fractures, change the environmental surface temperature. Most areas had a uniform temperature, although they were fractured, indicating that most of these joints are created by excavation. In the ventilation chamber, which is located in the dead end section of the VE drift, several traces of water-conducting features could be correlated with thermal anomalies.

The method was applied at the Äspö HRL/Sweden (crystalline rock) and the Tournemire Tunnel/France (clay formation) to identify water-bearing structures. Ventilation and high relative humidity of the atmosphere influence the resolution of the data. Hence, the tunnel surfaces were found to be homogeneous with respect to rock temperature.

3.2.7 DC geoelectric surveys

Desaturation of the tunnel near-field caused by ventilation affects the flow and transport properties of the near-field rock body. DC geoelectric surveys are suitable for determining changes in the water content due to desaturation, because the effective electrical resistivity of a rock mass is dependent not only on its porosity but also on the actual water saturation and the electrical resistivity of the porewater. An empirical formula for the effective resistivity of rock is given by Archie's equation. In a crystalline rock, the total porosity of the rock matrix is typically as low as 1 – 2 %. The purpose of the DC geoelectric surveys as part of the ZPM experiment was to show that resistivity measurements are suitable for determining in 3D the variations in water content due to saturation / desaturation effects, even for low permeability formations (KULL et al. 1999).

The methodology of DC geoelectric surveys for determining the 3D distribution of water content in the tunnel near-field includes field measurements, laboratory calibrations and modelling of the field data. Field measurements consist of long-term monitoring of the resistivity distribution in the rock mass during a well-defined ventilation sequence, using a multi-electrode array. The electrodes are located at the tunnel surface and in special small-diameter boreholes, respectively. The design of the electrode arrays depends on the size of the investigated rock volume. In order to relate the electrical rock resistivity to the water saturation, laboratory calibrations are required. For this purpose, small rock samples of about 30 mm length and 20 mm diameter are saturated in discrete steps and the corresponding saturation for each step is related to the electrical resistivity (cf. Figure 3.7). For constructing the calibration curve, additional pore properties such as porewater and surface resistivity, porosity and further empirical parameters are required. Based on the field data, the so-called measured apparent resistivities have to be converted to model calculated resistivity distributions.

The configuration of the geoelectric surveys applied within the framework of the ZPM experiment is shown in Fig. 4.11. Resistivities were monitored during desaturation and saturation phases. A significant difference in the results was not determined for the desaturation phase, either for the surface electrodes or for the borehole measurements (cf. section 4.4). During the wetting phase there were noticeable, ambiguous resistivity variations in the surface measurements. These can be attributed to pure surface effects caused by electrical charges irregularly distributed on the surface.

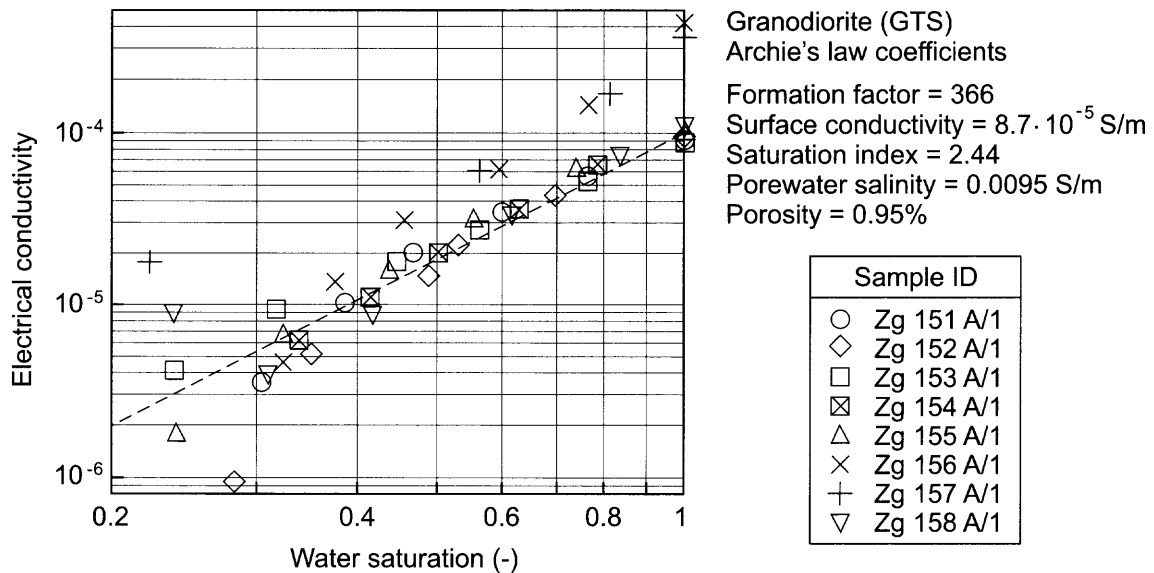


Fig. 3.7: Calibration curves for DC resistivity measurements. Electrical conductivity of a total of eight core samples (Central Aare granite) is measured as a function of water saturation

Before applying the method in the crystalline rock at GTS, geoelectric measurements had successfully been performed in several salt mines in Germany. Similar measurements are being carried out at the Äspö HRL, Sweden. Recently, testing of the method started in clay in the Tournemire underground laboratory, France.

3.2.8 Mini sonic probe

The mechanical properties of the wallrock in the tunnel near-field can be altered by increased fracture density due to the excavation process and / or by formation of an unsaturated zone due to ventilation of the tunnel. Seismic techniques provide a suitable tool for characterising the extent of alteration, because both phenomena result in significant reduction of the seismic velocity of the wallrock. A seismic borehole probe, called the mini sonic probe, was developed and tested as part of the ZPK experiment (LIEDTKE et al. 1999), aimed at detailed characterisation of the excavation disturbed zone and the unsaturated zone.

The mini sonic probe (Fig. 3.8a) is applicable in boreholes with a diameter of approx. 86 mm. It consists of a seismic source and two receiver stations 100 mm apart, each fitted with two accelerometers. At each station, one piezoelectric accelerometer is fixed by screws in a vertical position inside a half-open metal block, whilst another is screwed in a horizontal position onto the other side of the same metal block. The accelerometers have a frequency range of up to 20 kHz and a sensitivity of 100mV/g. Coupling of the metal block to the borehole wall is achieved by means of a pneumatic cylinder. This provides a strong repeatable surface pressure (6-8 bar). The maximum extension of the cylinder, and thus the acceptable variability of the borehole diameter, is approximately 10 mm.

The seismic sources for interval measurements are small, pneumatically operated hammers. The vertically positioned hammer strikes the borehole wall directly whilst the horizontally mounted hammer strikes a metal block (Figure 3.8a). This metal block is

also pneumatically coupled to the borehole wall. In addition, an alternative seismic source was developed to generate either S-waves or P-waves.

The mini sonic probe can be operated in three different modes. Interval velocities along the borehole are measured by excitation of seismic pulses with the internal seismic source. Average velocities are determined by generating the seismic signal with a pendulum hammer at the borehole mouth and measuring the travel times between source and downhole receivers. Finally, crosshole measurements between two (parallel) boreholes are performed by generating the signals with a piezoelectric transmitter. Crosshole measurements are not only aimed at determining radial velocity profiles but also at detecting velocity anisotropy.

Downhole and interval velocity measurements carried out at the GTS revealed considerable P-wave velocity reductions in horizontal and 45° upwards inclined boreholes in the tunnel near-field (<0.5 m). This velocity reduction is primarily attributable to the desaturation of the rock in the tunnel near-field zone. The velocity reduction disappeared after resaturation of the rock. Only the velocity of S-waves - which are unaffected by the phase conditions along the fractures - still showed a reduction in the tunnel near-field.

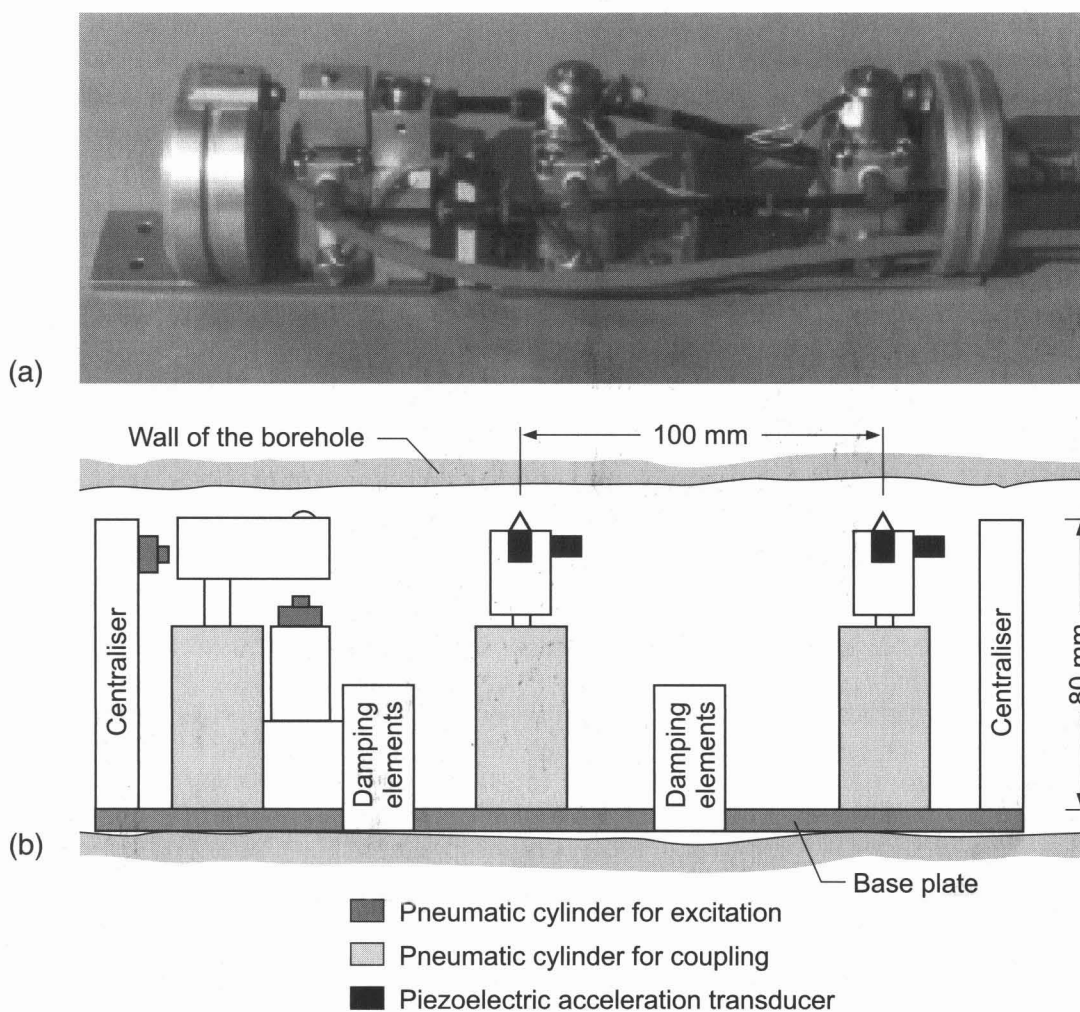


Fig. 3.8: The mini sonic probe: (a) photograph of the probe and (b) principle sketch

The observed P-wave velocity reduction cannot be solely attributed to desaturation: some of the reduction is also due to disturbance of the rock. This aspect is, however, masked by the resaturation of the rock with water. Therefore, the S-waves gain in importance when determining the excavation disturbed zone in water-saturated crystalline rock.

The mini sonic probe was tested successfully at the Mont Terri Laboratory (clay formation), as well as at the Äspö HRL (crystalline rock). At Mont Terri, the interval velocity measurements revealed the first 0.4 – 0.5 m as a zone where seismic energy is highly attenuated and P- and S-wave velocities are considerably reduced. At the Äspö HRL, reduced velocities could be observed only within the first 5 – 10 cm, measured from the borehole mouth (EMSLEY et al. 1997).

3.2.9 Sampling of shear zone cores

During underground site investigations, laboratory experiments with drillcore material are a well-established method for determining the hydraulic and two-phase properties of the host rock formation. In a fractured rock, where groundwater flow takes places in discrete features such as fractures and shear zones, the low cohesion of the brittle structures and the risk of washing out the fault gouge material complicates the recovery of good core samples considerably. Previous core drilling campaigns at the GTS showed that traditional techniques fail in providing shear zone core samples for quantitative permeability measurements. Motivated by the lack of suitable core drilling techniques, a refined overcoring technique was developed within the framework of the TPF experiment (MARSCHALL & CROISÉ 1999), aimed at minimising damage of the shear zone sample. The technique consists of four steps: (i) a borehole parallel to the fault gouge horizon is drilled with single core drilling equipment, (ii) the annulus of this borehole is filled with a resin, (iii) the inner core, protected by the resin coating, is overcored, and, finally, (iv) the outer core is removed from the wallrock (Figure 3.9).

With the above mentioned sampling technique, cores have been recovered with a typical length of 0.3 - 0.5 m. The diameter of the inner core was 86 mm. About 30% of the cores recovered by this technique could be used for quantitative laboratory experiments (gas permeability, porosity, capillary pressure); the remainder was disturbed by intrusion of the drilling fluid.

3.3 Equipment and methodology developments

Within the framework of the synthesis procedure (cf. Figure 2.1), the field data largely feed into the development of structural and process models of the tunnel near-field. The field data can be divided into the following categories, respecting the disciplines of field investigations:

- Geological data as input for a detailed structural model.
- Hydrogeological data, characterising the hydraulic and two-phase flow properties of the different fracture families and of the matrix.
- Rock mechanical data as input for coupled hydromechanical models of the EDZ.

In addition, mineralogical data may be needed to some extent for classification of the water conducting features. Table 3.3 gives an overview of the specific deliverables expected from the field investigations.

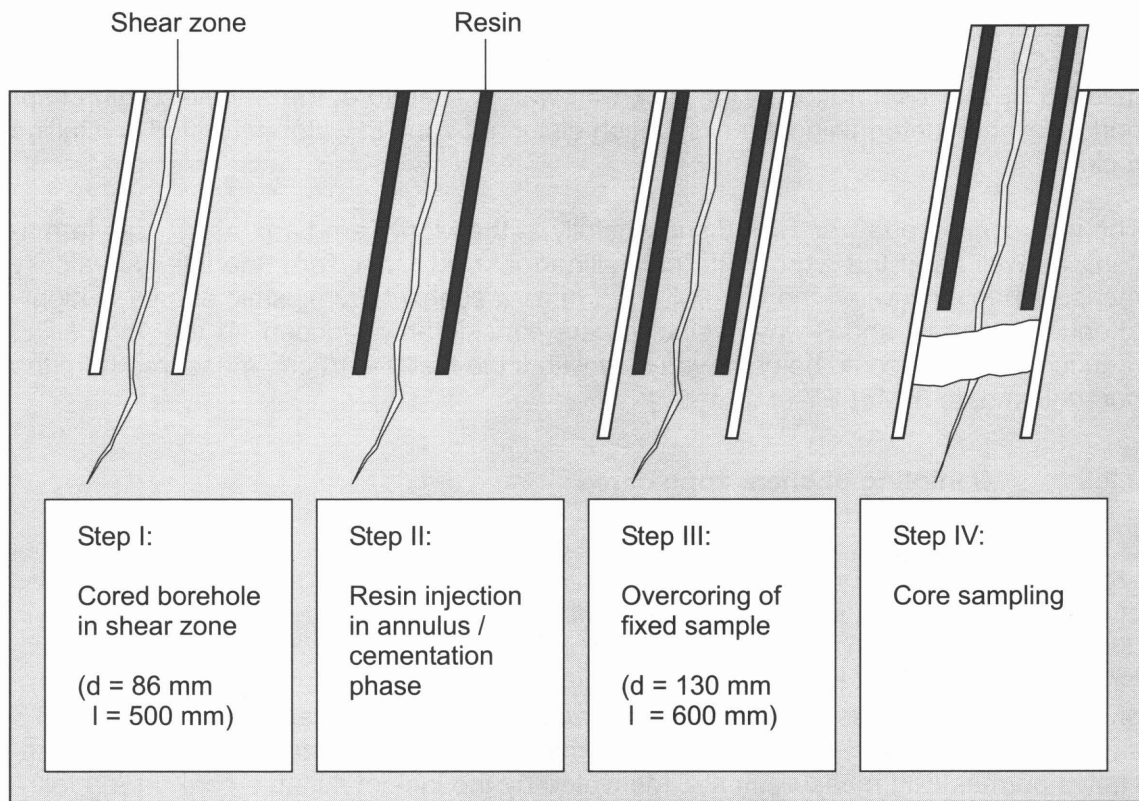


Fig. 3.9: Recovery of undisturbed shear zone core samples

Table 3.3: Field data and expected deliverables from tunnel near-field investigations

Field data	Deliverables for near-field conceptual models
Geological / mineralogical data	<ul style="list-style-type: none"> - identification and classification of main structural elements (natural and excavation-induced fractures, matrix zones) - structural properties of water-conducting features (orientation, spatial frequency, size, porosity, pore size distribution) - structural properties of matrix (cleavage intensity, porosity, pore size distribution)
Hydrogeological data	<ul style="list-style-type: none"> - transmissivity distribution of water-conducting features (mean values, variability, correlation length) - hydraulic conductivity of the matrix - hydraulic boundary conditions at the tunnel surface and state conditions (inflow to the tunnel, head distribution and phase conditions in the near-field) - two-phase flow properties of water-conducting features and matrix
Rock mechanical data	<ul style="list-style-type: none"> - elastic moduli and strength of matrix - residual strength of brittle structures - local measurements of stress tensor

The equipment and methodology developments in the Tunnel Near-Field Programme were focused on structural and hydrogeological characterisation of natural and excavation-induced fracture systems. Particular emphasis was given to determination of the connectivity of the fracture systems and of small-scale variability of the hydraulic properties. These data are required for conditioning hydraulic fracture network models (gas migration models, axial flow models; cf. sections 4.3 and 5.3).

When groundwater flow is simulated with stochastic fracture network models, critical input parameters are the fracture size and the internal variability of hydraulic properties along the fractures ("channeling factor", cf. NAGRA 1997). These parameters determine the effective hydraulic conductivity of the composite system of fractures. In particular, when the average fracture size (sometimes expressed by the average fracture area or the average number of intersections with other fractures) approaches the so-called percolation threshold of the fracture network, small changes in fracture size may change the effective hydraulic conductivity of the network by orders of magnitude (CHILÈS & DE MARSILY 1993). Sensitivity analyses of the influence of fracture size and internal variability of hydraulic properties on the average hydraulic conductivity of fracture networks were conducted as part of the Wellenberg Geosynthesis (NAGRA 1997).

The surface packer and the thermography equipment provide new tools for structural mapping of fracture networks at the tunnel surface. These fracture maps form the basis for the estimation of fracture sizes and fracture connectivity. Thermography is used for imaging the traces of water-conducting features at the tunnel surface. The method allows quick working progress and is therefore suitable for establishing a systematic inventory of water conducting features during the tunnel excavation phase. Spatial variability of temperature along the fracture traces may be a measure of the variability of fracture transmissivity. As part of a prestudy for the planned underground investigations at the Wellenberg site, Nagra has tested the method under real excavation conditions. The tests showed that the field equipment has achieved a high degree of maturity; the method was applicable under the severe conditions during the tunnel excavation phase. The interpretation of the results, however, is sometimes ambiguous due to a variety of possible disturbances (anchoring of the tunnel surface, drip points, tunnel ventilation). Thus, future developments should focus on the processing and interpretation of thermographic images, such that these data can be applied as quantitative input for fracture network models. An important requirement for successful interpretation of thermographic data is a detailed geological map of the tunnel surface.

The surface packer, combined with the leak spray method, proved an excellent technique for detailed mapping of fracture traces at the tunnel surface. The method allows determination of the geometry of the fracture traces and estimation of fracture connectivity. In addition, the transmissivity distribution along the fractures can be estimated in a semiquantitative-way. The observed transmissivity distribution is a measure of the internal heterogeneity of the water conducting features and can be expressed in terms of a variability and a correlation length as input for stochastic fracture network models.

The mini sonic probe was successfully applied to delimit the extent of the excavation disturbed zone around the tunnels. Major fractures could be identified. The method provides a reliable tool for fast surveying of the damaged zone during the tunnel excavation phase or, during a test phase, for mapping of structural and rock mechanical properties in greater detail.

Finally, the novel core sampling technique for recovery of low-cohesion cores from fracture zones opens a new field for laboratory investigations. The laboratory tests include quantitative microstructural analyses (porosities, pore size distributions, spatial correlation length), hydraulic column experiments (intrinsic permeability, two-phase flow parameters, transport parameters) and rock mechanical tests (elastic moduli, strength) of brittle structures.

The combined short interval packer and the MMPS are suitable for detailed profiling of interval transmissivity along boreholes with a spatial resolution in the decimetre range. By combined interpretation of the interval transmissivities with core logs or borehole imaging data, the transmissivities can be assigned to the water-conducting features and matrix, respectively. Both systems, short interval packer and MMPS can be applied for hydraulic interference tests, allowing estimation of the fracture network connectivity or - in other words - for upscaling of local transmissivities to effective properties of the composite system.

In addition, the MMPS was designed for long-term monitoring of hydraulic head profiles in the excavation disturbed zone. The slim hole piezometer proved a reliable system for long-term monitoring of hydraulic head in matrix zones of the tunnel near-field. Due to the very low interval volume, the piezometer is extremely sensitive to changes in the ventilation conditions in the tunnel and is therefore well suited for head measurements within the framework of unsaturated zone experiments.

The TDR device allows determination of water content profiles along boreholes. With this tool, water-conducting features can be localised with a spatial resolution in the cm-range and water saturation of the fractures can be determined. In combination with gas threshold pressure tests, TDR measurements are recommended for determining two-phase flow properties of the tunnel near-field. The TDR system is also suitable for long-term monitoring of water content in the rock matrix during ventilation tests.

The DC geoelectric measurements were aimed at measuring desaturation effects in a matrix zone of the ZPM site. No desaturation was observed. In the light of the available data, an evaluation of the method is not reasonable.

3.4 Applicability of equipment developments to other rock formations

Most of the equipment developments within the Tunnel Near-Field Programme have also been tested in other rock formations. Of particular interest is the applicability of the methods in soft rock formations such as clay or salt. These formations are characterised by a more plastic behaviour and do not show the typical brittle structures that hard rock formations do. Thus, it cannot be assumed a priori that the new methods are applicable in such environments.

The MMPS and the mini sonic probe were used successfully at Mont Terri (Opalinus Clay) and can be regarded as standard tools for structural and hydraulic characterisation of the EDZ. At Mont Terri, both methods consistently indicated a damaged zone of about 0.5 - 1 m around the tunnel surface. The hydraulic properties were several orders of magnitude higher than for the undisturbed rock matrix (COTTOUR et al. 1999). Interval velocity measurements (mini sonic probe) revealed the first 0.4 - 0.5 m as a zone where seismic energy is highly attenuated and P- and S-wave velocities are considerably reduced (ALHEIT et al. 1999). At the Äspö Hard Rock Laboratory, as part of

the ZEDEX experiment (OLSSON et al. 1996), reduced velocities could be observed only within the first 50 - 100 mm.

The TDR device is in use at Mont Terri for determination of water content profiles in the unsaturated zone of the tunnel near-field and for in-situ monitoring of gas migration processes. Furthermore, laboratory experiments were conducted in which TDR systems were applied for monitoring the saturation process in a large core sample (FRIEG et al. 1999).

Thermography was applied at the Tournemire mine (clay formation) and at the Äspö Hard Rock Laboratory.

Finally, DC geoelectric measurements were carried out at the Äspö Hard Rock Laboratory. Compared to the Grimsel experiments, the surveys at Äspö were carried out on a larger scale (deca – hundred metre scale). The aim was to detect major water-conducting features. The preliminary results seem to be very encouraging and the experiments are being continued.

3.5 Comprehensive overview of field methods for tunnel near-field characterisation

The field methods for characterisation of the tunnel near-field are essentially a subset of the methods commonly used in site investigation programmes. Given that any underground site exploration programme will depend on a multitude of scientific and economic constraints, it is not reasonable to strictly adopt a given suite of field methods for characterisation of the tunnel near-field. A comprehensive overview of suitable exploration methods, with focus on the particular deliverables of the methods, may assist in planning an underground exploration programme. It is the purpose of this section to give an overview of exploration methods, recommended for the characterisation of the tunnel near-field.

In Table 3.5, an overview of recommended field methods is given. The survey is structured as follows:

- the particular purpose of the proposed methods is specified and is linked to the corresponding geoscientific disciplines (geology, hydrogeology, rock mechanics; cf. chapter 3.3),
- the methods are grouped with respect to the rock exposure required (tunnel surface, boreholes, core samples). This item represents an economic and time factor to be considered when planning the exploration procedure.

Each method is set in relation to the exploration phase (excavation phase, test phase, long-term monitoring phase; cf. chapter 2.2) where it is most successfully applied. Those field methods which have been applied during previous GTS investigation phases are marked in italics.

Table 3.5 does not represent a complete survey of field methods for geoscientific tunnel near-field characterisation. Instead, as part of an integrated approach for planning a site investigation programme, the table is regarded as a useful tool for preselection of the most appropriate field methods. The approach is steered by the needs of the data suppliers ("Geodata set", cf. Figure 2.1) and by the technical, economic and time constraints of the siting programme.

Table 3.5: Proposed field methods for tunnel near-field characterisation

Exposure	Exploration Phase	Field method	Purpose		Geology							Hydrogeology							Rock mechanics						
			Classific. of struct. elements	Orientation WCF	Frequency WCF	Size WCF	Deformation state matrix	Microstructural properties	Interv. Transmissiv. profiling	Internal variability TWCF	Correlation length TWCF	Head profiling	Saturation profiling	Matrix potential profiling	TPF parameters of WCF	Inflow distribution	Water balance (total)	Longterm monitoring head	Stress distribution	RM parameters - matrix	RM parameters - fractures	Extension damaged zone			
Tunnel wall	1,2	Geological / structural mapping	x	x	x	x	x																		
	1,2	Hydrogeological mapping									x	x				x									
	1,2	Seismic surveys		x	x	x																			
	1,2	Thermography		x		x					x					x									
	2	Water sampling /plastic sheets														x	x								
	2	Evapometer														x	x								
	2	Surface packer				x				x	x	x													
	1,2,3	Convergence measurements																							
Boreholes	2	Petrophysical logging	x	x	x																				
	2	Core inspection	x	x	x		x																		
	2	Comb. Short Interval Packer								x	x	x	x			x	x								
	2,3	MMPS								x	x	x	x												
	3	Minipiezometers																							
	1,2	Fluid logging / flow logging																							
	2	Ultrasonic borehole seismics																							
	2,3	Time Domain Reflectometry																							
	2,3	Thermocouple psychrometers																							
	2	In-situ stress / overcoring																							
	2	Borehole slotter probe																							
Core samples	2	Borehole camera (bh imager)	x	x	x		x	x																	
	2	Thin sectioning	x				x	x																	
	2	Porosimetry																							
	2	Capillary pressure tests																							
	2	Relative permeability tests																							
	2	Rock mechanical lab tests																							
2	NMR-pore space visualisation																								
Exploration phase: 1 - investigations during excavation 2 - test phase 3 - longterm monitoring phase																									

4 GAS RELEASE AND THE UNSATURATED ZONE

After closure of a radioactive waste repository, two-phase flow conditions may be expected in the host rock formation, originating either from gas generation processes in the backfilled emplacement facilities or from desaturation of the tunnel near-field during the operational phase. Both perturbations are relevant for assessment of repository performance (cf. chapter 2.2), requiring an appropriate conceptualisation and quantitative description of two-phase flow *processes and parameters* in the host rock formation. This chapter is aimed at presenting the concepts for gas escape from a repository and for resaturation processes in fractured hard rock as achieved in the Tunnel Near-Field Programme. The chapter outline follows the structure of the overall synthesis approach, proposed in chapter 2.3:

- In chapter 4.1 fundamentals are reviewed in as far as they are required for establishing *process models* of two-phase flow in fractured media. The concept of equivalent porous media is introduced and the governing equations of mass flux in a two-phase system are given. The two-phase flow properties of the fractured hard rock formation are expressed in terms of parametric models (relative permeability, capillary pressure, gas entry pressure).
- Chapter 4.2 presents *site-specific information* on those rock properties which may impact two-phase flow processes at the GTS. A compilation of *interpreted field data* is given, characterising the structural, hydraulic and two-phase flow properties of the water-conducting features and the rock matrix at the GTS.
- Chapter 4.3 provides the framework for establishing a *system model* for gas release from the emplacement caverns of a repository in a fractured hard rock environment. The main gas flowpaths through the engineered barriers, the EDZ and water conducting features are discussed first. The relevance of the different gas flowpaths through the geosphere (*structural model*) is assessed and, applying the two-phase flow properties on the local scale (field scale / laboratory tests), an up-scaling concept for two-phase flow parameters is outlined.
- Chapter 4.4 consists of a comprehensive summary of investigations on resaturation processes in the tunnel near-field. This includes *experimental studies* and a simple *system model for resaturation*, for estimating the extent of the unsaturated zone in an underground facility and for determining the duration of the resaturation phase.

4.1 Modelling two-phase flow processes in fractured hard rock

4.1.1 The continuum approach

The host rock is assumed to consist of a fractured hard rock formation which behaves as a poro-elastic medium. The medium is in mechanical and chemical equilibrium. The pore spaces of fractures and shear zones form the main water-conducting features, determining groundwater flow by their transmissivity and connectivity. The rock matrix exhibits low porosity and permeability; its contribution to groundwater flow is of minor importance, but is not negligible. Within the context of two-phase flow processes, the pore size distribution across the fractures can significantly influence gas migration through the formation. In particular, the high permeability / high porosity channels of the fractures will be the dominant gas pathways. The rock matrix may also affect the evolution of two-phase flow conditions in the vicinity of the repository in two ways: (i) the water-filled pore spaces of the matrix act as a storage medium for dissolved gas and

thus may reduce build-up of gas pressure in the emplacement caverns and (ii) as soon as the pore spaces have been desaturated (e.g. due to ventilation during the operational phase), the matrix represents a capillary barrier, which prolongs the resaturation phase after closure of the repository (chapter 4.4).

For modelling of two-phase flow processes in fractured hardrock, equivalent porous medium approaches (EPM) have to be proved an appropriate conceptualisation (PRUESS & TSANG 1990). Both the medium and the fluids are represented as continua, each notionally present at all points of the model domain. It is assumed that the properties of the porous medium and of the phases are given as local averages over some representative elementary volume. Gas and liquid flow are governed by viscous, capillary and gravity forces. Darcy's Law extended to two-phase flow is assumed to apply, with a relative permeability for each phase described as a function of the degree of water saturation (flow equations for the two phases gas / liquid):

$$Q_{(g,l)} = - \frac{k \cdot k_{r(g,l)}(S_l)}{\mu_{(g,l)}} (\text{grad } p_{(g,l)} - \rho_{(g,l)} \cdot g)$$

with

$Q_{(g,l)}$ specific discharge of the phase (gas / liquid) (m/s)

k absolute permeability of the porous medium (m²)

$k_{r(g,l)}$ relative permeability / liquid saturation function for the phases (-)

S_l water saturation (-)

$\mu_{(g,l)}$ viscosity of the phases (Pas)

$p_{(g,l)}$ gas / liquid pressure (Pa)

$\rho_{(g,l)}$ phase density (kg/m³)

g gravity constant (m/s²)

The capillary pressure p_c , representing the difference between gas and liquid pressure in the porous medium, is described as a function of the water saturation:

$$p_c(S_l) = p_g - p_l$$

where the water saturation represents the fraction of the pore space occupied by water. The water and gas saturations add up to 1:

$$S_l + S_g = 1$$

Conservation of mass leads to the mass balance equation for each component κ (e.g. air, water). Ignoring the diffusive mass flux, the transport equation for component κ is given by:

$$\frac{\partial}{\partial t} (\phi \cdot \sum_{g,l} \rho_{(g,l)} \cdot S_{(g,l)} \cdot X_{(g,l)}^\kappa) = \text{div}(\sum_{g,l} \rho_{(g,l)} \cdot Q_{(g,l)} \cdot X_{(g,l)}^\kappa) + S_{(g,l)}$$

with:

$S_{(g,l)}$ source term for the phases (kg/m³/s)

ϕ porosity (-)

$X_{(g,l)}^{\kappa}$ mass fraction of component κ in phase (g,l) (-)

Non-isothermal conditions are accounted for by considering the conservation of energy and solving the coupled mass and energy balance equations. For the purpose of modelling gas release from the emplacement caverns and resaturation of the repository environment, thermal effects are normally ignored.

In most numerical two-phase flow simulators, the gaseous phase is treated as an ideal gas and generally consists of a mixture of water vapour and air. Phase transition between liquid and vapour and mass transfer of gas components between the gas and liquid phase (i.e. dissolution of gas in liquid) are accounted for. The solubility of a gaseous component (e.g. air) in the liquid phase is given by Henry's law, describing the solubility of gas as a function of temperature, pressure and molecular weight of the gas:

$$X_l^{\kappa} = p_{\kappa} \cdot K_H \frac{M_{\kappa}}{M_l}$$

with

p_{κ} partial pressure of the gaseous component (air) (Pa)

K_H Henry coefficient (1/Pa)

M_l molecular weight of the liquid component (water) (kg/mol)

M_{κ} molecular weight of the gaseous component (air) (kg/mol)

Common extensions of the above formulation of the two-phase flow problem include diffusion processes in the phases and mass transfer between the gaseous and liquid phase for a variety of gas components.

4.1.2 Parametric models of two-phase flow properties

The applicability of the continuum approach for modelling two-phase flow processes in fractured media depends critically on an appropriate description of the relative permeability and the capillary pressure as a function of liquid saturation. In the fields of hydrocarbon exploration and soil physics, simple parametric models were developed based on capillary bundle and parallel plate models. Those models have been shown to apply for porous media such as sands and soils but also, in a modified form, for fractured rock (PRUESS & TSANG 1990). In particular, when modelling two phase flow processes in shear zones, which are filled with fault gouge material, the porous medium approach represents an adequate conceptualisation (MARSCHALL & CROISÉ 1999).

The most common parametric models for the capillary pressure / water saturation relationship are the Brooks-Corey (BROOKS & COREY 1964) and the van Genuchten models (VAN GENUCHTEN 1980). In both models, capillary pressure is a function of the effective liquid saturation $S_{\text{eff},l}$, given by:

$$S_{\text{eff},l} = \frac{S_l - S_{lr}}{1 - S_{lr}}$$

with

S_l liquid saturation (water) (-)

S_{lr} residual liquid saturation (water) (-)

The residual liquid saturation S_{lr} indicates the component of bound water in the medium. Table 4.1 gives a compilation of the models and their parameters: the empirical parameters λ and n characterise the pore size distribution of the medium, while p_e and $1/\alpha$ are representative for the gas entry pressure, which must be applied to displace the water by gas. The main difference between the two models is that, when water saturation tends towards 1, the capillary pressure approaches a non-zero value (i.e. the gas entry pressure) in the Brooks-Corey model, whereas a continuous decrease to zero is observed in the van Genuchten model. The application of both models to various types of porous media has been validated by laboratory experiments (e.g. FISCHER et al. 1998).

Table 4.1: Parametric models for capillary pressure and relative permeability

Model	Capillary pressure	Relative permeability
Brooks-Corey / Burdine	$p_c = p_e \cdot S_{\text{eff},l}^{-1/\lambda}$ p_e - gas entry pressure (Pa) λ - pore-size distribution index (-)	$k_{rl} = S_{\text{eff},l}^{(2+3\lambda)/\lambda}$ $k_{rg} = (1 - S_{\text{eff},l})^2 (1 - S_{\text{eff},l}^{1+2/\lambda})$
Van Genuchten / Mualem	$p_c = \frac{1}{\alpha} \cdot (S_{\text{eff},l}^{\frac{n}{1-n}} - 1)^{1/n}$ $1/\alpha$ - gas entry pressure (Pa) n - pore size distribution index (-)	$k_{rl} = S_{\text{eff},l}^{1/2} \left[1 - (1 - S_{\text{eff},l}^{\frac{n}{n-1}})^{\frac{n-1}{n}} \right]^2$ $k_{rg} = (1 - S_{\text{eff},l})^{1/2} (1 - S_{\text{eff},l}^{\frac{n}{n-1}})^2$

Further extensions of the Brooks-Corey and van Genuchten models have been developed to account for capillary pressure hysteresis. Proper assessment of hysteresis effects requires extensive laboratory experiments with capillary pressure cells. Such data sets are not available for fractured rock material. For this reason, hysteresis models were not investigated in the present study.

The theoretical derivations of the relative permeability / saturation relationships from the capillary pressure parametric models are based on the representation of the pore structure as a bundle of capillary tubes with a certain tortuosity. The porous medium is idealised by a distribution of tube diameters. According to the Hagen-Poiseuille law for flow in a single capillary tube, the flow velocity is proportional to the square of the tube radius. Different integration schemes were used by BURDINE (1953) and MUALEM (1976) to calculate the mean hydraulic radius of a capillary bundle and, consequently, derive the relative permeability for water and gas, respectively. Based on these integration schemes, several variants of the relative permeability function were established, the most common of them being the Brooks-Corey / Burdine and the van Genuchten / Mualem models (Table 4.1). It should be noted that the effective liquid saturation of the relative permeability function is defined in a slightly different way than for the above mentioned capillary pressure relationship. The effective liquid saturation of the relative permeability function is given as:

$$S_{\text{eff},l} = \frac{S_l - S_{lr}}{1 - S_{gr} - S_{lr}}$$

with

S_{gr} - residual gas saturation (air) (-)

The residual gas saturation S_{gr} indicates the component of trapped gas which cannot be displaced by water. It is mainly determined by the pore geometry and the heterogeneity of the porous medium, but may also be influenced by the kind of displacement process (fast / slow, drainage / imbibition) and by the number of drainage / imbibition cycles.

In fractured porous media, it might be expected that gas flows preferentially in fractures with larger apertures, whereas water flows in the smaller fractures. In this case, the interference between the flow of water and gas would be negligible. GRANT (1977) introduced the following relationship for the relative gas permeability to account for this behaviour:

$$k_{rg} = 1 - k_{rl}$$

The Grant formulation of the relative gas permeability can be applied to both the Brooks-Corey and the van Genuchten model.

4.1.3 Empirical relationship between transmissivity and gas entry pressure

The gas entry pressure is the most critical parameter to be determined when characterising the two-phase flow properties of a fractured medium in terms of the above-mentioned parametric models. Unlike for porous media, where the two-phase flow parameters can be determined by laboratory tests in capillary pressure cells, derivation of gas entry pressure is complicated considerably for fractured materials. This is mainly because of the difficulties in recovering undisturbed core samples from a fractured rock body (cf. chapter 3.2.1). The so-called gas threshold pressure test (cf. chapter 4.2) represents an alternative field method for the determination of two-phase flow parameters in fractured rock. However, gas threshold pressure tests are an expensive type of packer test, which allow collection of only a limited number of data points. In particular, when the transmissivity distribution along the fractures is highly variable (channelling), it is not realistic to determine both hydraulic and two-phase flow properties with the same spatial resolution. A solution is to establish an empirical relationship

between the fracture transmissivity and the gas entry pressure. Thus, the distribution of gas entry pressures along the fracture plane can be derived indirectly by measuring the transmissivity distribution (cf. Chapter 3.1.2).

Based on the model of parallel plates and considering the cubic law, which relates the fracture transmissivity to the fracture aperture, the following power function between gas entry pressure and fracture transmissivity can be derived:

$$p_e = c_1 \cdot T_{fr}^{-1/3}$$

with

c_1 fitting coefficient

T_{fr} fracture transmissivity (m²/s)

This power law with the exponent -0.33 is restricted to the idealised conditions of parallel plates. The coefficient c_1 depends on the fluid properties and on the interfacial tension. The roughness of the fractures and fracture fillings as observed in the shear zones of the GTS (fault gouge material) can modify the coupling between gas entry pressure and fracture transmissivity. DAVIES (1991) compiled an extensive database of laboratory measurements on porous core samples (sandstones, carbonates, anhydrites, shales) and derived a correlation between intrinsic permeability and gas entry pressure with exponents ranging from -0.34 to -0.37 . As part of Nagra's site investigations for a L/ILW repository at Wellenberg, a similar correlation was established. Based on the results from hydrotests and gas threshold pressure tests in five investigation boreholes, the gas entry pressure was matched by a power function in k with a best fit exponent of -0.35 .

4.2 **Compilation of a GTS database on two-phase flow properties**

In fractured rock formations, specific discharge of the gaseous phase is dominated by the connectedness of the high permeability channels across the water conducting features. Detailed characterisation of the spatial variability and connectivity of the major hydraulic features is therefore required as input for quantitative assessment of gas migration processes (cf. chapter 3.3).

Rock masses subjected to weak or moderate ductile deformation processes are largely unfractured. Normally, the pore spaces of the unfractured rock matrix are occupied by the liquid phase, because the porosity of the matrix is made up of very small pores. The water-filled pores of the matrix are of interest as a potential storage volume for gas, which may be transferred by dissolution from the water-conducting features into the matrix domain.

In the following sections, the structural and hydraulic properties of the major water conducting features (including the undisturbed matrix) of the GTS, which are relevant for gas migration and repository resaturation in crystalline environments are compiled. The data are based on the results of previous investigation phases at the GTS. In addition, the efforts in determining two-phase flow properties, which were a key issue of the Tunnel Near-Field Programme are summarised.

4.2.1 Geological background

The GTS in the Central Swiss Alps is located in the southern part of the Central Aare Massif, around 400 m below ground surface. The rocks in this area are almost exclusively granitic, the northern part of the GTS being located in Central Aare granite and the southern part in the Grimsel granodiorite. The age of solidification of the granites is approximately 290 – 300 Ma; subsequently the rocks were intruded by sets of lamprophyres and aplites (250 Ma ago).

The whole Aar Massif was subjected to strong alpine deformation and metamorphism. The dominant overprinting of the rocks occurred some 20 – 25 Ma ago, associated with ductile deformation, indicated by a cleavage of variable intensity (orientated NE - SW), by ductile shear zones and mylonites.

During the subsequent uplift (which is still ongoing) and cooling, the deformation changed from ductile to brittle behaviour, resulting in fractures and fault breccias. Brittle deformation concentrated along the old cleavage planes, NE-SW-striking shear zones and along the lamprophyre / granite contacts. At present, these brittle structures represent the main groundwater flowpaths at the site.

In NAGRA (1985), a classification of the brittle structures is given, based on the orientation of the discontinuities. Four main categories of discontinuities are presented:

- S-zones, which are fracture bearing shear zones that generally dip steeply SE, parallel to the foliation in the rock,
- K-zones striking WNW and intersecting the rock fabric at a high angle,
- steeply dipping lamprophyres, which are highly discontinuous and are widely distributed at the GTS and finally,
- subhorizontal, poorly connected tension joints.

Several modifications of the classification scheme have been proposed by different authors, including criteria such as the mineral coatings on the fractures (KEUSEN et al. 1989) and chemical and hydraulic properties of the discontinuities (MARTEL & PETERSON 1990). BOSSART & MAZUREK (1991) adopted a conjugate shear zone model (S- and K-zones) to explain the mechanisms of brittle deformation at the site.

There are marked differences in the distribution of the brittle structures at the GTS (Figure 4.1). In the northern part of the laboratory, complex systems of conjugate shear zones (S- and K-zones) are observed, and are associated with the considerable water inflows towards the tunnel. In addition, sets of major lamprophyres intersect the laboratory tunnel at a steeply dipping angle. The BK area, which has been extensively explored by BGR (BRÄUER et al. 1989, PAHL et al. 1989, PAHL et al. 1992), is an example of such a complex fracture network.

In the central and the southern parts of the laboratory, the frequency of discontinuities decreases, the dominant rock type changing from a slightly deformed homogeneous Central Aare granite to Grimsel granodiorite. Brittle structures are linked to the ductile shear zones, largely parallel to the cleavage. The shear zones in the southern part of the GTS have been characterised in great detail by MAJER et al. (1990) and BOSSART & MAZUREK (1991).

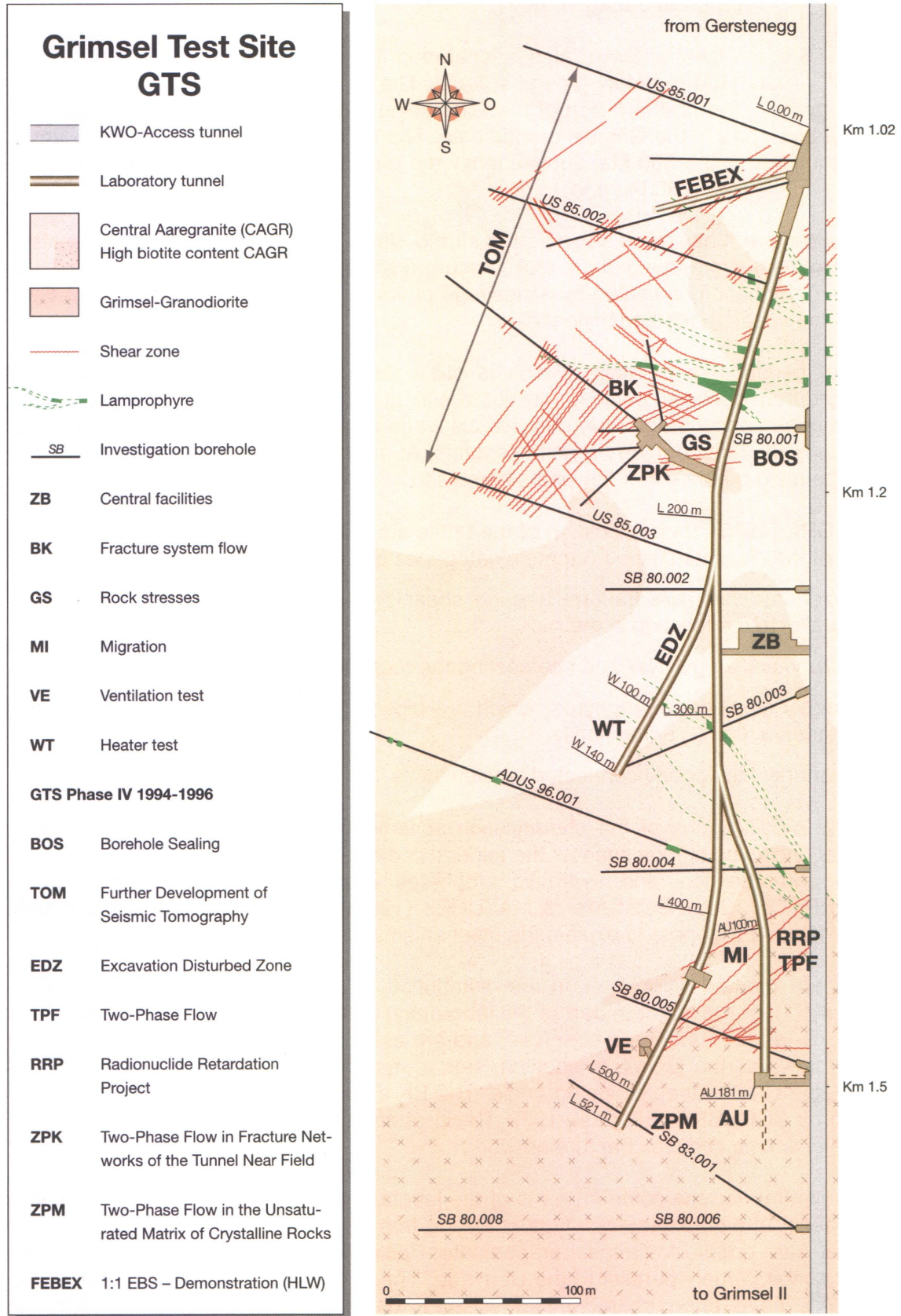


Fig. 4.1: Geological overview of the GTS

4.2.2 Structural and hydraulic properties of the rock

Interconnected S- and K-fracture systems in the northern part of the GTS

Most of the structural and hydraulic data were collected within the framework of the BK experiment (e.g. PAHL et al. 1992, LIEDTKE et al. 1994). Structural analyses of cores from more than 20 boreholes with a cumulative length of approx. 600 m showed a complex geometry of the fracture systems. In total, more than 2500 discontinuities were detected. The fracture frequency along the boreholes was highly variable, with a strong tendency for fractures to form in clusters. Typically, the fracture frequency within such clusters was 10 - 15 fractures / m. The fracture orientation at the site was also irregular, indicated by widespread distributions in the pole plots. About 50 % of the fractures were classified as open fractures, representing the actual water-conducting features at the site. BGR developed a hydraulic classification scheme for open fractures, which is based on visual inspection of cores (cf. PAHL et al. 1992). Table 4.2 summarises the results of a classification exercise at the BK site, based on the analysis of more than 750 discontinuities.

Table 4.2: Hydraulic classification of discontinuities at the BK site (762 fractures) based on an approach by PAHL et al. (1992)

Weighting class	Fraction of open fractures (%)	Description
W 1-2	51	Visual identification of fractures is possible
W 3-5	26	Fracture aperture < 1 mm
W 6-10	13	Fracture aperture ~ 1 mm
W 10-50	9	Several fractures with apertures > 1mm
W 50	1	Fracture zone with a total thickness in the dm range

Each borehole of the BK site was tested hydraulically by fluid logging and hydraulic packer tests. The transmissivities of the open fractures ranged typically from $1\text{E-}10$ to $5\text{E-}6$ m^2/s . The fraction of open fractures with transmissivities $> 1\text{E-}7$ m^2/s (classes W 10-50 and W 50) was approximately 10%.

The size of the major water conducting features is expected to be in the decametre range. Systematic analyses, however, were not performed.

Shear zones in the southern part of the GTS

The shear zones in the southern part of the GTS (MI shear zone, FRI shear zone, VE shear zone) were investigated by BOSSART & MAZUREK (1991), MAJER et al. (1990) and VOMVORIS & FRIEG (1992). Most of these shear zones exhibit a similar structure. The features are steeply dipping and the strike is predominantly NE-SW. Macroscopically the shear zones are characterised by:

- zones of ductile deformation with a thickness ranging from decimetres (e.g. MI zone: 0.15 – 0.90 m) up to 10 m (VE shear zone). The ductile zones are generally characterised by high cleavage intensity with mica-rich mylonite bands. Most of the shear zones have extents of decametres up to hundreds of metres.

- Brittle fault breccia horizons with a thickness of a few millimetres to 1 cm and more. The fault breccia horizons are located in the zones of greatest ductile deformation with an orientation parallel to the cleavage. They contain fine-grained, cohesionless gouge material. Frequently, several more or less parallel fault breccia horizons with undulating shape are observed. Fault gouge horizons may either intersect each other or are connected by fine channels along grain boundaries or sheet silicates (Figure 4.2a, see below).

The porosity of the fault gouge horizons is estimated at 10 – 30 vol %, although this was never measured in the laboratory (BOSSART & MAZUREK 1991). Recent studies as part of the TPF experiment (MARSCHALL & CROISÉ 1999) showed that the aperture distribution across the brittle structures is typically described by a log-normal distribution with mean values of about 0.2 – 0.5 mm and a cumulative thickness in the cm range. Figure 4.2 a shows a bitmap of a core sample which was impregnated with resin. The bold black channels represent two parallel fault gouge horizons. Figure 4.2 b shows the corresponding aperture distribution. The sheet silicate and grain boundary channels show apertures in the range of 0.001 – 0.05 mm.

The porosity of the ductile part of the shear zones is comparable to matrix porosity (see below).

As verified by hydrotests and tracer tests, the flowpaths along the shear zones are well connected over distances of decametres. Interconnection in the range of hecto- to kilometres has not been investigated but is considered likely. The connectivity to the rock matrix along both sides of the shear zones is weak but, nevertheless, detectable.

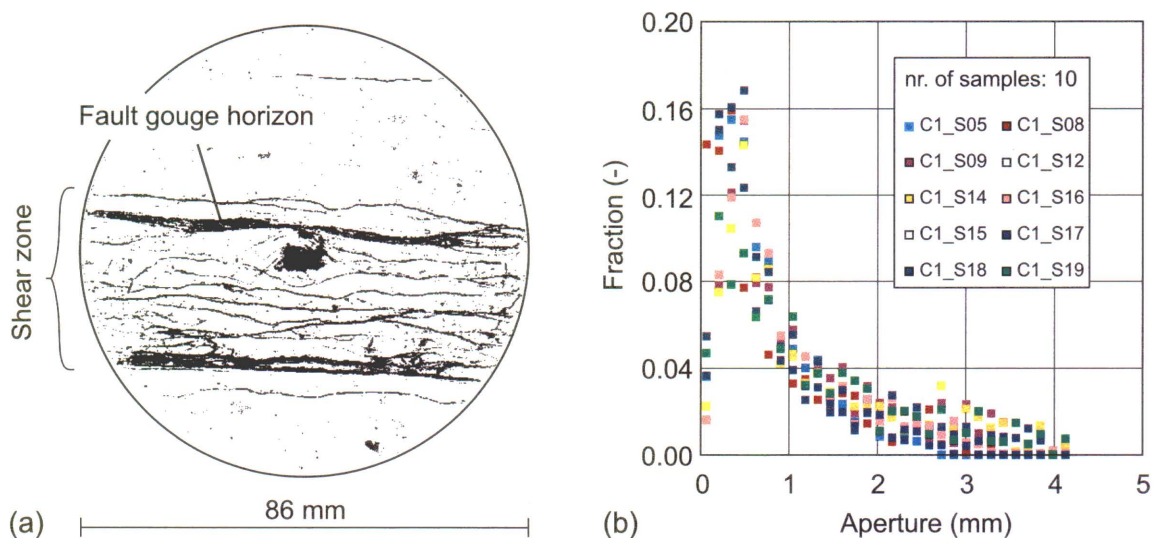


Fig. 4.2: Structural characterisation of core samples of shear zone material (from MARSCHALL & CROISÉ 1999): (a) bitmap of a core section and (b) aperture distribution of 10 core samples

The average transmissivity values of the different shear zones are highly variable. This is also true for the internal transmissivity distribution along the shear zones. MEIER (1997) analysed a set of hydraulic tests in the MI shear zone. Point measurements of

transmissivity ranged from $1\text{E-}10$ to $5\text{E-}6$ m^2/s . The geometric mean was in the range $2 - 4 \text{E-}7$ m^2/s . Hydrotests in the FRI zone as part of the experiments TPF and GAM (MARSCHALL & CROISÉ 1999, GEMPERLE 1999) showed point values in the range $7\text{E-}11$ to $1\text{E-}9$ m^2/s with a geometric mean of $2 - 5 \text{E-}10$ m^2/s .

Matrix

As part of the Ventilation Experiment (KULL & MIEHE 1995), the unfractured rock matrix was subjected to detailed structural and hydraulic characterisation. Structural investigations were based on resin impregnation methods, thin sectioning and petro-physical laboratory tests.

On a micro-scale the geometry of pore spaces in the crystalline matrix is defined by mineralogy, mineral morphology and degree of deformation (cf. Figure 4.3). Relevant parameters are the effective pore volume, the intrinsic permeability, storage capacity and the communication between matrix and main fracture systems. Four different types of pore spaces were identified by BOSSART & MAZUREK (1991):

- grain boundary porosity (connected, web-like pore space system along the grain boundaries of the minerals),
- mica porosity (pore space parallel to the orientation of the cleavage plane of sheet silicates),
- transgranular pores (microfractures and fissures),
- solution pores (pores with finely branching cavities extending from both sides of the pore channel into the mineral grain).

The effective pore volume of the matrix depends on the size and distribution of the inter-, intra- and transgranular pore spaces. The contribution of mica porosity is of minor importance. This pore space type is expected to be influenced by compressibility effects such as relaxation of the rock body. This leads to a contribution by the ductile component to the storage capacity of the matrix and, consequently, to fluid exchange with fracture systems.

Any kind of rock stress, e.g. excavation activities, can cause intragranular pore spaces within the grain size and transgranular pore spaces of larger extent. These microcataclastic fractures are the dominant flowpaths connecting the storage pore volume with a macro scale fracture system.

Results from quantitative porosimetry (BOSSART & MAZUREK 1991) showed that the average porosity of the granitic rock at the GTS is typically less than 1 vol. %. The undeformed granodiorite has porosities in the range 0.8 – 1.5 vol. % which decrease to 0.5 – 0.9 vol % in mylonitic granodiorite. With increasing degree of deformation the effective porosity also increases. Strongly deformed mylonite core samples showed porosities up to 2 vol. %, which is probably due to brittle deformation on the micro scale (microfracturing).

The distribution of pore diameters of the undeformed and mylonitic granodiorite covers a range of 3 orders of magnitude, with values between 0.02 to 2 μm and a mean value of about 0.2 μm . In strongly deformed matrix zones the distributions of pore diameters scattered from sample to sample probably due to microfracturing. Mean values as high

as 2 μm were observed. Furthermore, solution pores and microfissures were observed with diameters up to 50 μm .

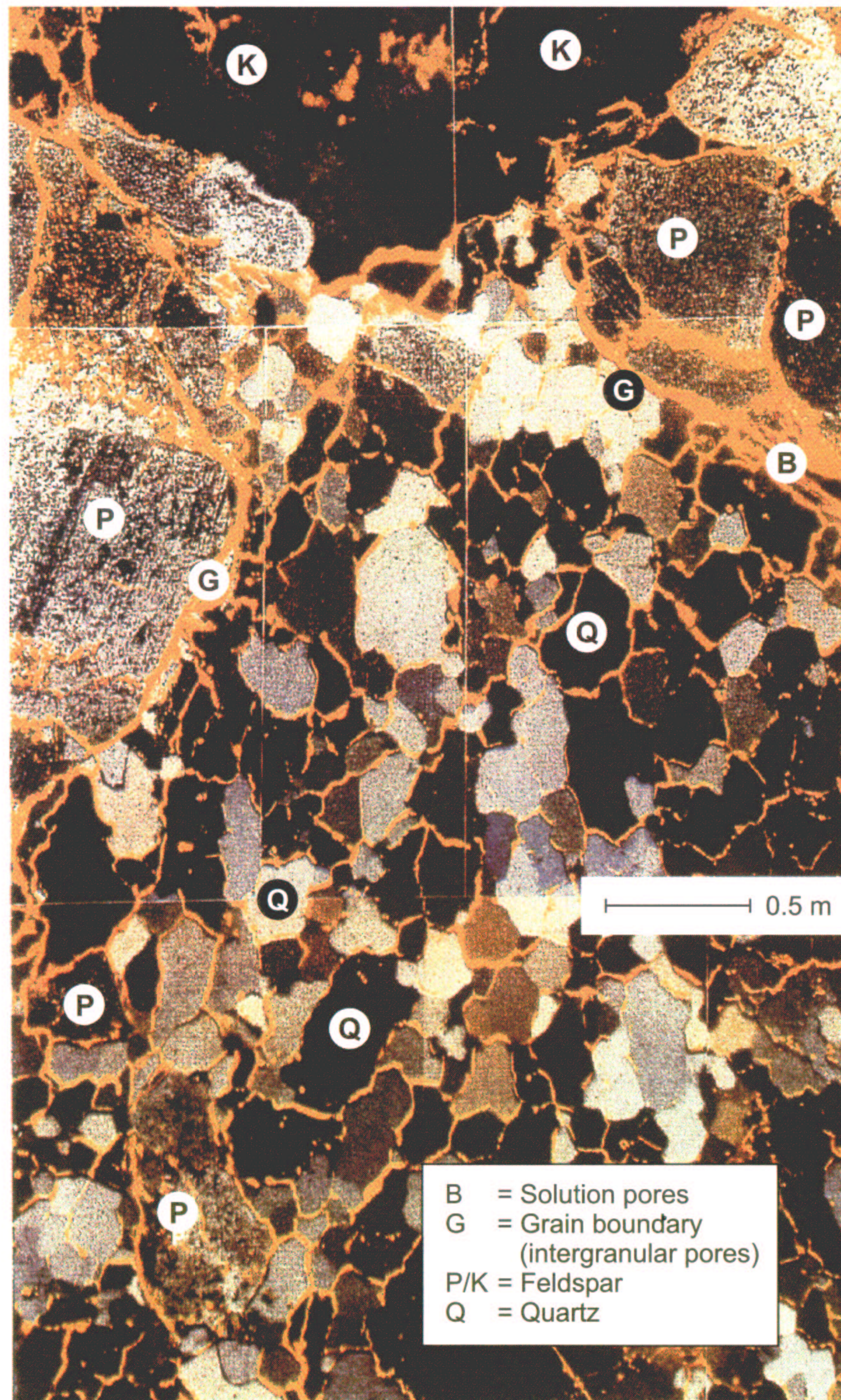


Fig. 4.3: Thin section of a typical granodiorite-granitic rock matrix. Pore spaces are yellow coloured (G) by fluorescent resin. Small intergranular pores between the grain boundaries are expected to be the main pathways of the matrix

KULL & MIEHE (1995) performed a set of gas and water permeability tests with matrix cores. The intrinsic permeability (after Klinkenberg correction) was determined to be in the range $0.55 - 6.5 \text{ E-}18 \text{ m}^2$. No dependence between effective porosity and permeability was observed.

The results of hydraulic packer tests in the matrix are reported in VOMVORIS & FRIEG (1992). The range of hydraulic conductivities varies between $4 \text{ E-}12$ and $2 \text{ E-}10 \text{ m/s}$. The authors mention that all test intervals were located close to the VE shear zone and some of the tests may partly reflect the shear zone properties.

The specific storage capacity of the water-saturated rock matrix was determined by hydrotests. The uncertainty of the parameter estimates is large due to the low sensitivity of hydrotests to specific storage. Best estimates for the specific storage were around $1 \text{ E-}7 \text{ m}^{-1}$.

4.2.3 Two-phase flow parameters

Systematic investigations of two-phase flow properties of matrix zones and shear zones material were conducted by KULL & MIEHE (1995), LIEDTKE et al. (1999) and MARSCHALL & CROISÉ (1999). The investigations include:

- in-situ gas threshold pressure tests
- capillary pressure and relative permeability measurements with core samples

Two-phase flow properties of shear zones

Two-phase flow experiments were carried out within the framework of the TPF experiment (MARSCHALL & CROISÉ 1999). In total, five gas threshold pressure tests were conducted in two different boreholes intersecting the FRI shear zone. The tests were analysed by modelling the pressure transients with the two-phase flow simulator TOUGH2 (PRUESS 1991). The analyses included (i) identification of the most likely two-phase flow parametric model, (ii) determination of the model parameters (gas entry pressure, pore size distribution index, residual water / gas saturation) and (iii) their uncertainty.

In addition, shear zone samples were recovered with the novel core sampling technique described in chapter 3.2.9. The two-phase flow parameters of the samples were determined by laboratory experiments.

The two-phase property measurements indicate that, on the core and field scale (cm to metres) gas mobility along the fault gouge horizons is high. The most likely parametric models derived from data analyses were the conventional van Genuchten / Mualem model and the Grant model for enhanced gas mobility. The estimated gas entry pressures ranged between 9 kPa (Grant model) and 263 kPa (conventional van Genuchten model). When analysing the gas threshold pressure tests, the pore size index and the residual gas saturation were given as input parameters rather than estimated through the test analysis. This is because these parameters are not very sensitive to the measured pressure transients. Laboratory experiments indicated that the best estimate for the pore size index was $n = 1.4$. The residual gas saturation S_g was determined by gas permeability tests on cores. Typical values for S_g were about 0.2. The estimated residual water saturations for the gas threshold pressure tests were model-dependent and

ranged between 0.23 (conventional van Genuchten model) and 0.6 (Grant model). The results of both the laboratory and the field tests are given in Table 4.3.

Table 4.3: Two-phase flow properties of the FRI shear zone

Tests	Most likely parametric model	Gas entry pressure (kPa)	Pore size index (-)	Residual saturation (-)	
				Gas	Water
Gas threshold pressure tests	vG / M vG / M – Grant	9 – 263	$n = 2.4^1$	0.0 ¹	0.23 – 0.60
Laboratory tests	vG / M	50	$n = 1.4$	0.2	-
vG / M - van Genuchten / Mualem					
¹ - value assumed					

Two-phase flow properties of the matrix

Laboratory experiments on core samples were focused on determination of relative permeability, gas entry and capillary pressure. The experimental work was performed at the Division of Reservoir Engineering, Technical University of Clausthal (NYIKES et al. 1997). It should be noted that these kinds of measurements are not 'standard' due to the very low intrinsic permeability of the core material and the 'Hassler Cell' equipment used as well as the methodology had to be modified (KULL & MIEHE 1995).

The relative permeability function was determined using a modified Penn-State-Method (HONARPOUR & KOEDERITZ 1986) called the Stationary-Phase-Displacement-Method. The modification became necessary because it was not possible to induce a stationary parallel gas and water flow in matrix samples. Hence, in a first step the relative gas permeability and the capillary pressure were calculated from stationary gas flow at defined injection pressure. The change in water saturation was measured gravimetrically by core sample weighting. In a second step the relative water permeability was determined for the same desaturation conditions.

For gas entry pressure measurements, the breakthrough of a gas bubble through a water-saturated core specimen was monitored. To reach breakthrough, the injection pressure is increased stepwise. One pressure step can last several weeks. A less time-consuming procedure is the Backward Break-Through-Time Extrapolation (NYIKES et al. 1997). Using much higher pressure increments the breakthrough appears within a short time. The pressure curve is extrapolated to an infinite breakthrough time at the pressure axis, which is equal to the gas entry pressure. In laboratory experiments on core samples the gas entry pressure was determined to be in the range of 0.4 to 0.8 MPa.

Gas entry pressure was also measured in-situ. The test procedure consisted of multi-step constant head gas injection using the slim hole piezometer systems (cf. chapter 3.2.4). The gas injection pressure was increased stepwise by 0.2 to 0.5 MPa up to 3 MPa, which is the limit of the test equipment. By definition, a sharp pressure drop after shut-in signified that the entry pressure p_e had been reached. From field testing the entry pressure of the fully water saturated rock matrix seems to be much higher (Figure 4.4). p_e values of 1.5 MPa were measured at a distance of about 0.3 m from the tunnel

surface. At 2.4 m from the tunnel surface the gas entry pressure was about 3 MPa. The results of both the laboratory and the field tests are given in Table 4.4.

Table 4.4: Two-phase flow properties of matrix zones at the VE site

Tests	Most likely parametric model	Gas entry pressure (kPa)	Pore size index (-)	Residual saturation (-)	
				Gas	Water
Gas threshold pressure tests	-	1500 - 3000	-	-	-
Laboratory tests	Brooks-Corey	400 - 800	$0.7 < \lambda < 2$	0.	0.4 - 0.45

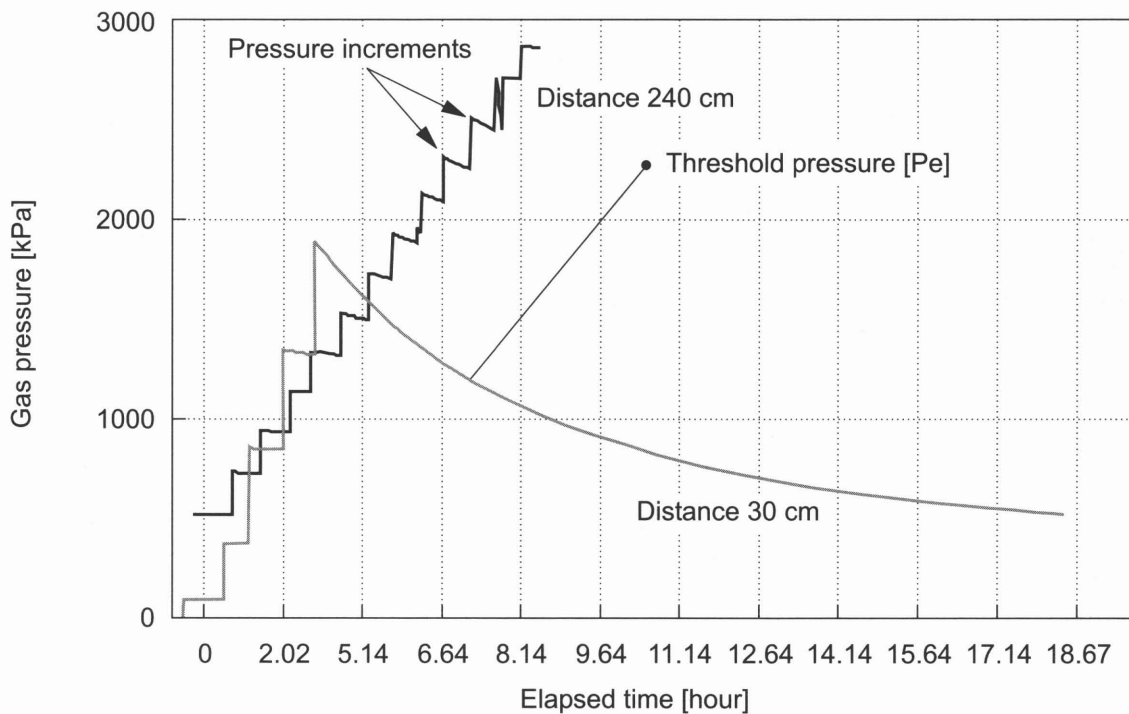


Fig. 4.4: Multistep constant head gas injection tests for determination of gas entry pressure in matrix zones at the ZPM site. Piezometers located at 0.3 and 2.4 m from the tunnel wall

4.3 System models for modelling gas migration through fractured hard rock

Gas escape from the emplacement caverns of a radioactive waste repository is determined by a multitude of factors including the repository concept and the geological host rock environment (cf. chapter 2.2). In a fractured hard rock environment, the major water conducting features are expected to represent the most important flowpaths for gas from the repository through the geosphere. This chapter is aimed at developing a conceptual framework for quantitative assessment of gas migration in a fractured hard

rock formation. Relevant gas migration processes are discussed in chapter 4.3.1. In chapter 4.3.2 two different conceptualisations of water-conducting features are derived, representing reasonable structural models of the crystalline rock formations at the GTS. Finally, chapter 4.3.3 emphasises the issue of upscaling of two-phase flow parameters in order to derive effective parameters as input for system models of large-scale gas migration.

4.3.1 Relevant processes and gas flowpaths

Assuming (post-closure) that the repository has fully resaturated and gas generation due to corrosion and degradation processes has started, gas will accumulate in the upper part of the emplacement caverns and the gas pressure in caverns will rise. The accumulated gas may be released into the geosphere (i) by dissolution in groundwater and transport in the liquid phase, and (ii) by displacement of water along one of the following pathways:

- through the bentonite seals, which plug the caverns,
- through the EDZ around the seals,
- through major water-conducting features of the host rock.

It is expected, that the bentonite seals - if fully saturated – will not form major gas flowpaths due to the very high gas entry pressure of the bentonite. The ability of the EDZ and the water-conducting features to transmit gas depends largely on the effective two-phase flow properties of these potential gas migration routes on the deca- to hectometre scale.

Dissolved gas

Dispersal of gas in solution is mainly determined by total groundwater flow through the emplacement caverns. Assuming that the specific discharge in the host rock is:

$$q = K \cdot i \text{ (m/s)}$$

with:

K effective hydraulic conductivity of the host rock formation in the vicinity of the repository (m/s)

i regional hydraulic gradient (-)

the total flow through the cavern area A_c can be estimated as:

$$Q_l = F_e \cdot q \cdot A_c \text{ (m}^3\text{/s)}$$

F_e flow enhancement factor (-)

A_c cross section area of the cavern (m²)

The flow enhancement factor accounts for the focused groundwater flow through the caverns due to their high hydraulic conductivity and can be determined either analytically or by numerical groundwater modelling on the site scale. The flux of dissolved gas is then given by Henry's Law:

$$Q_g = Q_l \cdot p \cdot K_H \quad (\text{m}^3/\text{s})$$

p hydraulic pressure (Pa)

K_H Henry constant (1/Pa)

In order to assess the effectiveness of gas dissolution in avoiding major overpressures, the flux of dissolved gas has to be compared with the gas generation rate in the emplacement caverns.

Gas migration through water-conducting features

The main gas flowpaths through the geosphere are through the EDZ around seals and along major water-conducting features intersecting the caverns. Quantitative assessment of the gas flux from the repository to the biosphere requires an appropriate conceptualisation of the two-phase flow processes along these flowpaths. As shown in MARSCHALL & CROISÉ (1999), the porous medium concept (chapter 4.1) provides a suitable framework for modelling two-phase flow processes in a single fracture. The input parameters are the structural properties of the fracture (e.g. porosity, pore size distribution), hydraulic properties (mean and spatial variability) and two-phase flow properties (parametric models of relative permeability and capillary pressure, gas entry pressure). Site-specific values for these properties, representative for the GTS are given in chapter 4.2.

In order to simulate gas migration on a larger scale (deca- to hectometres), the network effect must be considered: gas flow takes place in a network of intersecting fractures and the connectivity of the fractures impacts the effective two-phase flow properties of the entire network. For this reason, a structural model of the water-conducting features is an important prerequisite for determination of effective two-phase flow properties on a large scale.

4.3.2 Structural models for gas migration at the GTS

Within the framework of the geological synthesis of the Wellenberg site investigations (NAGRA 1997), Nagra applied a simple 1D model for estimating the effective two-phase flow properties of the host rock formation on a 100 m scale. The major water-conducting features were modelled as a set of 1D columns, connecting the emplacement caverns with the biosphere. Each column was divided into segments with variable hydraulic properties. The variability of the hydraulic parameters was consistent with the internal variability of the water conducting features as determined by field investigations (packer testing and fluid logging). The empirical relationship described in chapter 4.1.3 was used to assign a gas entry pressure to each of the segments. Finally, a Brooks-Corey model (pore size index $\lambda=2$) was applied to describe the capillary pressure and relative permeability relationships for each segment of the columns. Gas flow through the EDZ was not considered.

The representation of the water-conducting features by columns (channels) with variable transmissivity distribution may be an oversimplification of reality. In particular, such a simple 1D model is expected to contradict the complex 3D fracture network models usually applied for modelling (single phase) groundwater flow at the site.

The conceptual model for gas migration in fractured rock depends strongly on the complexity of the fracture networks, representing the main gas flowpaths through the geosphere. Two different back-of-the-envelope model variants may be considered:

- a) the water-conducting features form a complex network of intersecting fractures (e.g. BK site)
- b) the water conducting features are subvertical and of large size. The internal transmissivity distribution is highly variable, but the features do not intersect each other (e.g. shear zones at the MI site, FRI site and VE site)

In case (a), gas flow will occur along a 3D network of those channels with the highest transmissivity. In case (b), gas migration can be treated as a 2D problem (cf. Figure 4.5). In both cases, gas flow will occur along the most permeable channels of the water-conducting features.

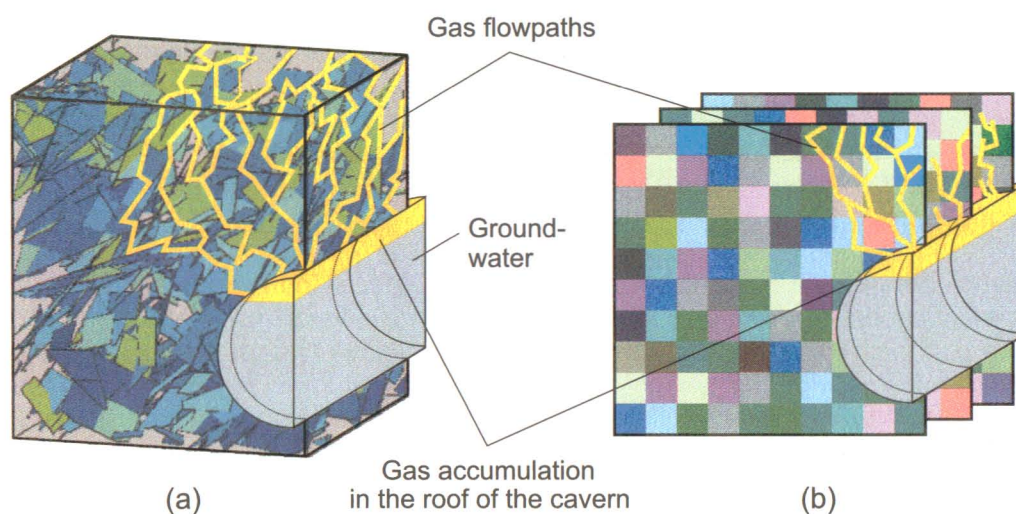


Fig. 4.5: Model variants for gas flow through a fractured host rock formation: (a) the water-conducting features form a complex network and (b) the water-conducting features are highly variable in transmissivity, but do not intersect each other

4.3.3 Effective two-phase flow parameters (upscaling approach)

Fracture network models for groundwater flow in fractured hard rock are well established (cf. NAGRA 1997). In order to ensure consistency between groundwater and gas migration models, it would be favourable to simulate gas migration with the same structural models as groundwater flow. To date, however, the numerical tools do not exist for modelling two-phase flow processes in complex fracture networks. Therefore, an abstraction scheme is required to simplify the complex groundwater flow models without losing the essential elements for gas flow.

An upscaling approach for derivation of effective two-phase flow parameters on the block scale (cube with sides in the order of 100 m) is presented. Based on a fracture network conceptualisation of the host rock on the local scale (scale of field tests: approx. 1 – 10 m), the host rock is described as a continuum on the block scale, each

block being characterised by uniform two-phase flow parameters. The approach consists of the following steps:

- establish a hydraulic fracture network model on the block scale (cube with sides of 100 m), based on geostatistical representation of the water-conducting features,
- simplify - if necessary - the groundwater flow model by discarding the low transmissivity features,
- simulate two-phase flow experiments through the cube at different / variable water saturation and derive the empirical capillary pressure and relative permeability relationship,
- match the relative permeability and capillary pressure relationship with a continuum model which is homogeneous on the block scale. The best fit two-phase flow parameters represent the effective parameters.

The hydraulic fracture network model

The hydraulic fracture network model consists of a structural model based on a geostatistical description of the water-conducting features (orientation, fracture frequency, size) and assignment of hydraulic properties to the individual fractures (transmissivity distributions, variability, correlation length). This type of model may be applied for simulation of groundwater flow in the near-field of emplacement caverns or for determining effective hydraulic parameters on the block scale (NAGRA 1997).

Simplified fracture network for modelling two-phase flow processes

As described in chapter 4.3.2, two bounding cases for fractured host rock may be considered, the complex fracture network and the system of subvertical and non-intersecting features. In the second case, a simplification of the fracture systems is not needed, because common numerical two-phase flow simulators (cf. chapter 6) can handle such 2D structures. Complex fracture networks, however, have to be simplified in a manner that is consistent with the original hydraulic model. The following procedure for simplification of fracture networks is based on an approach by LANYON (1998).

Given a complex hydraulic fracture network (e.g. cube with sides of 100 m), steady-state groundwater flow calculations through the cube must first be carried out. The next step consists of simulating advective particle transport through the network for identification of the pathways. The paths of the particles are tracked so that it is possible to identify major pathways (i.e. Those where a large fraction of the particles have followed the same pathway). The elements belonging to the selected important pathways are then extracted for further calculations. Figure 4.6 gives an example of the simplification process. The numerical approach for identification of the major water-conducting features was developed by LANYON (1998).

The next step consists of assigning the two-phase flow parameters to the individual segments of the flowpaths. As shown in Figure 4.6 (c), the water-conducting features may consist of patterns with variable transmissivity, describing the internal variability of the hydraulic properties. Two-phase flow parameters (parametric model for capillary pressure and relative permeability, gas entry pressure, pore size distribution index, residual gas / water saturation) must be determined for each segment. This can be accomplished directly by calibration / conditioning with field data (e.g. gas threshold

pressure tests) or by deriving site specific empirical relationships between the hydraulic and two-phase flow parameters (cf. chapter 4.1.3).

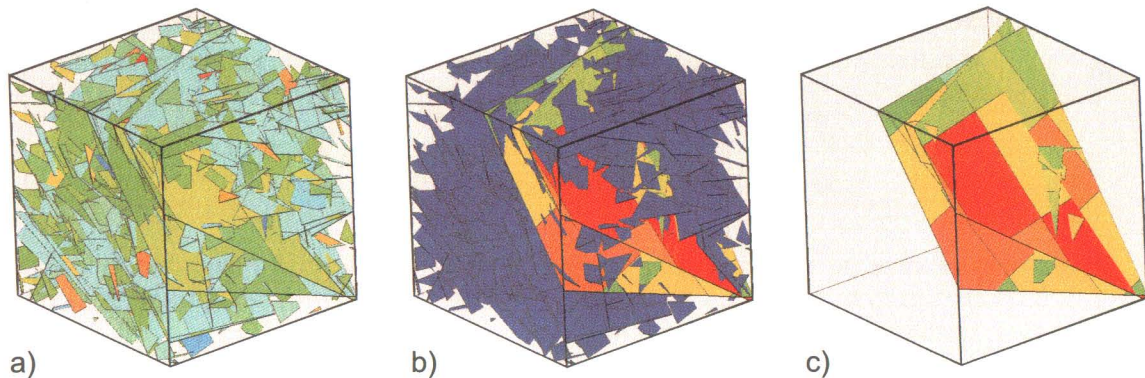


Fig. 4.6: Derivation of simplified fracture network models for two-phase flow simulations, which are consistent with the original hydraulic models: (a) original hydraulic model with colour-coded log transmissivities of the water-conducting features, (b) identification of the major pathways by particle tracking and (c) discarding of all minor flowpaths

Simulated two-phase flow experiments in the simplified fracture network

Following implementation into a numerical two-phase flow code, the simplified fracture network is subjected to simulation of two-phase flow processes under well defined boundary conditions. For this purpose a two-phase flow-field is established between two opposite sides of the cube (Figure 4.7). The flow-field between the two sides may be realised at constant head or constant flow (gas and liquid) boundary conditions. All other sides of the cube are defined as no-flow boundaries. Determining the pressure drop across the cube and the gas / liquid flow rates at steady state conditions, Darcy's law can be applied to calculate the relative gas / liquid permeability at a given degree of liquid saturation (chapter 4.1.1). By repeating the simulations with different ratios between gas and liquid flow through the cube, the relative permeability function can be determined for different degrees of saturation. The final result is a relationship between relative gas / liquid permeability and liquid saturation derived from numerical simulations. Uncertainty analysis is accomplished by repeating the entire procedure for an appropriate number of realisations of the fracture network.

Capillary pressure is determined by displacing the liquid phase in the cube at different gas pressures. Liquid saturation at a given pressure difference between the two opposite sides of the cube is determined by measuring the amount of displaced water as a fraction of the total pore volume of the cube.

Effective two-phase flow parameters

The final step in deriving effective two-phase flow parameters on the block scale is to match the synthetic relationships for relative permeability and capillary pressure with simple parametric models as given in chapter 4.1.2. It seems reasonable to determine the residual liquid saturation as the ratio between the pore spaces of the discarded minor water conducting features ('immobile' water, i.e. water which cannot be displaced by gas) and the total pore volume of the fracture network.

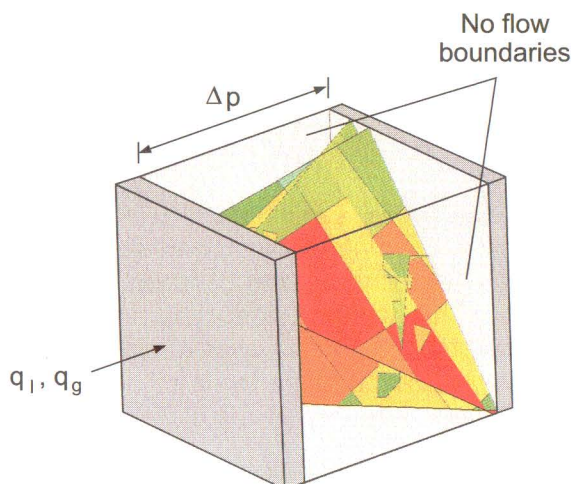


Fig. 4.7: Determination of synthetic relationships for relative permeability / capillary pressure and liquid saturation by numerical simulations of two-phase flow processes through the simplified fracture network

4.3.4 Issues for future investigation

The proposed approach for determination of effective two-phase flow parameters on the block scale provides a promising tool for estimation of total gas flux from the emplacement caverns of a repository through the host rock. In addition, the procedure can be applied to assess the efficiency of the EDZ as a gas flowpath (cf. conceptual model of the EDZ in chapter 5.3). The great advantage of the method is its consistency with the corresponding single-phase groundwater flow models (hydraulic fracture network models on the block scale).

No verification of the upscaling approach has been carried out in the Tunnel Near-Field Programme. This is mainly due to the lack of a suitable hydraulic fracture network model describing groundwater flow at the GTS on the block scale. Future investigations of gas migration in fractured rock should be focused on detailed verification of each step of the upscaling procedure. The studies need not be based on data from the GTS. For example, the hydraulic fracture networks established within the Wellenberg synthesis (NAGRA 1997) would form an ideal data set for testing the procedure. The verification exercise should include the following items:

- sensitivity study on the threshold for discarding the minor water conducting features. From economic reasons it would be favourable to simplify the fracture network as much as possible by discarding all water-conducting features below a given threshold. On the other hand the numerical simulations must lead to stable two-phase flow parameters. Sensitivity studies will help to optimise the threshold for discarding the features.
- check of the Representative Elementary Volume (REV) for gas migration processes. The above-mentioned block size of 100 x 100 x 100 m is the REV for groundwater flow on the block scale as determined in the Wellenberg programme. For gas migration at the repository scale, a different scale of REV may be required. A sensitivity study could investigate the dependence of the effective two-phase flow parameters on the side length of the block.

- determination of the optimum initial and boundary conditions for simulation of the two-phase flow processes through the fracture network. Possible cases are constant head, constant gas / water flow and constant gas flow at fully saturated initial conditions.

4.4 Resaturation of the tunnel near-field

In the context of performance assessment, the duration of the resaturation phase following closure determines the time when radionuclide migration from the repository to the biosphere is initiated (chapter 2.2). Assuming a fractured host rock formation, the phase conditions in the tunnel near-field may have a significant influence on the resaturation of the emplacement caverns after repository closure if:

- the effective hydraulic conductivity of the water-conducting features is very low, i.e. it is of the same order of magnitude as the matrix conductivity (reduced effective water permeability in matrix zones due to ventilation during the operational phase),
- the groundwater is characterised by a high content of dissolved gases (degassing of groundwater, generating increased resistance to groundwater flow towards the tunnel).

At the GTS, the gas content of groundwater is rather low and, therefore, degassing effects may not play a major role. On the other hand, as indicated by previous long-term groundwater inflow measurements in an isolated section of the VE site, the total inflow from matrix zones was a factor of 3 – 10 times lower than water inflow from discrete water-conducting features (FRIEG & VOMVORIS 1994). These conditions may allow the formation of an unsaturated zone, which acts as a skin zone around the tunnel with reduced effective permeability. As part of the ZPM experiment, investigations on the phase conditions in the tunnel near-field focused on the following topics:

- How does an unsaturated zone develop and what are the properties and extent of an unsaturated zone within a homogeneous rock matrix?
- Do the two-phase flow properties of the matrix show any hysteresis effects?

Summarising the main results of the ZPM investigations, this chapter gives an overview of the relevant two-phase flow processes in the tunnel near-field (chapter 4.4.1). The experimental work for verification of these processes is presented (chapter 4.4.2). Finally, the results of scoping calculations, which were conducted to assess quantitatively the relevance of the unsaturated zone for repository performance are discussed (chapter 4.4.3).

4.4.1 Two-phase flow processes in the matrix

As noted in chapter 4.2.2, formation of a mobile gas phase is not very likely in the rock matrix due to the small pore sizes of the inter- and transgranular pores (Figure 4.8). Nevertheless, unsaturated conditions are observed in matrix zones of the tunnel near-field, which originate from:

- evaporation due to tunnel ventilation,
- gas evolving from the liquid phase, when the hydraulic pressure is lowered below the bubble point (degassing).

Both effects may considerably reduce groundwater flow towards the tunnel.

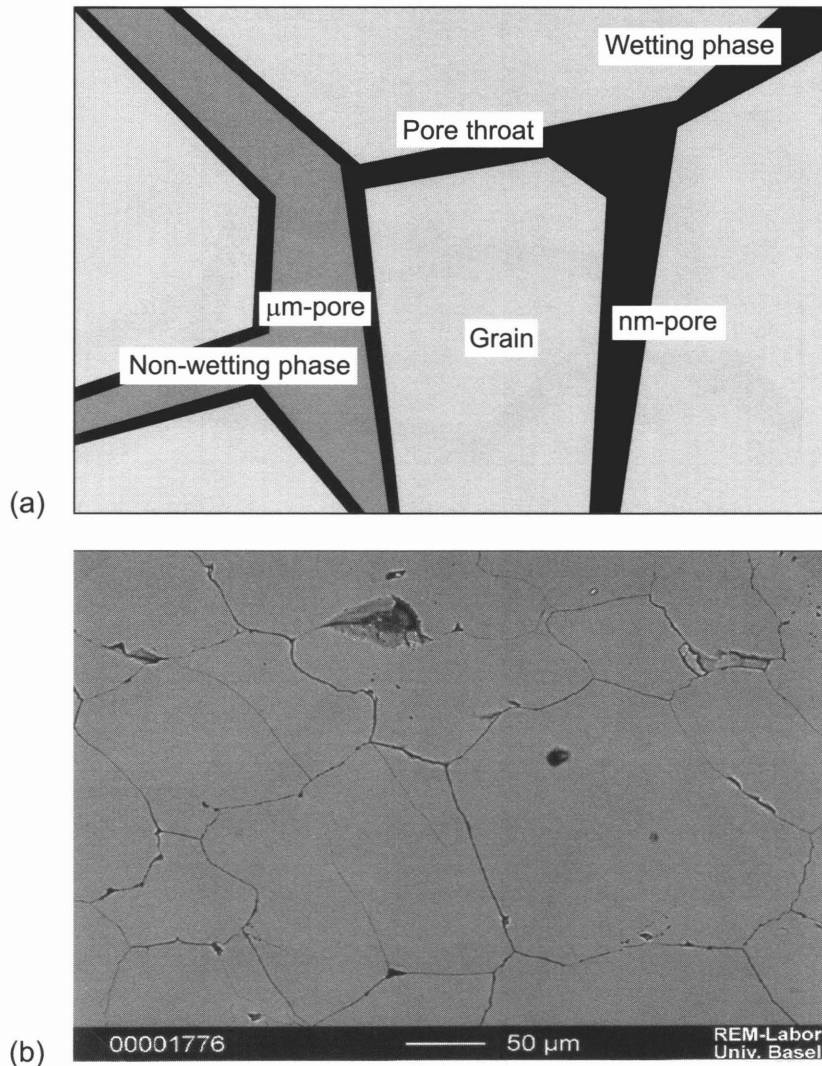


Fig. 4.8: Conceptualisation of two-phase flow conditions in the rock matrix: (a) due to the very small pore sizes of the inter- and transgranular pore channels formation of a continuous (and mobile) gas phase is restricted to the condition of very low water saturation (wetting phase); (b) thin section of a typical quartz matrix and nanometre-size intergranular pores spaces

Evaporation effects

Evaporation effects are mostly linked to tunnel ventilation. When the evaporation of water at the rock surface exceeds the water inflow to the tunnel through the low permeability rock matrix, water saturation in the matrix changes. Assuming that the pore spaces of the matrix are in contact with the atmosphere, the partial pressure of vapour in the atmosphere is expected to control the phase transition of the porewater. Movement of a desaturation front into the rock matrix is determined (i) by the pore size distribution affecting the capillary forces in the medium and its intrinsic permeability and (ii) by the hydraulic gradient towards the tunnel surface (Figure 4.9).

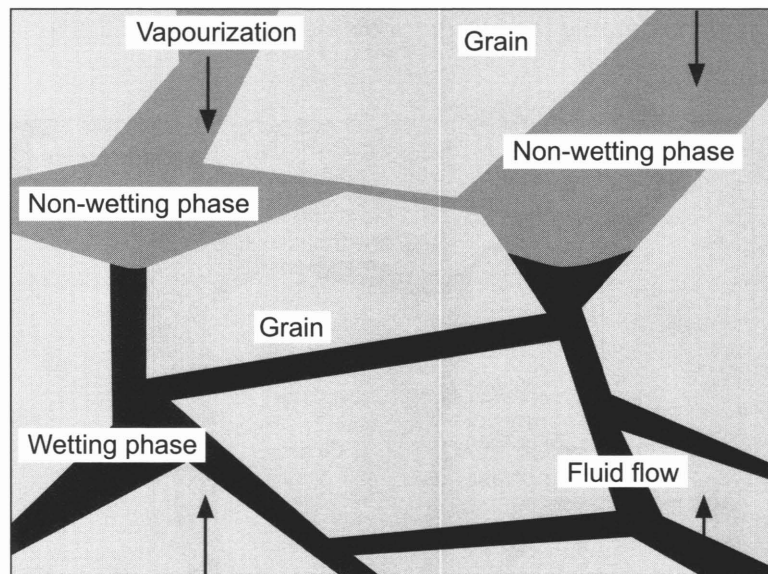


Fig. 4.9: Movement of a desaturation front into the rock matrix: the balance between evaporation and advective flow of the liquid phase determines the extent of the unsaturated zone

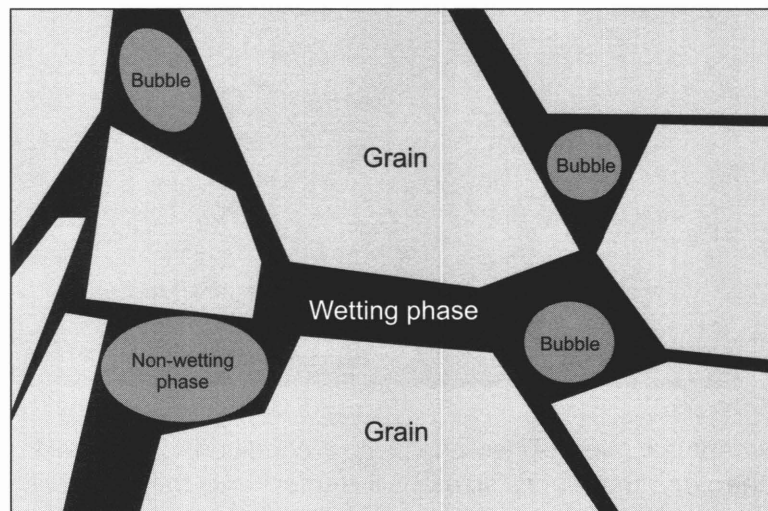


Fig. 4.10: Two-phase flow conditions in the rock matrix due to degassing. Spontaneous degassing is observed when the hydraulic pressure of the liquid phase is lowered below the bubble pressure of the dissolved gas component

In the excavation damaged zone of the tunnel near-field as part of the excavation disturbed zone (cf. Chapter 5), enhanced desaturation could result from the low interfacial tension of pore spaces and low hydraulic gradients.

Degassing

Degassing is observed in groundwater systems with a high content of dissolved gas. Gas evolving from the liquid phase is observed when the hydraulic pressure is lowered

below the bubble pressure (cf. Figure 4.10). Such pressure drops may originate either from a highly heterogeneous permeability distribution or from pressure sinks such as boreholes or underground excavations. In general, degassing depends on the partial pressure of initial dissolved natural gas components (nitrogen, carbon dioxide, oxygen, hydrocarbons) and is described by Henry's law (chapter 4.1.1). Degassing around tunnels has been investigated extensively within the Stripa and Äspö projects (OLSSON 1992, GELLER & JARSJÖ 1995).

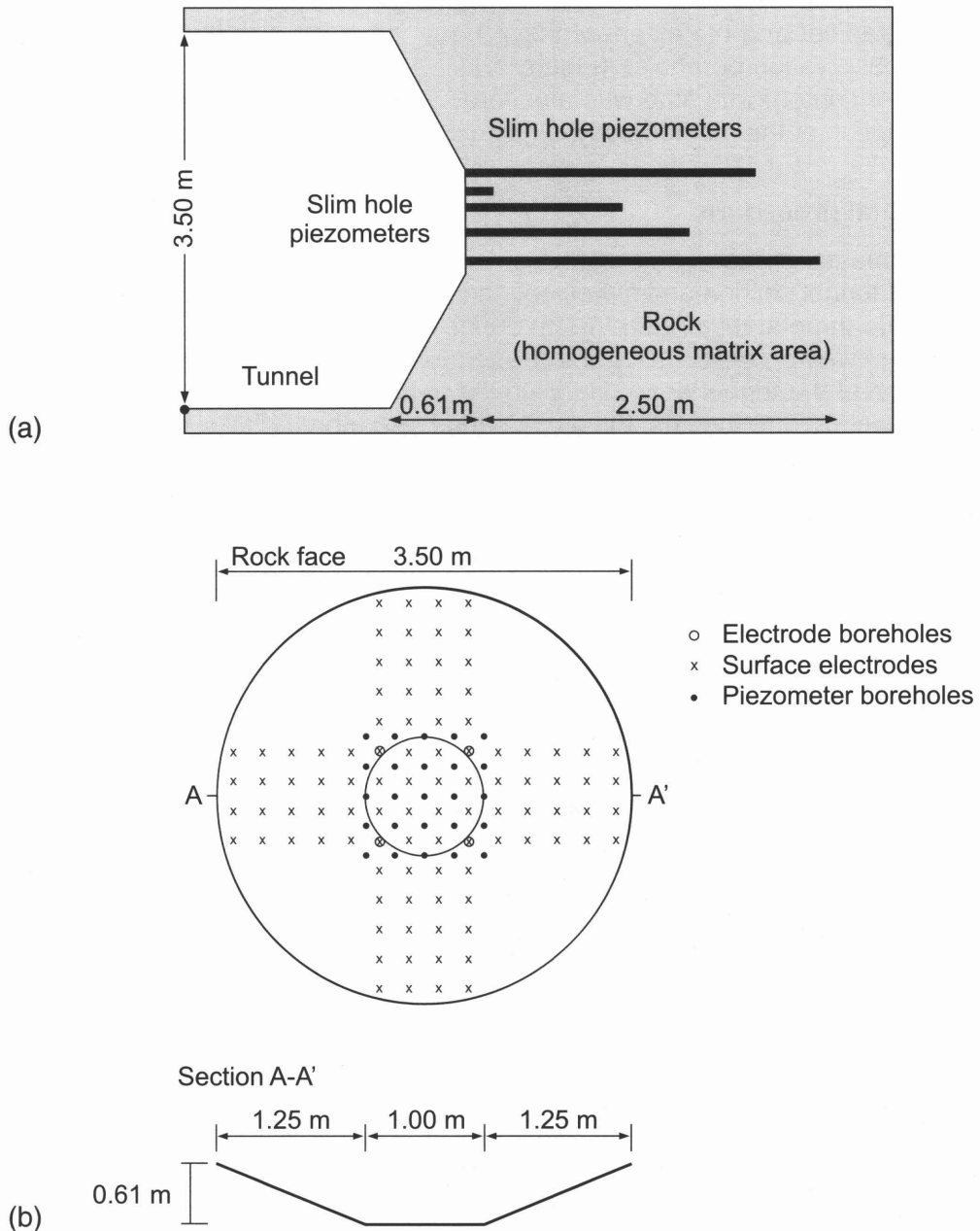


Fig. 4.11: The ZPM experimental site in the dead end section of the VE drift: (a) vertical section of hydraulic pressure monitoring system and (b) electrode array for electrical resistivity measurements at the tunnel face

4.4.2 Experimental verification

Experimental set-up

The desaturation of crystalline rock matrix was investigated on a local scale in field tests. The tests were run under controlled climatic conditions in a closed ventilation chamber at the GTS. The hydraulic measurements, including the determination of effective water permeability and gas entry pressure (cf. chapter 4.2.3), were performed in a homogeneous matrix area of granodiorite at the ZPM site to a depth of 2.5 m from the tunnel surface. The influence of tunnel ventilation on pressure evolution and on the hydraulic gradient and the extent of the zone of influence was investigated in a dense cluster of observation boreholes (Figure 4.11). At the same time, the assumed change in porewater content with time was monitored by electrical resistivity measurements. A brief description of the methodology is given in chapter 3.2.

Experimental procedure

The experimental procedure consisted of long-term monitoring of the phase conditions in a closed tunnel section under well defined ventilation conditions. The procedure was divided into three steps (Figure 4.12): during the first 12 months (step I), the humidity in the tunnel was close to 100% and the temperature was 14°C. Step II was aimed at desaturation of the tunnel near-field. Humidity was lowered to 30% at a temperature of 20°C for a period of 6 months. Finally, a period of 6 months followed where the saturation increased from 30 to 100% and temperature was reduced from 20 to 14°C. During steps I and III the closed tunnel section was not ventilated. Pressure monitoring, geoelectric surveys, hydrotests and gas threshold pressure tests were carried out during all experimental phases to characterise the phase conditions up to 2.5 m distance from the tunnel wall.

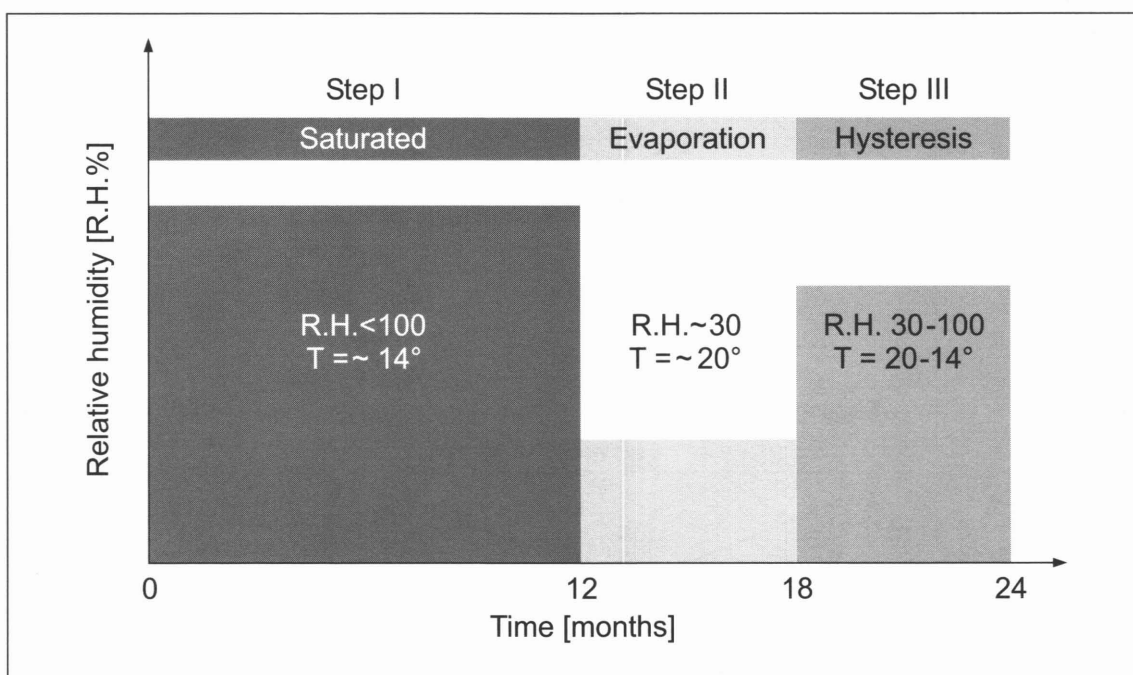


Fig. 4.12: Ventilation steps to induce the movement of an unsaturated zone into rock

Experimental results

A clear correlation was determined between the tunnel climate and the pore pressures in the tunnel near-field. At the end of step I, with quasi-stationary conditions, a steep increase in the pressure profiles was monitored, with atmospheric pressure at the tunnel wall and about 1 MPa (absolute pressure) at a depth of 2.4 m (Figure 4.13, curve no. 1). Already 10 cm from the tunnel surface the water pressure increases up to 100 kPa above atmospheric pressure. The form of the pressure curve supports the assumption of a homogeneous rock volume. Hydraulic structures with enhanced transmissivity, e. g. brittle deformations, are not recognised, nor are any indications of an excavation damaged zone given.

Curve no. 2 shows the water pressure after 5 months of constant ventilation during step II. Pressures close to atmospheric were measured up to a distance of 1 m. Remarkable are the pressures below atmospheric at distances between 0.2 and 1.0 m. At 0.4 m from the tunnel surface the hydraulic pressure is approximately 50 kPa below atmospheric. This 'underpressure zone' indicates that the gas phase is not mobile due to increasing water content. In contrast, the pressure values for the first 0.2 m represent more or less atmospheric conditions, indicating that the gas phase is more or less continuous. Fully saturated conditions are observed at a depth of more than 1 m. Absolute pressure at 2.4 m is about 0.7 MPa.

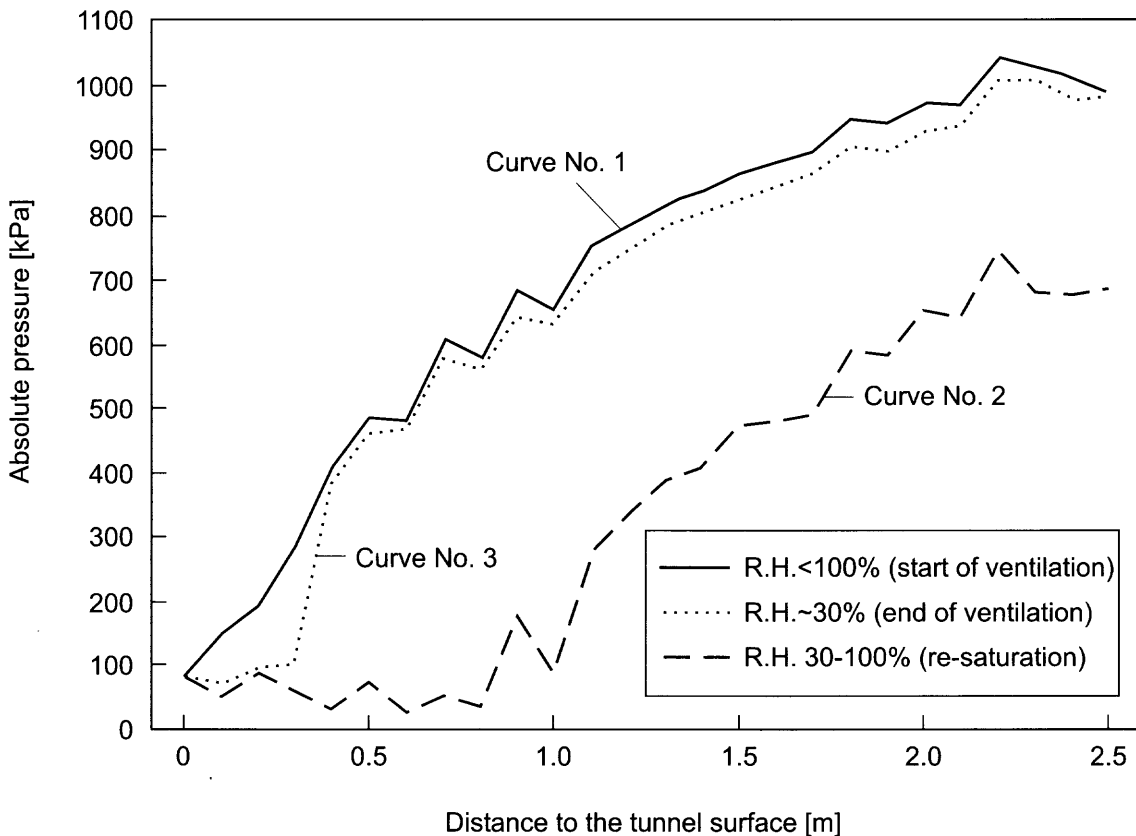


Fig. 4.13: Pressure profiles in the tunnel near-field during different ventilation phases

When the ventilation was stopped (step III), the hydraulic pressure increased again until it reached nearly the initial pressure head. Curve No. 3 represents the hydraulic pressure distribution 4 months after starting resaturation. The depth of partial desaturation seems to be limited to a distance of 0.3 m from the tunnel surface. Pressure hysteresis may be a matter of observation time.

Effective permeability measurements were conducted with the slim hole piezometers as an indirect measure for water saturation at the location of the piezometer interval. The results were obtained from constant head injection (water) tests during step I and step II of ventilation. It has to be emphasised that all calculated effective permeability data are obtained from analysing the 'early time' period of the pressure recovery period after 'shut-in'. The dependence of matrix permeability on the distance to the tunnel surface and on step of ventilation is demonstrated in Figure 4.14. During step I the effective permeability of the rock matrix is in the order of $4.0\text{E-}18\text{ m}^2$, which corresponds with previous measurements of intrinsic permeability for Grimsel granodiorite (chapter 4.2). A slight increase in the permeability with distance to the tunnel surface is observed.

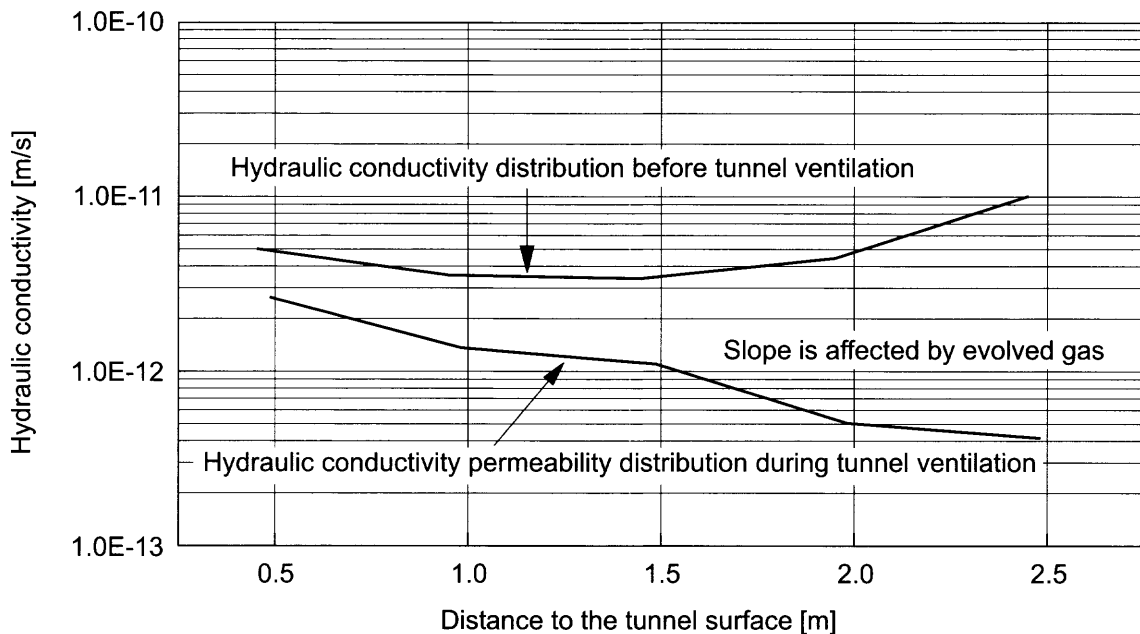


Fig. 4.14: Effective permeability distribution in the tunnel near-field during steps I and II

During step II the effective permeability decreased by up to one order of magnitude. It should be noted that the deviation seems to increase with the distance to the tunnel surface. The reason for this is not clear, because unsaturated conditions are expected for distances lower than 1 m (see above).

Gas threshold pressure tests were carried out during step I to determine the gas entry pressure of the granodiorite matrix (cf. chapter 4.2.3). The tests were repeated during step II. Generally, the displacement pressures (i.e. the pressure, at which gas starts to become mobile) were lower, which can be explained by the presence of a gas phase in the rock matrix. For instance at a distance of 0.2 m from the tunnel surface the entry

pressure was found to be less than 1.5 MPa. From the pressure recovery curve of the same test a displacement pressure of 0.8 MPa was derived.

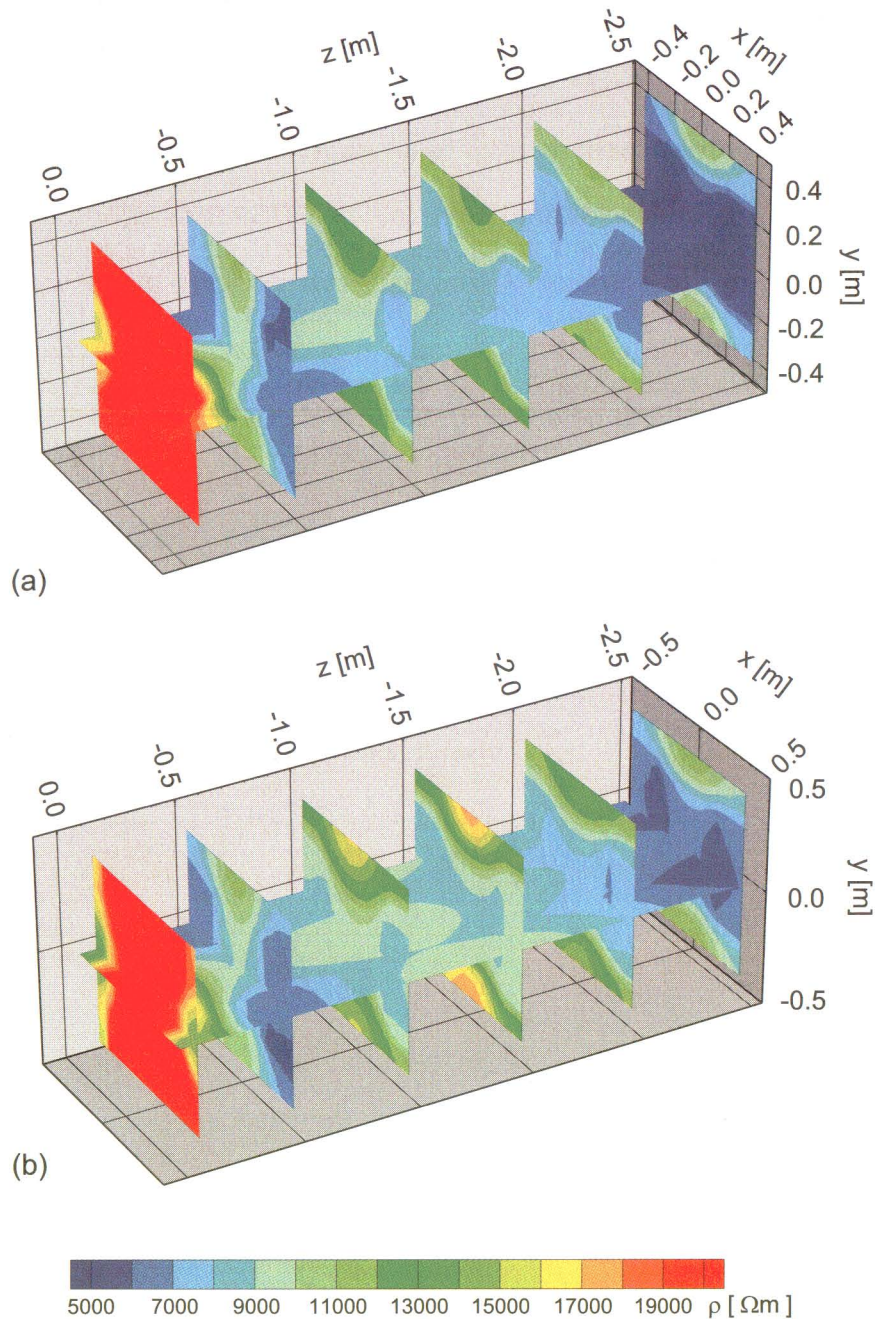


Fig. 4.15: The change in resistivity distribution was measured 0.25 and 2.5 m from the surface of the tunnel and sections between the borehole electrodes (edges of the 3D pictures): (a) at the beginning of step II; (b) after 3 months of ventilation

DC-geoelectric resistivity measurements (cf. chapter 3.2) were carried out for 3D imaging of changes in water saturation during the different experimental phases. Except for the first decimetres, with resistivity values higher than 20000 Ωm , the resistivity dis-

tribution is rather uniform (5000 to 10000 Ωm , cf. Figure 4.15), with a tendency to decrease with depth. The relative changes in saturation are too small to be detected by the geoelectric method. Obviously the electrical resistivity distribution was not affected by ventilation. Also no indications are given for formation of an unsaturated zone. This leads to the conclusion that the altered zone is limited to approximately 50 cm from the tunnel surface.

4.4.3 Quantitative assessment of resaturation scenarios

Numerical scoping calculations were carried out by GRS for modelling two-phase flow processes in matrix zones of the tunnel near-field as input for scenario analyses on post-closure repository resaturation. A simple, one-dimensional model was established using the multiphase flow simulator MUFTE-THERMO (cf. chapter 6.1.1). The scoping calculations were aimed at estimating the extent of the unsaturated zone after a long ventilation period (i.e. a period which compares with the duration of the operational phase of a repository) and at determining the spatial distribution of water saturation in the tunnel near-field. The simulations demonstrated clearly the strong dependence of the pressure distribution in the tunnel near-field on the saturation of the rock matrix (KULL et al.1999).

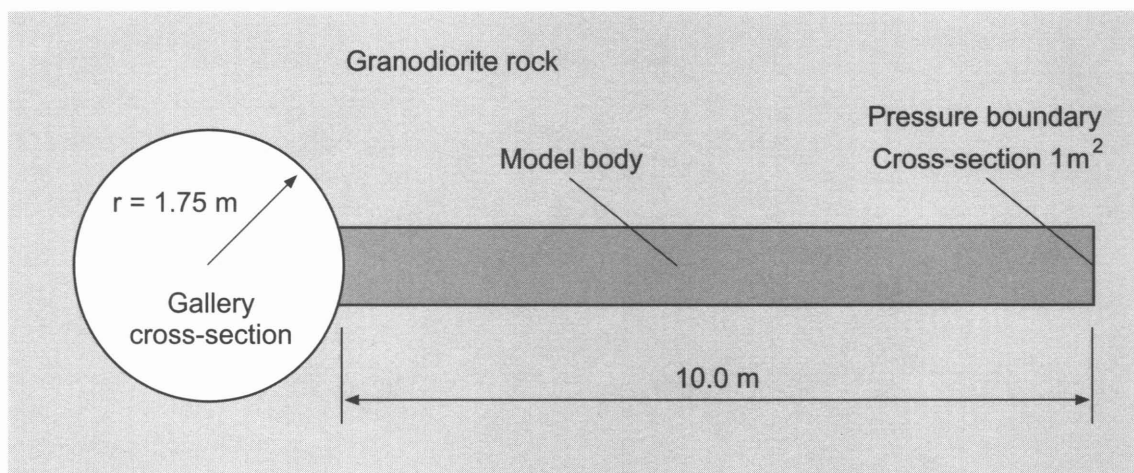


Fig. 4.16: Model Region for the 1D desaturation simulations

The model region extends from the tunnel surface radially into the rock zone over a length of 10 m (Figure 4.16). Thermal and mechanical properties of the cylinder with a cross-sectional area of 1 m² are assumed to be constant. The parametric models used to describe the two-phase flow properties of the rock are given in Table 4.4. Fluid exchange through the mantle area of the cylinder is not allowed. Also diffusion of water vapour is not considered.

Fully saturated conditions are assumed as initial conditions. At the endpoint of the model region, the pressure and water saturation conditions are held constant. For the rock cavity, pressure is assumed to be atmospheric. Two different cases were assessed with respect to the water saturation at the model boundaries: (i) case 1 with very low water saturation at the tunnel wall ($S_w = 0.001$) is aimed at simulating strong ventilation with low humidity in the tunnel atmosphere, (ii) case 2 with very high water saturation at the wall to ($S_w = 0.999$) corresponds to nearly unventilated conditions.

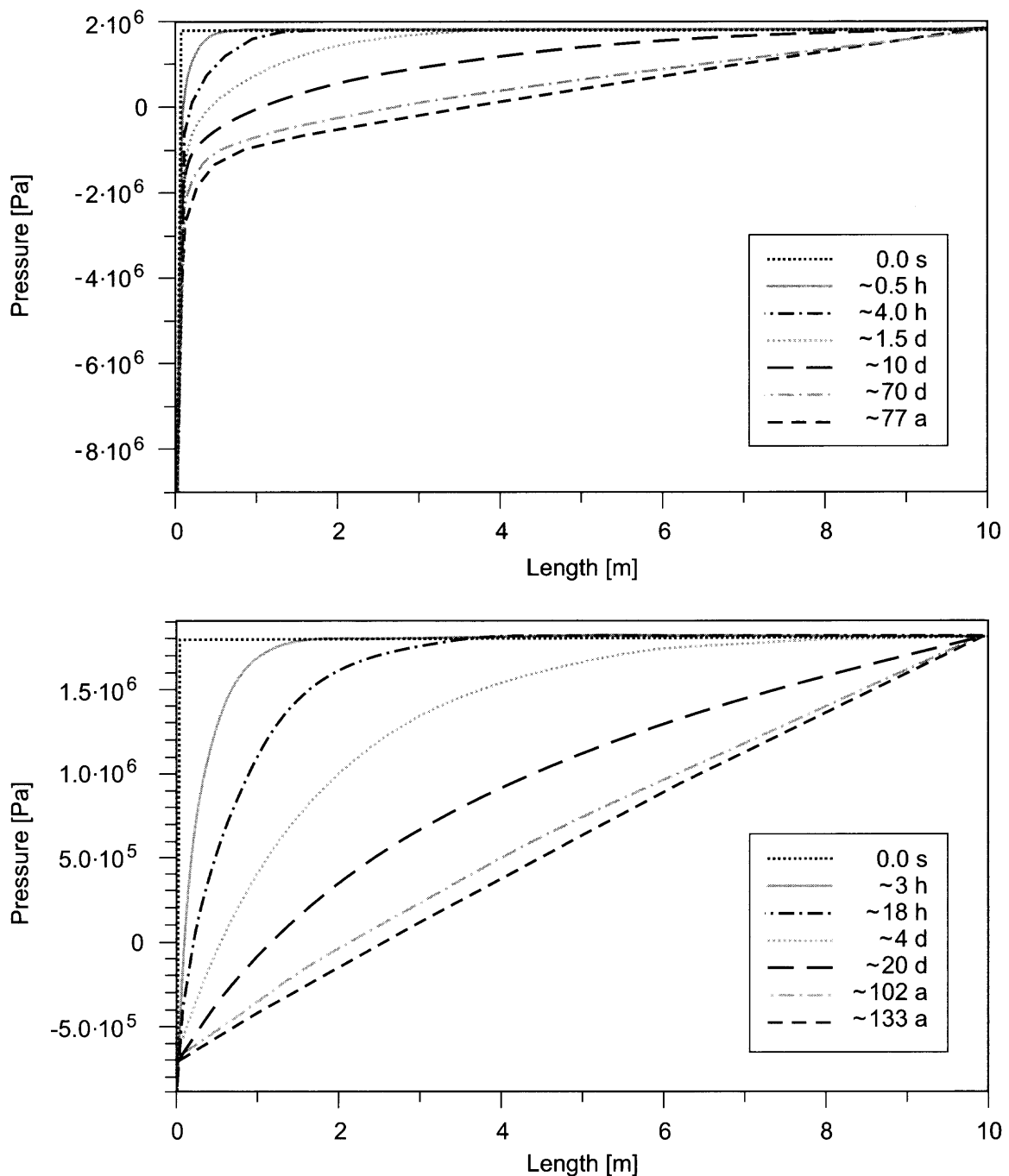


Fig. 4.17: Evolution of water pressure profiles after start of ventilation for (a) case 1 representing conditions of strong tunnel ventilation and (b) case 2 with tunnel ventilation at a minimum

nel and the higher one in the rock slowly decreases by balancing processes (case 1, cf. Figure 4.17a). For the annular zone around the tunnel with a width of 2 - 3 m, negative pressures are obtained. This is due to the low water saturation prescribed at the tunnel wall which creates a gas phase in the tunnel near-field. Water is vapourised when the pressure declines to the water vapour pressure level. After 70 days, quasi-stationary state conditions are achieved with a strong pressure gradient across the first 0.5 m next to the tunnel surface and a more or less linear pressure drop towards the outer

boundary. The pressure profile indicates a decrease in effective water permeability, which can be explained by the formation of a gas phase in the immediate vicinity of the tunnel surface. It is remarkable that this low permeability zone does not change significantly in extent for the entire period of 77 a.

The pressure curve in case 2 indicates steady state conditions after approximately 100 d. The linear transition of the pressure profile does not correspond to field observations, but is determined by the prescribed pressures at the model boundaries (Figure 4.17 b). A significant reduction of effective water permeability is not observed.

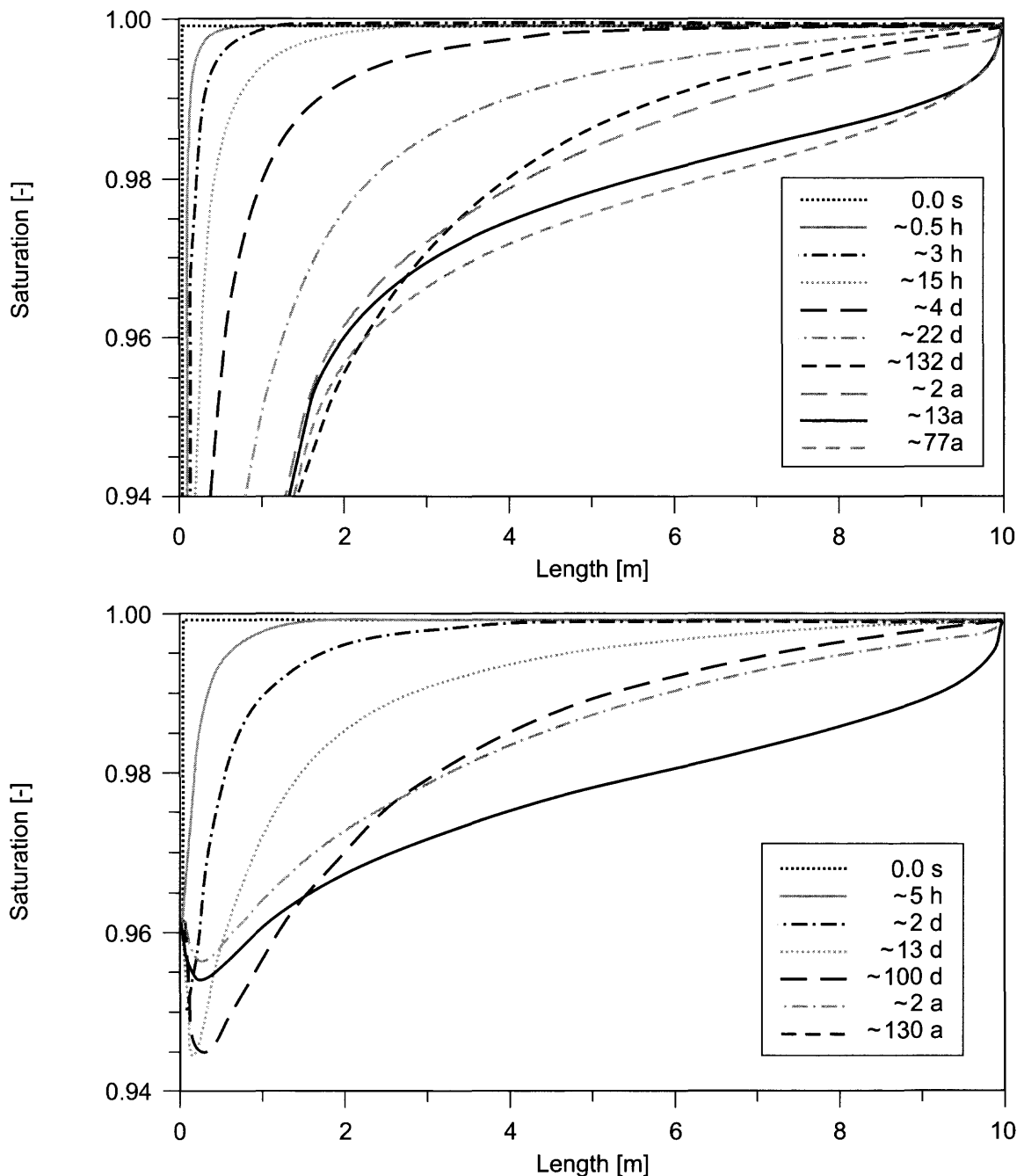


Fig. 4.18: Evolution of water saturation after start of ventilation for (a) case 1 and (b) case 2

The comparison of the results for case 1 and 2 (cf. Figure 4.18) shows that tunnel ventilation influences the radial distribution of water saturation only within a range extending up to 0.5 m into the rock. For case 1, a significant desaturation is observed in the immediate vicinity of the tunnel surface ($S_w < 0.9$ at a distance < 1.0 m to the tunnel surface). This zone corresponds to the low permeability zone which was observed in the pressure profiles. For case 2, no significant desaturation occurs in the tunnel near-field ($S_w > 0.94$). The long-term evolution of the saturation profiles (i.e. $t > 100$ d) is not representative of real conditions either for case 1 or for case 2, because the influence of the prescribed pressure and saturation at the outer boundary starts to dominate the the shape of the profiles.

The calculated mass flux density of water along the model axis is almost constant after 100 days (Figure 4.19). On the assumption of low water saturation at the boundary (case 1), a value of $0.2024\text{E-}6 \text{ kg m}^{-2} \text{ s}^{-1}$ has been obtained; for case 2 the value is about 15% less.

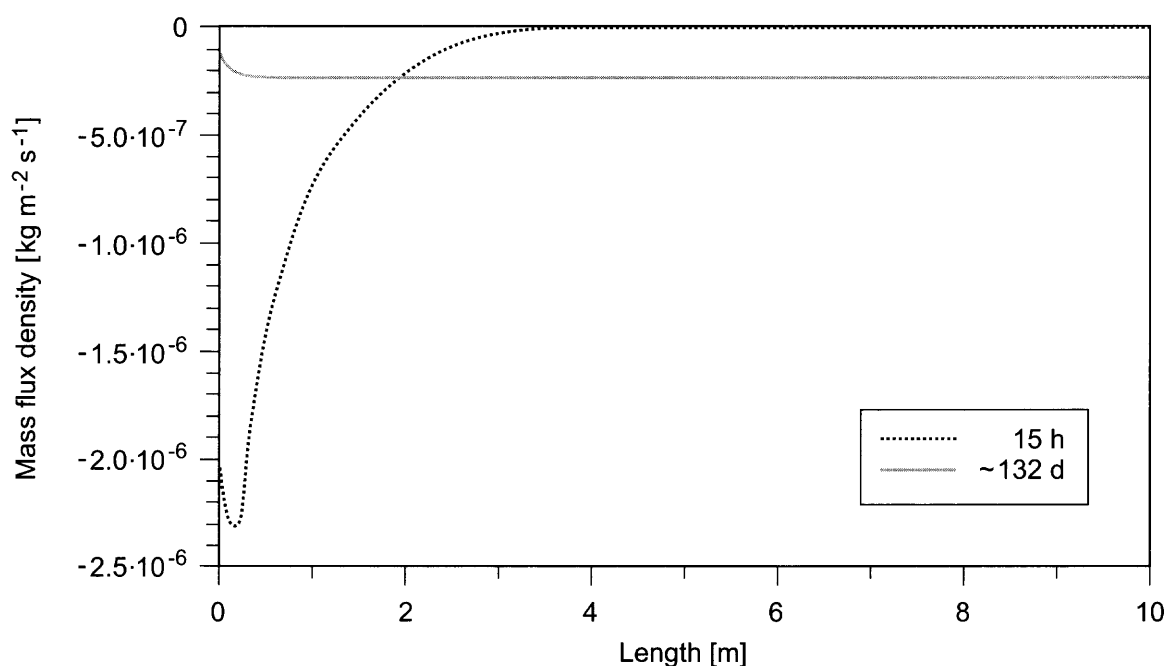


Fig. 4.19: Water mass flux density along the model axis for case 1 at a very early time (15 h) and at almost steady-state after 130 days

In contrast, the air mass flux density is not constant along the model axis and increases in the immediate vicinity of the tunnel wall (Figure 4.20). After 10 years the mass flux dependency is linear except for the zone close to the boundary. The increase of air mass flux density in the flow direction is a result of the mass increase from the degassing and the evaporation of the water phase. After 48 years, the theoretical gas mass flux density into the tunnel attains, for case 1, a constant level of $0.1\text{E-}9 \text{ kgm}^{-2}\text{s}^{-1}$ or $3.15\text{E-}9 \text{ kgm}^{-2}\text{a}^{-1}$ and 80% less for case 2.

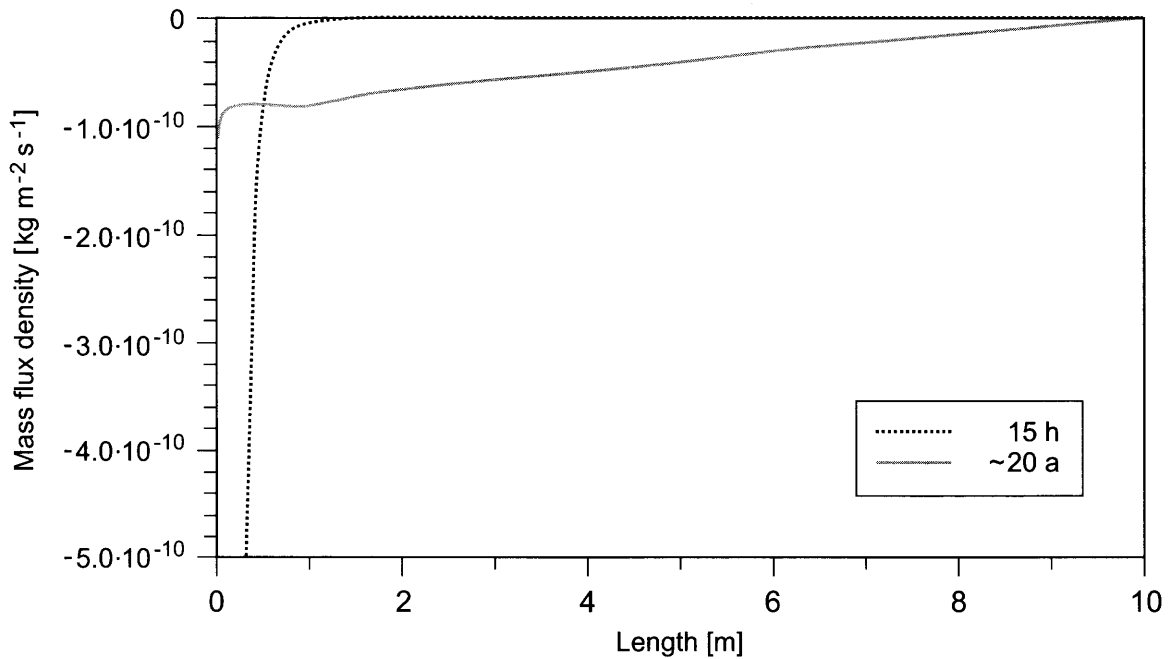


Fig. 4.20: Air mass flux density along the model axis for case 1 at a very early time (15 h) and at almost steady-state after 20 years

4.4.4 Concluding remarks

Evolution of an unsaturated zone during the operational phase may impact post-closure repository performance in low permeability host rock formations such as clay, salt or sparsely fractured crystalline rock. The ZPM experiment was aimed at developing process models of the unsaturated zone in the near-field of underground excavations. Complementary field investigations were carried out to provide a data base for model validation. The main conclusions gained from the ZPM experiment are summarised as follows:

- Experimental evidence was found for the existence of an unsaturated zone in ventilated tunnel sections of low permeability. The extent of the unsaturated zone is mainly determined by the humidity and temperature evolution in the tunnel. Desaturation of the tunnel near-field is a reversible process. No hysteresis effects were observed between the desaturation and the resaturation process.
- The unsaturated zone around tunnel sections of low permeability is restricted to the immediate vicinity of the tunnel surface. Scoping calculations indicate, that significant desaturation may be expected in a zone of 0.5 - 1.0 m thickness around the tunnel. Assuming constant ventilation conditions, this zone does not grow with time but stays stable in size and magnitude of desaturation. Thus, the unsaturated zone may be conceptualised by a low-permeability skin zone around the tunnel.
- Due to their high gas entry pressures matrix zones are practically impermeable with respect to gas flow (capillary barriers). The scenario of an axial gas flow through the EDZ of a seal section is not very likely, when the seal is placed in a tunnel section characterised by homogeneous rock matrix.

5 EXCAVATION DISTURBED ZONE

The excavation of any underground opening creates a zone of disturbed rock around the opening. Close to the excavation, the magnitude of the disturbance may be sufficient to cause fracturing or failure of the intact rock such that its properties are significantly altered. The characterisation of these excavation disturbed and excavation damage zones has been the subject of considerable experimentation over the last twenty years in connection with characterising the near-field rock around repositories for radioactive waste. The term EDZ has been used ambiguously in the past to cover both the excavation disturbed and damage zones. Here the EDZ is used to refer to the excavation disturbed zone, of which the damage zone is a part as illustrated in Figure 5.1. The usage follows that of EMSLEY et al. (1997) who give the following comment on the two zones in connection with the ZEDEX experiment:

„there is a damaged zone closest to the drift wall dominated by changes in material properties which are mainly irreversible and there is a disturbed zone outside the damaged zone dominated by changes in stress state and hydraulic head and where changes in rock properties are small and mainly reversible and it is considered that there are no, or insignificant, material property changes.“

The boundary between the two zones is gradational, as is the boundary between the disturbed zone and the undisturbed rock. The position of any defined boundary or envelope of the disturbed zone will differ according to the properties of interest and the magnitude of changes that are deemed to be significant in a particular investigation.

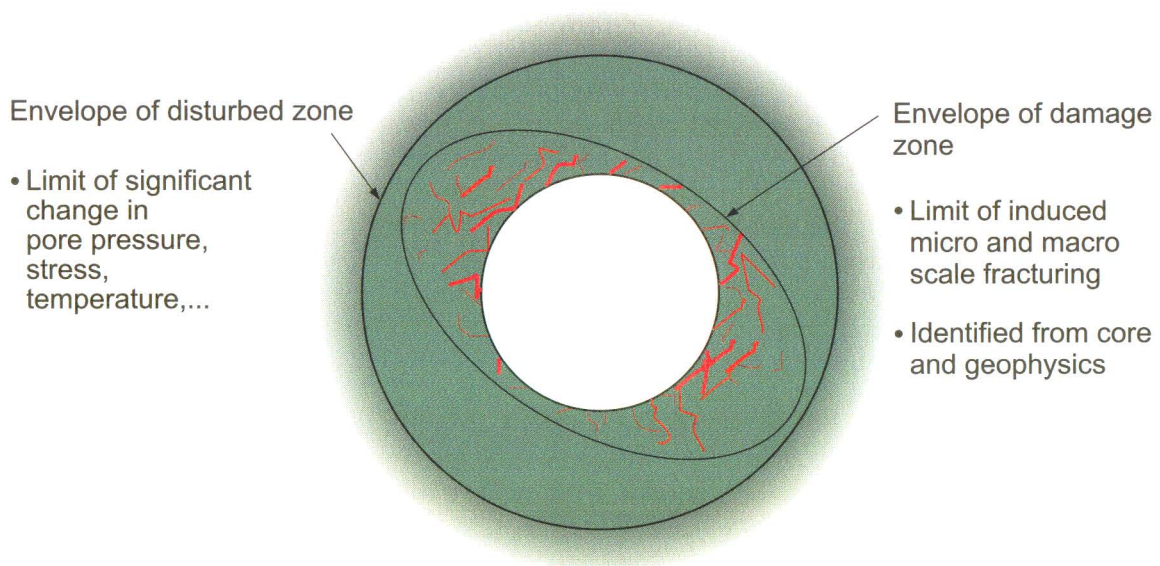


Fig. 5.1: Schematic illustration of excavation damage and disturbed zones

This chapter is aimed at presenting the concepts for quantitative assessment of axial flow around repository seals and of the distortion of the natural groundwater flow fields around emplacement caverns due to flow enhancement in the disturbed zone. The concepts are applicable to fractured hard rock formations, characterised by a network of natural and excavation-induced fractures which determines the large-scale effective hydraulic conductivity. They are less suitable for soft rock formations (e.g. clay), where

plastic deformation and hydrochemical alteration of the wallrock may have a strong impact on the hydraulic properties of the EDZ. The chapter is structured as follows:

- Chapter 5.1 presents an extended discussion of the role of the EDZ in performance assessment, addressing axial flow around repository seals and large-scale flow enhancement around emplacement caverns. Further aspects are mentioned, such as transport properties and long-term evolution of the EDZ.
- Chapter 5.2 gives a compilation of site-specific information on those rock properties, which may impact groundwater flow processes in the tunnel near-field at the GTS. The data include structural data from tunnel and core mapping, stress measurements and hydraulic characterisation of the tunnel near-field.
- In chapter 5.3 different types of conceptual models for flow in the EDZ are described. Deterministic models, assuming a circular zone of increased permeability around the tunnel are compared with fracture network models. Finally, results of sensitivity analyses are shown.
- Chapter 5.4 presents a brief discussion of unresolved issues. In particular, possible experiments are proposed for validation of numerical models of axial flow.

5.1 Importance of the EDZ for repository performance

The EDZ issues relevant to performance assessment were briefly presented in chapter 2.1. This section describes possible effects of the EDZ in more detail and presents discussions intended to highlight the requirements of performance assessment.

5.1.1 The disturbed zone around repository seals

In an assessment of the safety of a deep repository for spent nuclear fuel, SKB described plans for “plugging” access drifts and shafts with highly compacted bentonite (SKB 1992). It was also suggested that such seal zones might be placed so as to isolate fracture zones intersected by tunnels containing spent fuel deposition holes. Similar seal zones have been designed for the proposed L/ILW repository at Wellenberg. The current design includes seal zones within the access tunnels and at the entrance to each emplacement cavern (NAGRA 1997). The existence of a permeable EDZ around such seal zones could compromise the effectiveness of the seals and lead to higher groundwater flow through the excavations.

As seal zones are only required to be of limited size and number (sufficient to cut any high permeability path), it is possible to select suitable zones for the seals and to implement additional engineering measures to ensure their integrity. Such measures might include the excavation of “EDZ Cut-offs” (slots of increased radius to cut the EDZ, cf. MARTIN et al. 1996) and selection of favourable excavation methods and shapes (READ 1996). Thus, although the potential impact of the EDZ may be most important when considering seal zones, there may also be the greatest opportunity to mitigate the effects of the EDZ.

5.1.2 The disturbed zone around emplacement caverns

The second effect that needs to be considered is the ability of the EDZ to focus flow from the host rock into a more permeable EDZ and possibly into the waste emplacement excavations. For the case of a spent fuel repository in crystalline rock,

BENGTSSON et al. (1991) considered the case where regional flow was either perpendicular to an emplacement tunnel or parallel to it. They assumed that, for the purpose of the calculations, the rock could be treated as an effective porous medium. For the case of flow perpendicular to the tunnel they estimated that flow through the EDZ would increase by a maximum of a factor of 2 over that expected when the EDZ was not significantly more permeable than the host rock. However for flow along the tunnel they suggest that the increase in flow is almost proportional to the increase in permeability of the disturbed zone to the surrounding rock mass. Given that existing assessments have suggested permeability enhancement factors of 100 or more (e.g. SKB 1992 and NAGRA 1985a, 1994), the consequences of such a flow redistribution need to be included any assessment of groundwater flow around the repository. Such effects may be even greater where flow is in discrete fractures and an assumption of equivalence to a porous medium may not be valid at the scale of the EDZ (order of metres).

The size of emplacement caverns for L/ILW may limit the choice of position and engineering to reduce EDZ effects. It is therefore necessary to account for the effects of the EDZ in the flow models. Detailed modelling of groundwater flow and transport around excavations using both equivalent porous medium (NAGRA 1997 and NIREX 1997) and discrete fracture network approaches (NAGRA 1997) has included explicit representations of the EDZ. In continuum models, zones of increased conductivity have been added around the excavations, while in the fracture network models local fracture transmissivities have been increased. In both cases relatively simple models of permeability enhancement have been used. In simple geometries where the excavation can be considered as an "inclusion" of higher permeability rock within a lower permeability host rock, the effects of the EDZ around excavations can be scoped using analytical methods similar to those from Potential Theory (LANDAU & LIFSHITZ 1984).

5.1.3 Evolution of the disturbed zone

It is important to note that, although the focus has been on the role of the EDZ in the post-closure situation after several tens of years of operation and subsequent resaturation, it is expected that the EDZ will change with time. These changes will be rapid during initial excavation and desaturation but may continue for some time after this with the development of a drying front. In addition, thermal loading due to emplacement of heat-generating waste and chemical disturbances due to waste and backfill will perturb the system. With regard to mechanical processes, PUSCH (1993) considers the effects of time-dependent strain on a repository in crystalline rock and the possibility for long-term evolution of the EDZ. It is suggested that such effects typically result in strain rate following a "power law". A special case that has some support from experimental evidence is where strain rate changes with the inverse power of time resulting in total strain changes proportional with log-time. Observation of strain changes early in the excavation would allow some degree of prediction of whether the suggested "log-time" dependence occurs. PUSCH concluded that time-dependent strain effects were unlikely to cause significant changes in the rock around emplacement holes, but that the unsupported roof of an emplacement cavern might fail over timescales of a few hundred years. Such long-term evolution of the disturbed zone is, however, outside the scope of this report.

The experimental work at GTS and other sites has however demonstrated that it is important to address the changes that occur immediately after excavation and the initial desaturation of the rock around a tunnel. Furthermore the requirement to describe the post-closure situation means that it is necessary to anticipate the consequences of

tunnel backfilling (by sealing or waste emplacement) and resaturation of the excavations. Simple analytical models of the rock mass response have been used in the studies for GTS Phase IV, but ideally measurements of the near-field should be made under conditions as close as possible to those relevant to post-closure to minimise the uncertainties that will derive from any extrapolation of conditions.

5.1.4 Performance assessment

In performance assessment the excavation disturbed zone presents a potential fast flow for transport of radionuclides from the repository to the biosphere. The properties required for such an assessment relate to the permeability, porosity and fracture surface properties of the rock in the EDZ together with their spatial distribution. In previous studies the focus has been on describing a region of enhanced permeability and transport properties of the EDZ have received relatively little attention. Tracer experiments for characterising the porosity of the EDZ have been performed at the Underground Research Laboratory at Pinawa in Canada and further experiments are planned (FROST & EVERITT 1997, CHANDLER 1998). Calculations described in BENGTTSSON et al. (1991) suggest that additional porosity and fracture surface area should be ascribed to the damage zone. Fresh fracture surfaces may also be more reactive than natural fractures (PUSCH 1993). Such properties are however difficult to characterise and typically it has been assumed that the EDZ is simply a zone of enhanced permeability with other matrix and fracture properties similar to those of the host rock. In host rocks other than crystalline porosity changes may be significant; see for example FREEZE et al. (1998).

5.2 EDZ investigations at the GTS

This section focuses on the results from recent EDZ investigations at the GTS. Much of the data are specific to the particular location at which they were measured and it is expected that EDZ properties will be dependent on the following:

- Excavation method – tunnel boring machine (TBM) or drill and blast
- Excavation shape and orientation
- Rock strength, modulus and anisotropy
- Stress field – magnitude and orientation of the local stress field relative to excavation
- Fracturing – local fracture density, orientation and mechanical properties
- Degree of deformation – relationship to major shear zones or faults
- Pore pressure and saturation changes
- Temperature changes

The data described here come from three test zones within the GTS (cf. Figure 1.2):

- I. The EDZ site in the WT drift where small scale hydraulic tests were conducted using the Modular Multipacker System (MMPS, cf. Chapter 3.2) in the boreholes EZ-95.001 to 95.003. Three further boreholes (EZ-95.004 to 95.006) were drilled and used as part of the characterisation at this site.

- II. The ZPK site located between the BK and GS sites, where an integrated programme of EDZ investigations was performed in two parallel fans of four boreholes AZ-94.001 to 94.008.
- III. The BK site cross tunnel where additional tunnel mapping was performed.

All three sites are in the Central Aare granite although the EDZ site is close to the boundary of a volume of Central Aare granite with higher biotite content. The position of the sites at the GTS is shown in Figure 5.2. During the measurements, the tunnel walls in both areas were sealed with a resin to allow resaturation. It is expected that pore pressures and temperature are similar at both sites.

The EDZ site was in a section of tunnel excavated using a tunnel boring machine with a diameter of 3.5 m oriented 30 - 210° approximately parallel to the expected minimum horizontal stress. The experiments were deliberately performed in a region where an unusual level of tunnel wall damage occurred. The causes of the spalling observed in this area are uncertain although it may relate to operation of the TBM or a particular stress regime close to a lamprophyre dyke. A geological map of the tunnel is shown in Figure 5.3.

The ZPK site is located in an approximately 4 m square section of drill and blast tunnel connecting the GS and BK test sites. The connecting tunnel is oriented at approximately 335° almost parallel to the expected maximum horizontal stress direction in that part of GTS. Two sets of 4 boreholes arranged in a plane normal to the tunnel were the subject of an integrated programme of geological, geophysical and hydraulic tests. A shear zone feature cuts the GS tunnel obliquely while a major shear zone intersects the BK site. The test site lies in relatively unfractured rock between these two structures.

The cross-tunnel site was used for surface packer testing and geological mapping and is close to the ZPK site. It is again in a drill and blast tunnel of 4 m square cross-section.

Although stress measurements were performed at the ZPK site, no measurements were made of the local stresses prior to excavation for any of the sites. The expected stresses have however been estimated for both the EDZ / WT and ZPK / BK sites. The estimates of pre-excitation stresses are given in Table 5.1. The stresses estimated for the WT site were derived from a three-dimensional model of stress around the GTS (KONIETZKY 1995). The expected stresses for the BK site were derived from previous rock mechanics investigations (PAHL et al. 1989). The expected stresses around the BK and WT excavations are shown in Figure 5.4. The local stresses are shown as contours of the property:

$$\sqrt{\frac{(\sigma_1 - \sigma_2)^2 + (\sigma_2 - \sigma_3)^2 + (\sigma_1 - \sigma_3)^2}{2}}$$

This property is related to the second stress invariant and the octahedral shear stress.



Fig. 5.2: GTS Map showing the two ZPK and the EDZ experimental sites

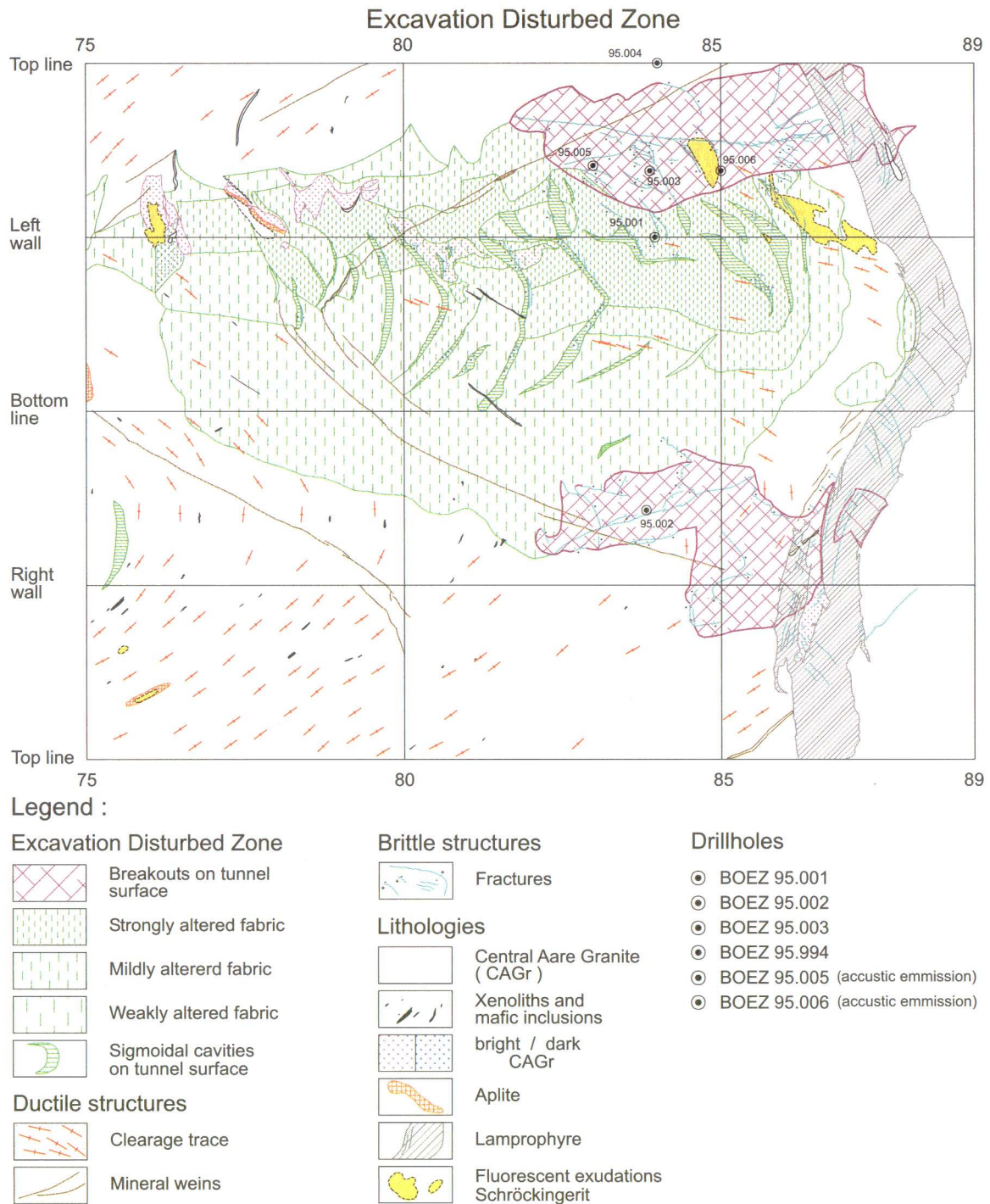


Fig. 5.3: Geological map of the EDZ site showing the breakout zone

The stresses around the ZPK / BK tunnel have been calculated using the Adina finite element program (ADINA FEM Programming System Version 6.1.5) while the stresses for the EDZ / WT tunnel are calculated analytically from the Leeman-Hayes equations (HAYES 1966). Stresses close to the tunnel wall are higher in the EDZ / WT site because the tunnel is approximately parallel to the minimum stress, while the ZPK / BK tunnel is parallel to the maximum stress and only a small stress anisotropy is expected between the intermediate and minimum stress.

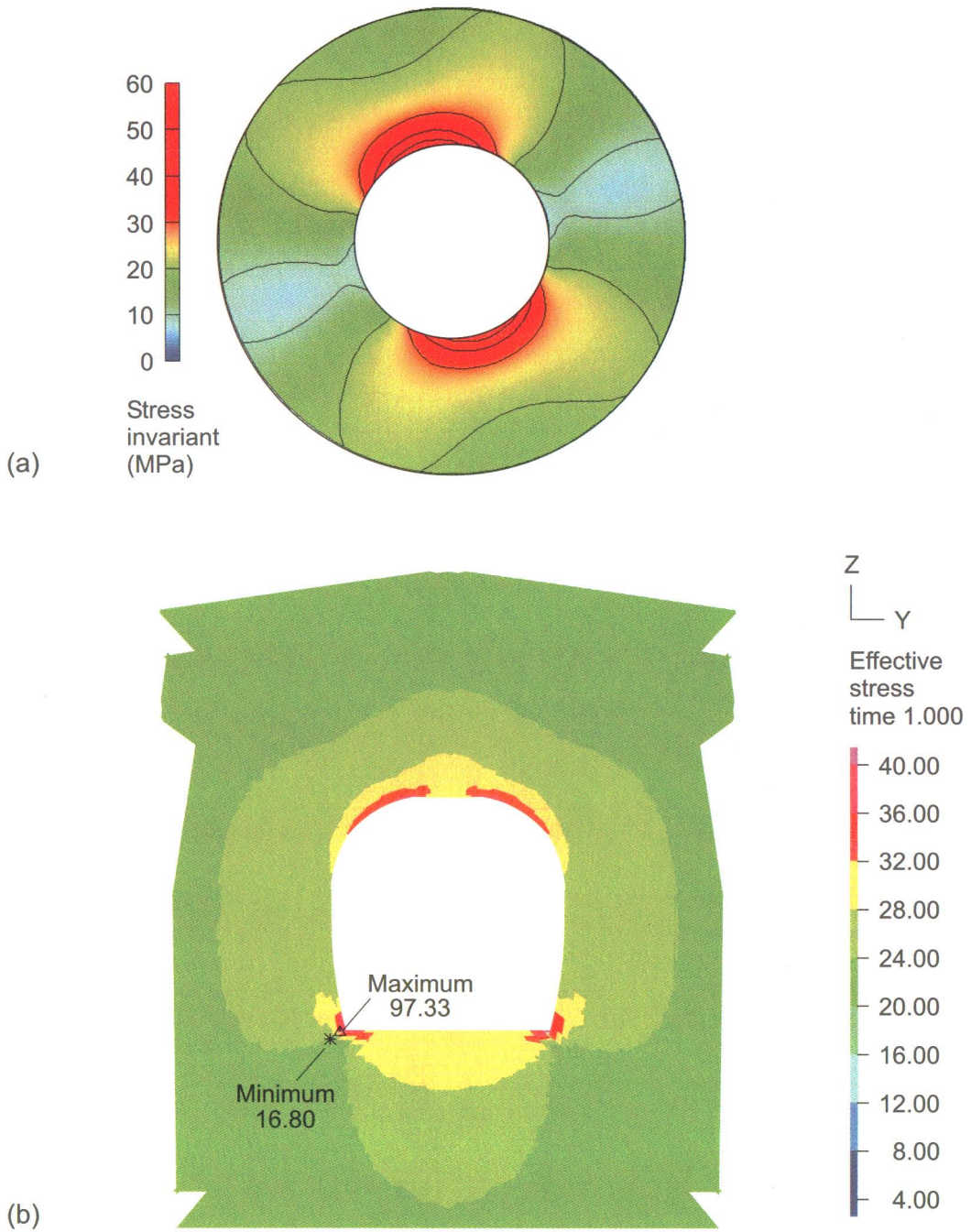


Fig. 5.4: Stresses around the EDZ/WT and ZPK/BK tunnels: (a) stress invariant for EDZ / WT area tunnel calculated from analytical solution for continuum homogeneous linear elastic material and (b) stress invariant for ZPK area tunnel calculated using the Adina finite element system.

Table 5.1: Interpretation of stresses at the ZPK / BK and EDZ / WT sites

	Predicted Stresses for EDZ / WT site		Predicted Stresses for ZPK / BK site	
	Magnitude (MPa)	Orientation Dip/Dip Direction	Magnitude	Orientation Dip/Dip Direction
σ_1	25.7	18 / 125	35	Parallel to BK tunnel (σ_H)
σ_2	12.9	32 / 23	15	Orthogonal to BK tunnel (σ_h)
σ_3	7.7	52 / 239	10.15	Vertical (σ_v)

tes at the GTS, results from the work can be compared with results from a variety of other sites (see Chapter 6). Comparisons with the Underground Rock Laboratory in Canada at similar depths are not appropriate because of the much higher horizontal stresses encountered at that site.

5.2.1 Rock matrix in the disturbed zone

The properties of the rock matrix have been studied using a range of techniques:

- Optical microscopy of thin sections from borehole cores
- Single and crosshole sonic measurements
- Core gas permeability measurements
- Surface and short interval air and water packer tests

Geological and geophysical properties of the matrix

The results from optical microscopy of core taken from one borehole at the ZPK site show that micro-fracturing is clearly associated with observed discontinuities and a set of "EDZ" micro-fractures were identified which were unmineralised and had a distinctive zig-zag geometry. Such features were common close to the tunnel wall and were limited to a distance of about 0.3 m from the tunnel wall. The distribution of microcracks and fractures for a single borehole core is shown in Figure 5.5.

Sonic measurements both along hole and cross-hole at the ZPK site showed considerable reductions in P- and S-wave velocities in the regions with 0.5 m of the tunnel. However after sealing and resaturation of the rock around the tunnel these effects were considerably reduced, especially with regard to the P-wave measurements. However there is still evidence for some reduction in velocity after resaturation within the first 0.3 m of rock and close to specific features. The observed dependence on saturation demonstrates the importance of making measurements of rock properties under fully saturated conditions.

At the EDZ site only limited geological characterisation of the boreholes was possible due to poor core recovery and limited geophysical imaging. Estimates of the depth of breakout zone were made based on the observed dinking and core recovery, which suggested that in two of the boreholes, a "breakout zone" might extend up to 1.5 m from the tunnel wall.

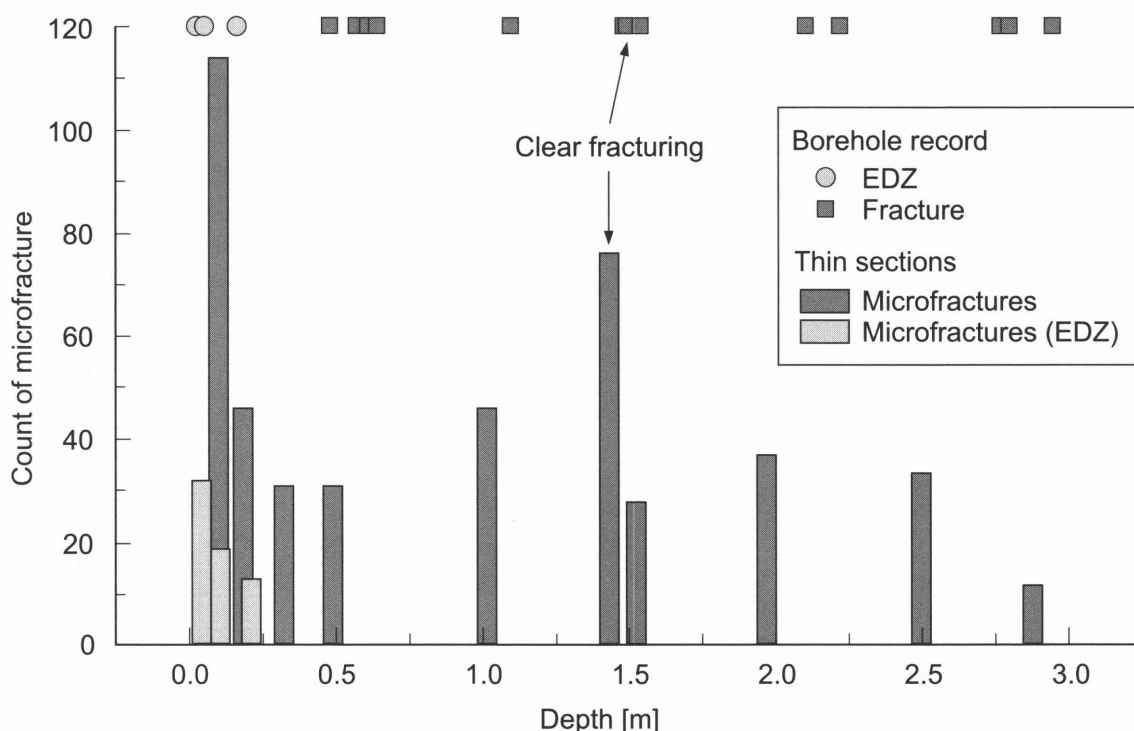


Fig. 5.5: Depth dependence of micro-fractures in AZ-94.006 from ZPK/BK site

EDZ matrix permeability

A compilation of intrinsic permeability values for the rock matrix close to the tunnel wall is given in Table 5.2. The results are drawn from both core and packer tests. Values are summarised as mean ± two standard errors, the range for all measurements is given in brackets. Where multiple tests have been performed on a single interval, the results have been averaged for each interval for the purpose of calculating the mean and standard error.

Gas permeabilities were measured for cores from one borehole at the ZPK / BK site. The core samples may have additional micro-fracturing due to drilling. Packer testing was performed both at the BK and EDZ sites and data from intervals without identified macroscopic fractures have been selected in Table 5.2. Tests at the ZPK / BK site used both air injection and combined air/water tests. Analysis of the MMPS tests from the EDZ / WT site provided estimates of hydraulic conductivity which have been converted to intrinsic permeability assuming a density of 1000 kg m⁻³ and a viscosity of 10⁻³ Pa.s.

The results are remarkably consistent for all measurements within 1 m of the tunnel wall. Permeabilities range from 1 to 4 · 10⁻¹⁸ m² in both the sites. In general no significant depth trend is visible over the first metre of tunnel wall within each dataset. However the more distant 0.5 m long MMPS intervals have a permeability of 2-3 · 10⁻¹⁹ m² almost an order of magnitude lower than the values for short intervals close to the tunnel wall.

Table 5.2: Matrix intrinsic permeability measurements at the EDZ sites.

Data Source	All tests performed			Tests within first 0.5 m	
	Permeability (m ²)	No. of tests	Depth range (m)	Permeability (m ²)	No. of tests
BK EDZ site / gas permeability core AZ-94.002	$3.2 \pm 0.6 \cdot 10^{-18}$ ($1.9 - 4.0 \cdot 10^{-18}$)	6	0.1 - 3	$3.2 \pm 1.0 \cdot 10^{-18}$ ($1.9 - 4.0 \cdot 10^{-18}$)	4
ZPK site/ air permeability short interval tests in AZ-94.001-94.006	$2.5 \pm 0.5 \cdot 10^{-18}$ ($0.1 - 4.0 \cdot 10^{-18}$)	16 tests in 8 intervals	0 - 1	$2.5 \pm 0.5 \cdot 10^{-18}$ ($0.3 - 3.6 \cdot 10^{-18}$)	10 tests in 5 intervals
EDZ site / MMPS data for EZ-95.001 and 95.003	$1.8 \pm 0.9 \cdot 10^{-18}$ ($0.8 - 3.0 \cdot 10^{-18}$)	10	0.1 - 1	$2.5 \pm 0.6 \cdot 10^{-18}$ ($2.0 - 2.4 \cdot 10^{-18}$)	4
EDZ site / MMPS data (0.5m intervals) EZ-95.001 to 95.003	$2.3 \pm 0.7 \cdot 10^{-19}$ ($2.0 - 3.0 \cdot 10^{-19}$)	3	2.0 - 2.5		

Summary of matrix properties of the EDZ

There appears to be evidence for a zone of induced micro-fracturing extending 0.3 m around the tunnels at the BK site. Observations from the EDZ site suggest that such micro-fracturing may extend further to about 1.5 m in particular directions around the tunnel. This difference probably relates to the different stress fields around the excavations.

The zone around the ZPK / BK site may be associated with a reduction in P- and S-wave velocity. However the extent of this zone can only be determined when the rock is fully saturated. No measurements of sonic velocity are available from the EDZ site.

Measurements of matrix permeability in the zone from 0 to 1 m around the tunnel wall from both sites suggest a value of approximately $3 \cdot 10^{-18}$ m². The permeability of the rock matrix outside this zone may be lower and the MMPS results for intervals 2 to 2.5 m from the tunnel show a value of $3 \cdot 10^{-19}$ m². This suggests that, around the excavation there is a zone of elevated matrix permeability extending to a maximum of 2 m. Beyond this zone, matrix permeability is unchanged with a value of approximately $3 \cdot 10^{-19}$ m². A single core analysis from AZ-94.002 at 2.88 m depth gave a permeability of $3.7 \cdot 10^{-18}$ m² but this higher value may result from microfracturing induced by coring. It should be pointed out that this increase in matrix permeability is unlikely to have a significant impact on groundwater flow if fracture flow dominates.

The very low values of matrix permeability measured in the near-field at GTS suggest that unless fracture flow is significant the dominant flowpath around any seal may relate to the interface between the seal and the host rock.

The porosity of the matrix may be slightly greater than the undisturbed matrix because of the increased microfracturing. However this is likely to be a small effect and can be ignored. It should be noted that, at more extreme stresses (eg. those found at the

URL), the matrix may totally fail, resulting in a zone of highly fractured rock with a permeability much greater than those given above. Measurements in the "Mine-By" tunnel at the URL suggest a permeability of 10^{-13} m^2 within a shallow failure zone around the notch (CHANDLER et al. 1996).

5.2.2 Fractures in the disturbed zone

It is expected that the dominant flowpaths within the disturbed zone will relate to fractures. These may be natural or induced fractures. Fractures may be induced by the excavation process itself or by stress redistribution caused by the existence of the void. The term fracture is used here to cover a range of scales.

Fractures in the EDZ were characterised using

- Geological mapping from core and tunnel walls
- Borehole logging using television systems
- Sonic measurements in boreholes
- Packer testing using air and water in selected intervals containing fractures

Ideally the natural fracture system should be characterised away from the disturbed zone in order to determine a representative characterisation of the host rock. Once this has been accomplished it would then be possible to compare characteristics between fractures inside and outside the EDZ. A problem arises however in that near-field studies necessarily involve a smaller scale of investigation and measurement. For example, the tunnel wall may act as a constant head boundary and hence limit the range of investigation of any hydraulic test to a few 10s of centimetres. Properties measured at this smaller scale may not be directly comparable with those measured in the host rock away from excavations. For example, the very high resolution packer testing (typically 0.1 m interval length) conducted in the EDZ work is difficult to compare with other testing performed at the GTS.

Geological and geophysical characterisation of the fractures in the EDZ

Geological mapping of the EDZ site (excavated using a TBM) identified EDZ fractures in the tunnel wall and in the first 0.2 m of two boreholes. In one of these boreholes, the EDZ fractures were associated with a single natural fracture that ran along the borehole.

Geological mapping of the tunnel wall at the ZPK / BK site also identified EDZ fractures at the tunnel wall which were correlated with features observed in the borehole. In general such fractures were shorter in extent than the natural fractures. In addition not all EDZ fractures in the boreholes could be extrapolated to the tunnel surface, suggesting that they may terminate within the rock mass. Data from boreholes at the ZPK / BK site show a clear reduction in open discontinuities with distance from the tunnel wall, with such features being much less frequent beyond the first 0.3 m of the tunnel wall.

The observations support a picture where EDZ fractures are limited to a small volume around the tunnel of less than 0.3 m at the ZPK / BK and EDZ sites. However there were difficulties in imaging the AZ boreholes so it is possible that EDZ fractures may exist at greater distances from the tunnel wall. It is also likely that such fractures may exist at greater distances where the rock is either weaker, influenced by a fault or shear

zone or where the tunnel orientation is sub-parallel to the natural fracture system. At the ZPK / BK site it was observed that the EDZ fractures connect with the natural fracture system and are in general sub-parallel to the tunnel wall. Pre-existing natural fractures may also be disturbed and re-opened.

Sonic measurements identified open fractures in a small number of cases where there was significant attenuation across the fracture. This occurred both before and after sealing and resaturation.

Fracture flow properties in the EDZ

At all the experimental sites natural fractures were observed to be associated with flow. At the EDZ site the most permeable intervals characterised by the MMPS system were related to a single natural fracture that ran along one borehole. However the fracture was not uniformly permeable. At the ZPK / BK site, air injection tests showed heterogeneous flow paths through the EDZ and natural fractures. When air was injected into fractured intervals in boreholes, air bubbles were observed in clusters of 0.2 m to 0.3 m in extent along the length of the fractures and at fracture intersections in the tunnel wall. This suggests typical "channel" widths of the same dimension for flow within the EDZ at the GTS. This is in agreement with the results from testing along the fracture intersected by the MMPS system. There may in addition be finer scale channelling.

In order to be consistent with previous discussion of intrinsic permeability in m^2 , the hydraulic property of an interval or of a single feature is described here by its transmissibility in $\text{m}^2 \text{m}$, which is the permeability times interval length or feature height. Figure 5.6 shows the pattern of transmissibility of 0.1 m intervals from air injection tests at the ZPK / BK site. These tests were performed over 0.1 m intervals in the horizontal and upward pointing boreholes. The air injection tests were analysed assuming steady state flow to a fixed pressure boundary at constant radius. The position of the tunnel wall may have led to an overestimate of transmissibility for the tests closest to the tunnel. The bottom part of the graph is shaded below the line corresponding to the transmissibility of a 0.1 m interval of matrix permeability $3 \cdot 10^{-18} \text{m}^2$ for comparison. Intervals identified with fractures or breaks are shown in red, while matrix intervals are shown in blue. There is a very clear reduction in transmissibility with distance from the tunnel wall, with little effect beyond 0.5 m. Subsequent focused testing using both water and gas confirmed the results from the air injection tests, although typically the water permeabilities were slightly lower than those estimated from the gas tests. These combined tests were analysed using a Finite Element programme and gas entry pressures were also determined for each feature tested.

Measurements of the transmissibility (permeability x thickness) of induced and natural fractures in the EDZ come from both the ZPK / BK and EDZ sites. Table 5.3 gives the results from analysis of the air/water injection tests at the ZPK / BK site targeted on fractures as well as the results from testing of intervals associated with a single natural fracture using the MMPS at the EDZ site.

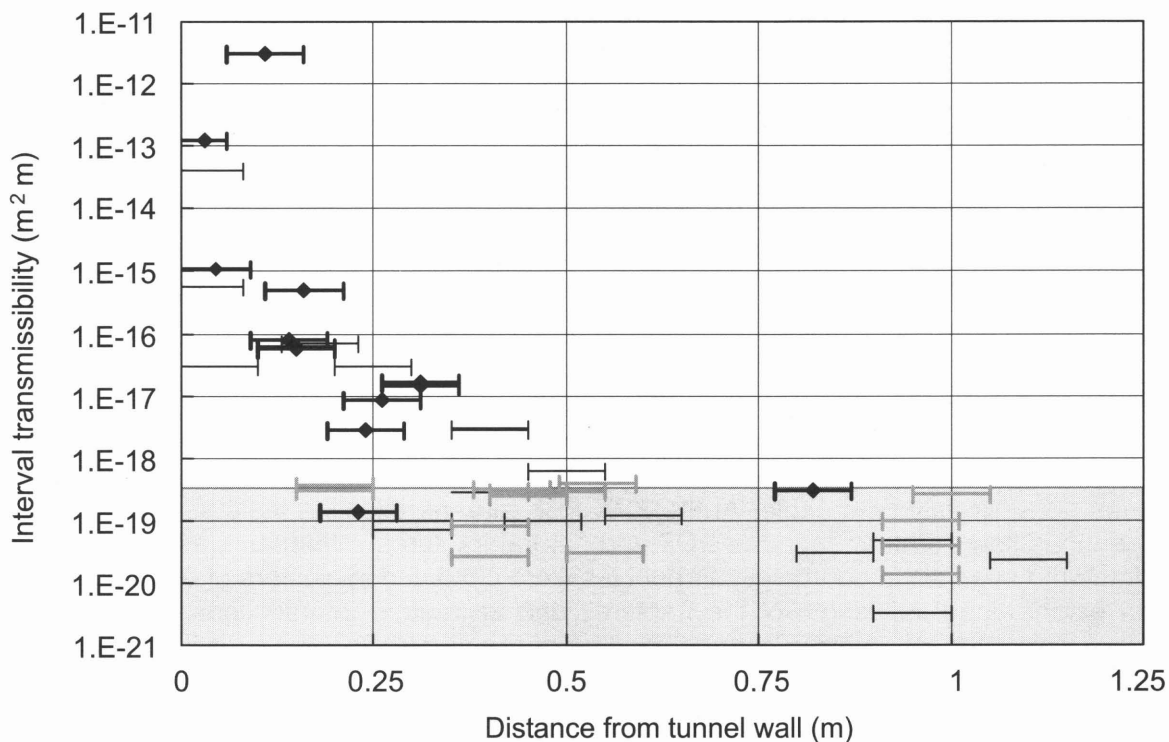


Fig. 5.6: Interval transmissibility with distance from tunnel

Table 5.3: Fracture transmissibility

	Transmissibility Range	Comments
ZPK / BK site - Air Injection Test Intervals identified as containing "fractures or breaks"	$1 \cdot 10^{-19} - 3 \cdot 10^{-12} \text{ m}^2 \cdot \text{m}$	Only possible to perform tests in horizontal and upper holes Strong dependence on distance from tunnel wall.
ZPK / BK site – Air / Water Injection Test	$4 \cdot 10^{-19} - 1 \cdot 10^{-14} \text{ m}^2 \cdot \text{m}$	Water transmissibility for selected intervals
EDZ site	$1 \cdot 10^{-19} - 3 \cdot 10^{-15} \text{ m}^2 \cdot \text{m}$	5 Intervals (length 0.1 m) cut by single fracture running along bore-hole

Summary of fracture properties in the EDZ

Results from the ZPK / BK site air / water injection tests suggest fracture permeabilities ranging from 10^{-11} to 10^{-15} m^2 and transmissibilities from $4 \cdot 10^{-19}$ to $10^{-14} \text{ m}^2 \cdot \text{m}$. The testing using the MMPS system suggested that the transmissibility of a single fracture ranged from 10^{-19} to $3 \cdot 10^{-15} \text{ m}^2 \cdot \text{m}$. The results demonstrate that the fracture system is very heterogeneous containing features that are: slightly more transmissive than a few cm of matrix; permeable channels in fractures and even more permeable open breaks or ruptures. It is expected that the groundwater flow will be controlled by the connectivity of the most permeable features.

Work on the results from the ZPK / BK site has allowed a detailed classification of the feature system in which individual features have been examined to determine whether they are induced or natural fractures and a sophisticated hydraulic classification for each feature. This has also allowed the identification of EDZ fractures in the tunnel walls and estimates of EDZ fracture size for this site to be developed. The nature of the interconnections between the different features is, however, difficult to determine. The experimental results suggest that while the induced and natural fractures are interconnected, such connections are not simple and may be highly tortuous.

Measurement of properties within the disturbed zone

It should be noted that, at both EDZ sites, it was found that the properties of the matrix and fracture system were dependent on saturation. This was evident in both the geophysics and the hydraulic measurements. The requirement to predict post-closure properties means that the effects of such saturation changes must either be well understood or minimised between the characterisation conditions and those expected post-closure. Realistically, given the complex geometry both within fractures and of the fracture network itself, it is preferable to minimise such differences and to make the characterisation measurements under conditions as close as possible to those expected post-closure. Unexpected effects around tunnels and drifts have been reported by LONG et al. (1992), that are believed to be due to groundwater degassing and resulted in changes in hydraulic properties local to a drift of one or more orders of magnitude (cf. chapter 4.4).

5.3 Conceptual model of flow in the excavation disturbed zone

The conceptual model for flow in the disturbed zone derived from the GTS results and experience at other sites is described below. The model is based on the groundwater flow paths discussed above.

Within the disturbed zone there may exist a “failure zone” where the intact rock has substantially lost its competence and which may have a high permeability. No such zone was identified at either of the GTS sites. Where such failure zones do exist they may be very sensitive to state changes (MARTIN et al. 1996). In general predicting the properties of such a zone will be difficult and excavation techniques (orientation and support) should be chosen to avoid the creation of such zones.

There may also be a damage zone where the intact rock has a greater density of micro-fracturing and macroscopic fractures. In addition to new fractures, existing discontinuities may have been reactivated and opened. The nature of this induced fracturing and reactivation will be dependent on the excavation method and stress redistribution caused by excavation and associated changes in temperature and pore pressures.

In hard crystalline rocks changes in matrix permeability will be relatively small and confined to a zone close to the tunnel wall. Unless the fracture density of the rock is very low, it is not expected that these changes will have a significant impact on groundwater flowpaths.

The dominant changes in hydraulic properties will be due to changes in the transmissibility of natural fractures and the creation of induced fractures. The relationship between natural and induced fractures is expected to be complex and result from interactions of the excavation process with the natural fracture system. The ability of the EDZ to act as a flowpath at scales above that of a single fracture will be controlled by the

connectivity of the fracture network which may be difficult to determine. At the GTS, results indicate that the heterogeneous fracture network around the tunnel will be complex and flowpaths may be highly tortuous.

5.3.1 Conceptual model of the EDZ around the ZPK / BK site

The use of drill and blast excavation and the relatively low anisotropy expected between the vertical and horizontal stresses acting around the tunnel at the ZPK / BK site suggests the following model:

Matrix permeability is approximately $3 \cdot 10^{-18} \text{ m}^2$ in the zone within 1 m of the tunnel wall. At greater distances matrix permeability reduces to approximately $3 \cdot 10^{-19} \text{ m}^2$.

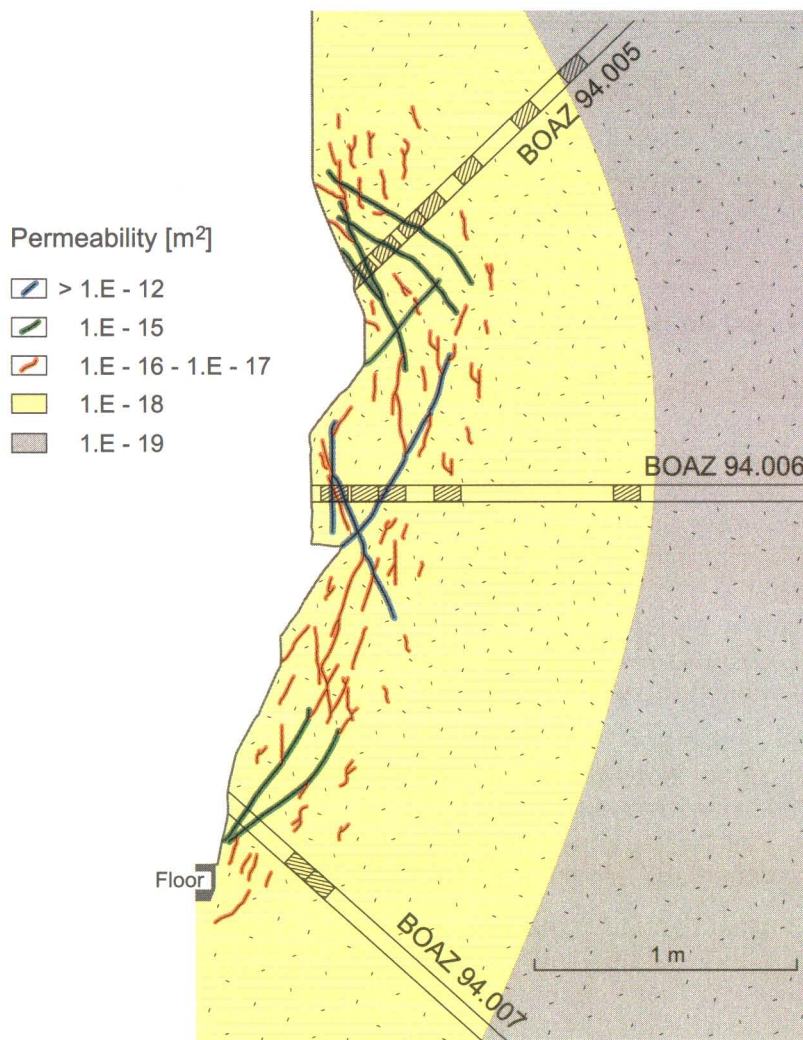


Fig. 5.7: Conceptual model of permeability distribution in the EDZ around the BK site

Induced fractures have been created within the first 0.3 m of the tunnel wall and natural fractures may have been re-opened. The damage zone containing such fractures appears to be confined to the first 0.5 m. Outside this zone there is no evidence of per-

meable fractures. Fracture permeability ranges from 10^{-11} to 10^{-15} m² in the EDZ. Figure 5.7 illustrates the conceptual model of permeability distribution developed for this site.

The network of induced fractures and permeable channels within natural fractures has been observed to be tortuous, but connected over several m.

Uncertainties in the extent of induced fracturing are due to the limited data coverage of the gas testing as higher levels of damage are frequently seen in tunnel floors and Figure 5.4 shows stress concentrations created by the excavation geometry in the tunnel floor.

Significant stress redistribution and pore pressure changes will extend over many metres from the tunnel, potentially changing the hydraulic properties of stress-sensitive fractures. The focus of the experimental programme close to the tunnel, together with the low frequency of permeable natural fractures, means that it is not possible to determine the importance of the effect from the observations. Instead any estimates of the importance of this effect must be derived from estimates of fracture stiffness and magnitude of effective stress change.

5.3.2 Conceptual model of the EDZ around the EDZ site

The use of a tunnel boring machine and the higher anisotropy expected between the vertical and horizontal stresses acting around the tunnel at the EDZ site suggests the following model:

Matrix permeability is approximately $3 \cdot 10^{-18}$ m² in the zone within 1-2 m of the tunnel wall. The pattern of this permeability enhancement may be related to the stress anisotropy and induced micro-cracking. At greater distances from the tunnel, matrix permeability reduces to approximately $3 \cdot 10^{-19}$ m².

Induced fractures have been created within the first 0.3 m of the tunnel wall and natural fractures may have been re-opened to a greater distance. The damage zone containing such fractures appears to be confined to the first 1 - 2 m. The most permeable intervals around the tunnel were associated with a natural fracture in a single borehole. The lack of core and limited ability to image the boreholes makes the relative importance of induced fractures and natural fractures uncertain.

Cross-hole testing between boreholes indicated very limited connection around the tunnel, while pore pressure measurements suggest that channels within the natural fracture connect back to the tunnel wall.

Uncertainties in the extent of induced fracturing are caused by the limited number of boreholes as the pattern of induced stresses may be complex as shown in Figure 5.4.

Significant stress redistribution and pore pressure changes will extend over many m from the tunnel, potentially changing the hydraulic properties of stress-sensitive fractures. The focus of the experimental programme close to the tunnel, together with the low frequency of permeable natural fractures, mean that it is again not possible to determine the importance of the effect from the observations. The lack of pre-excavation measurements means that it is not clear whether the permeability of the single natural fracture tested has changed. Estimates of the importance of induced stress changes

must be derived from estimates of fracture stiffness and the magnitude of effective stress change.

5.3.3 Description of the disturbed zone for performance assessment

The conceptual model developed for the EDZ site has been used as the basis for development of analytical and numerical models of EDZ permeability for input to performance assessment. Uncertainties about the nature of induced fracturing led to the development of two models illustrated in Figure 5.8. Simple mechanical models based on a homogeneous linear elastic continuum have been used in this study. It was felt that uncertainties in fracture properties and the generic nature of the work did not justify a more sophisticated approach. However more complex discontinuum models of the EDZ site were considered by KONIETZKY (1995) and, in similar work for the Wellenberg project, heterogeneous continuum models have been used (VOMVORIS et al. 1997).

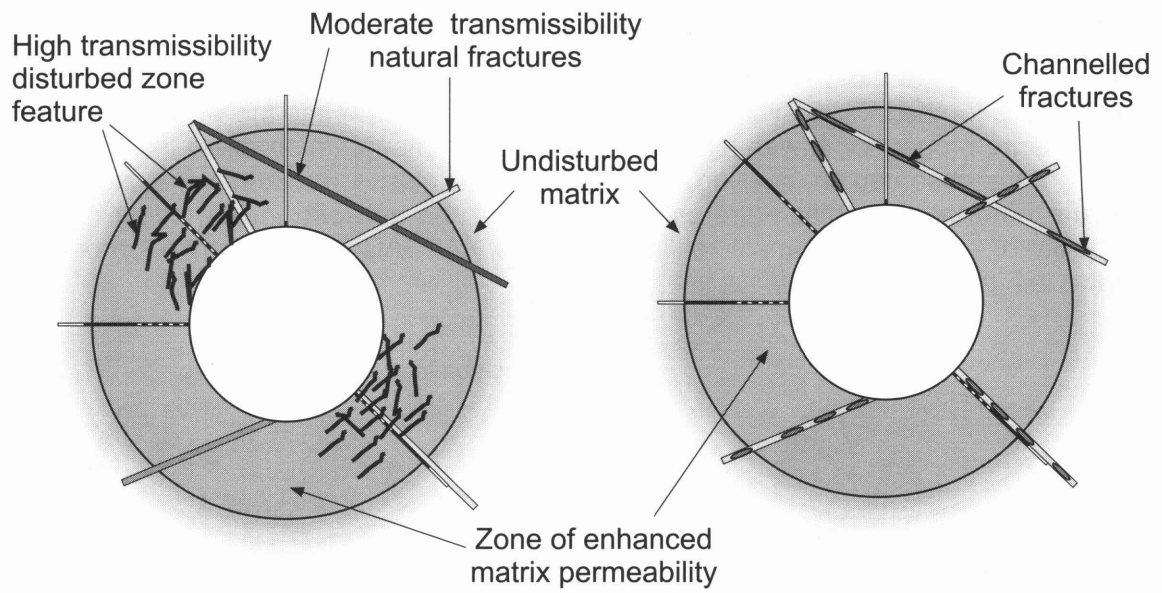
Upper bound for effective permeability around the tunnel

If it is assumed that the measurements of permeability made with the MMPS system are typical of the disturbed zone and that this may extend to a maximum of 2 m around the tunnel, it is possible to calculate an upper bound for the axial permeability. Assuming that the permeable features are infinite in length and arranged parallel to the tunnel, a maximum effective permeability can be calculated as the arithmetic mean of the individual measurements. The arithmetic mean permeability of the 15 intervals is $2.2 \cdot 10^{-15} \text{ m}^2$; however, the standard deviation is large and the standard error on the mean is $2 \cdot 10^{-15} \text{ m}^2$ implying a 95% confidence limit for the mean of $6.5 \cdot 10^{-15} \text{ m}^2$. This assumes that backfilling of the tunnel and resaturation have no significant effect on the permeability of the disturbed zone. The mean estimate of $2.2 \cdot 10^{-15} \text{ m}^2$ corresponds to a factor of 2000 increase over the estimate of the effective permeability for the back-ground rock at the GTS (i.e. excluding shear and fracture zones) of approximately 10^{-18} m^2 . This higher permeability zone might extend between 1 and 2 m from the tunnel wall. The calculation of this limiting value is based on assumptions of extensive tunnel-parallel uniformly transmissive features.

5.3.4 Numerical modelling of effective permeability around the tunnel

The analytical estimate of EDZ permeability assumed a highly connected system of tunnel-parallel conductors. Results from the both the EDZ and ZPK / BK sites suggest a heterogeneous system with tortuous flowpaths. The analytical estimate is therefore very over-conservative.

In order to investigate more realistic models of the EDZ it was decided to develop numerical models of the fracture system around the tunnel. Two model variants were considered: one where the high permeability intervals observed were related to damage zone fractures and the second where they were channels in natural fractures. The two models are illustrated in Figure 5.9 together with the profiles of hydraulic conductivity from the MMPS testing. The NAPSAC discrete fracture network code (HARTLEY 1998) was used throughout this study to implement the models.



(a) Model variant 1

(b) Model variant 2

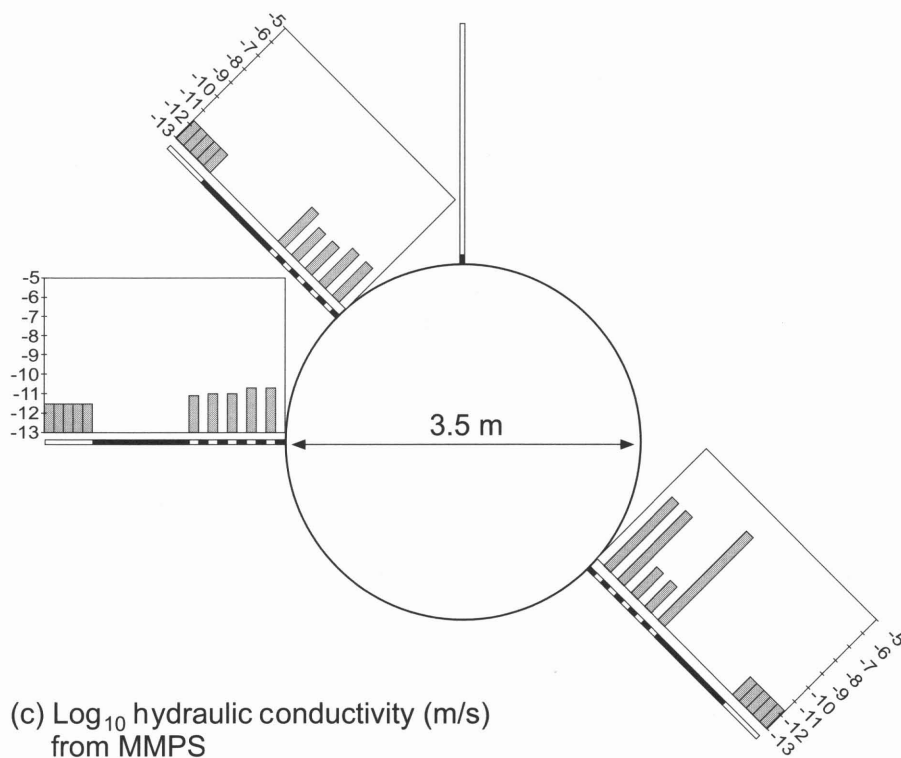


Fig. 5.8: Model variants used in axial flow calculations and field data from the GTS: (a) variant 1 - high transmissibility intervals are damaged zone features, (b) variant 2 - high transmissibility intervals are channels in natural fractures and (c) hydraulic conductivity profiles measured in the EDZ / WT area

NAPSAC discrete fracture network models of the EDZ

A generic model of the GTS fracture system had been previously developed for design calculations for the MMPS system. This model was taken over into the work to consider post-closure properties. It was felt that there was not enough information to develop a model of the observed channelling, so uniformly transmissive fractures were used. The fracture network properties were calibrated so that the network had an effective permeability of 10^{-18} m^2 . A sample realisation of the NAPSAC fracture network model is shown in Figure 5.9a.

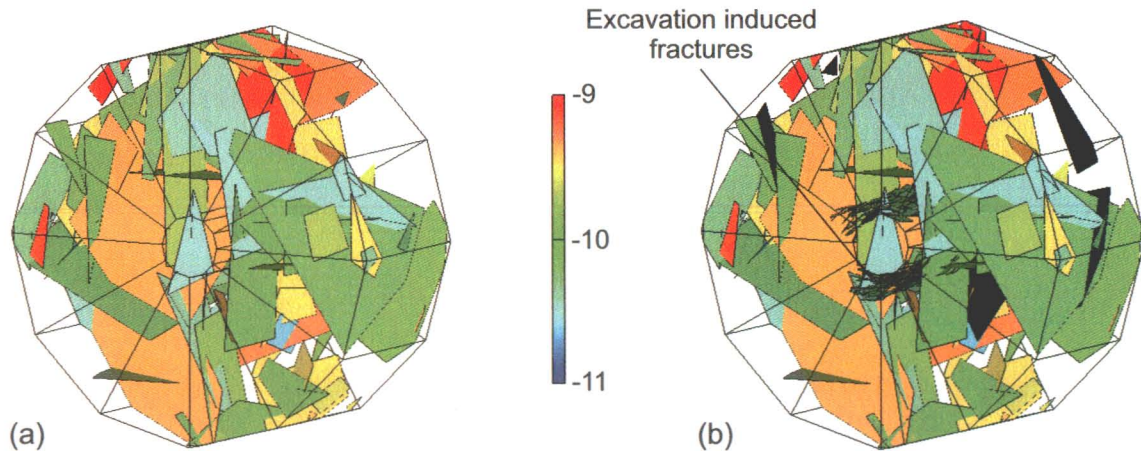


Fig. 5.9: Sample realisation from different models of fracture system around tunnel at EDZ site: natural fracture network (a) without damage zone and (b) with stress induced damage zone

The second model variant included additional EDZ features. There was very little information on the scale of such features and a variety of length scales were thus considered. In one case it was assumed that the features were relatively small (1 m square) oriented perpendicular to the local minimum principal stress (approximately tunnel parallel) while in a second case they were assumed to extend approximately 10 m along the tunnel. The density and transmissibility of such high permeability features were taken from those observed in the MMPS system, while the volume containing the features was delimited by a strain threshold derived from the predicted stress field. Figure 5.9b shows a realisation of this model of fracturing around the tunnel.

In order to predict post-closure flow and resaturation it was necessary to account for changes in pressure and stress between the situation during EDZ characterisation and that post-closure. The models used assumed that the major influence would be due to changes in effective stress normal to fractures. The approach is similar to that used in KELSALL et al. (1984). Shear deformations were assumed to be of minor importance but would require investigation as part of any more comprehensive analysis. Other factors such as temperature, fluid chemistry and fracture mineralisation might also be relevant but have not been considered here. The change in effective stress is due both to changes in total stress, from excavation and backfilling of the tunnel, and to changes in pore pressure.

While it has been possible to account for the pore-pressure and stress changes using analytical or numerical models, changes in saturation are more difficult to deal with. There is evidence of partially saturated behaviour in the well test data from the GTS

experiments but it has been assumed that, as properties of the more conductive intervals have been derived largely from recovery after injection, the effects should be minimised.

Stress from analytic solution for cylindrical void in homogeneous linear elastic material

Analytic solution for uniform pressure applied on a circular boundary
Operational phase pexcavation = 0.1 MPa
Post-closure phase pexcavation = 4.0 MPa

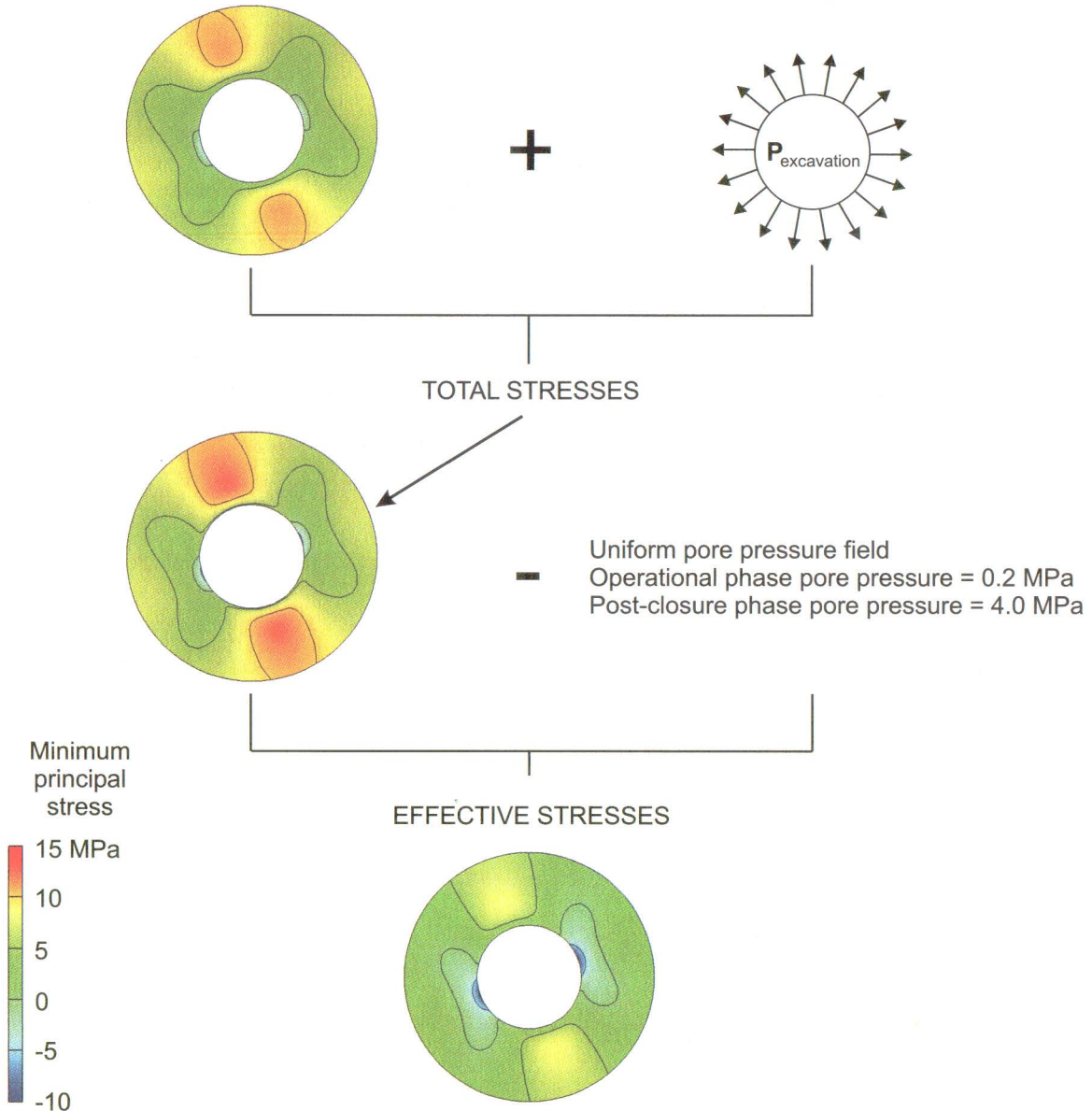


Fig. 5.10: Methodology for calculating total and effective stress around an excavation

The scheme used for calculation of stresses after backfilling and resaturation is illustrated in Figure 5.10. Figure 5.11 shows the total and effective stresses calculated for the operational and post-closure phases. It can be seen that the most important changes are in the effective stresses where pore pressure change is important. In particular

a large zone of tensile effective stresses is predicted in the post-closure case in zones away from the damage zone fractures. The existence of a tensile zone at the URL is discussed by MARTIN et al. (1996), where acoustic emission techniques were used to image excavation processes.

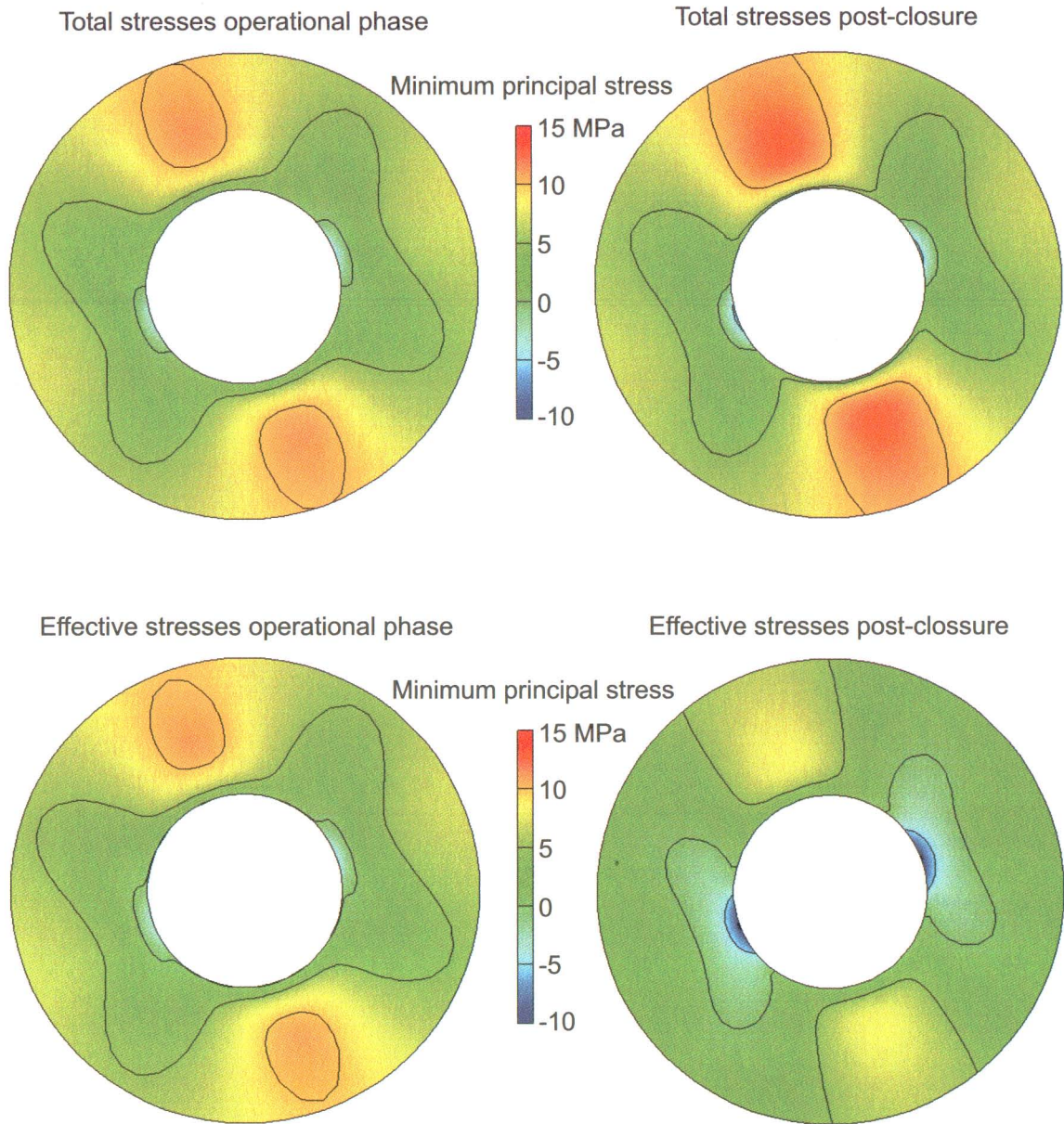


Fig. 5.11: Total and effective minimum stress for the operational and post-closure phases

It is necessary to consider whether backfilling and resaturation might induce further damage and changes to material properties. Inspection of the predicted total stresses suggest this is unlikely unless the backfill were to induce significant swelling pressures, in which case tensile failure might occur, creating new fractures away from the existing damage zone.

The coupling between changes in effective stress and changes in feature transmissivity has been based on a simple power law of the form:

$$\frac{T}{T_0} = \left(\frac{\sigma'}{\sigma_0'} \right)^{-b}$$

Where T is transmissivity in m²/s and σ' is effective stress in MPa. The 0 subscript refers to the conditions of an original measurement. Thus the law implies that the ratio of transmissivities at two different effective stresses is equal to the ratio of the effective stress to the power -b. DERSHOWITZ et al. (1991) reviewed a range of core measurements from fractures in granite and suggested values for b between 0.2 and 2. For the calculations performed in this study b values of 1 or 2 were used.

Alternative models could have been used such as those of Barton and Bandis (see for example BARTON & BAKHTAR 1987); however very little characterisation information on fracture properties is available from the GTS site and this simple approach was thought to be sufficient for the purposes of the modelling. Ideally information on fracture stiffness and shear behaviour should be acquired from core and in-situ testing. This would reduce uncertainty in stress-transmissivity coupling and in fracture storage properties.

The NAPSAC model volume used for effective permeability calculations was a hollow cylinder with inner radius 1.85 m and outer radius either 3.85, 5.55 or 12 m. The models with a small external radius consider flow only in the zone close to the tunnel, while the larger models are used to estimate an effective permeability for the damage zone, disturbed zone and natural fracture system as a whole. 12 m corresponds to over 6 excavation radii, beyond which point it is assumed that disturbed zone effects are insignificant. In addition some models calculated the effective conductivity for an annulus from 5.55 m to 12 m (i.e. excluding the damage zone) to investigate changes in hydraulic properties outside this zone.

For the calculation of effective axial permeability a pressure gradient was applied across the two end faces of the hollow cylinder while all other faces are set as no-flow boundaries. The effective permeability was then estimated using Darcy's Law. The imposition of no-flow boundaries on the cylindrical faces of the models reduces connectivity close to the boundaries and effective properties of the thin annuli may thus be underestimated in sparse or poorly connected fracture networks. The effective axial permeability of each model was calculated over 10 realisations.

Computed effective axial permeability

The results from the effective permeability calculations are given in Table 5.4.

Table 5.4: Effective axial permeability averaged over different annuli around tunnel

Damage Zone fracture size (m)	Cylinder Length Scale (m)	Inner Radius (m)	Outer Radius (m)	Stress Coupling	Mean $k_{\text{eff-axial}}$ (m^2)	Standard deviation $k_{\text{eff-axial}}$ (m^2)	Mean $\text{Log}_{10} k_{\text{eff-axial}}$ $\log(\text{m}^2)$	Standard Deviation $\text{Log}_{10} k_{\text{eff-axial}}$	Minimum $k_{\text{eff-axial}}$ $\log(\text{m}^2)$	Maximum $k_{\text{eff-axial}}$ $\log(\text{m}^2)$
None	20	Tunnel	12	Yes	1.2E-18	7.6E-19	-18.1	0.4	1.1E-19	2.4E-18
None	20	Tunnel	12	No	1.2E-18	8.3E-19	-18.0	0.4	1.5E-19	2.8E-18
1	10	Tunnel	3.85	Yes	1.8E-18	2.7E-18	-20.0	3.0	3.3E-25	8.8E-18
10	10	Tunnel	3.85	Yes	5.4E-16	3.8E-16	-15.4	0.4	8.5E-17	1.1E-15
10	20	Tunnel	3.85	Yes	1.5E-16	7.0E-17	-15.9	0.2	4.9E-17	2.6E-16
1	10	Tunnel	5.55	Yes	1.2E-18	1.2E-18	-19.2	2.6	1.5E-25	3.6E-18
10	10	Tunnel	5.55	Yes	2.9E-16	1.8E-16	-15.6	0.3	7.9E-17	5.8E-16
10	20	Tunnel	5.55	Yes	8.2E-17	4.4E-17	-16.1	0.2	2.6E-17	1.7E-16
1	10	5.55	12	Yes	1.4E-18	8.2E-19	-17.9	0.3	4.1E-19	2.8E-18
10	10	5.55	12	Yes	1.4E-18	8.1E-19	-17.9	0.3	4.1E-19	2.8E-18
1	10	Tunnel	12	Yes	1.3E-18	8.5E-19	-18.0	0.4	1.3E-19	2.9E-18
10	10	Tunnel	12	Yes	5.0E-17	3.1E-17	-16.4	0.2	2.5E-17	1.2E-16
10	20	Tunnel	12	Yes	1.7E-17	7.9E-18	-16.8	0.2	1.8E-20	3.7E-17
1	10	Tunnel	12	No	1.2E-18	8.1E-19	-18.0	0.4	1.1E-19	2.7E-18
1	20	Tunnel	12	No	8.8E-19	4.6E-19	-18.1	0.2	4.2E-19	1.8E-18
10	10	Tunnel	12	No	2.4E-17	1.2E-17	-16.7	0.2	1.2E-17	5.0E-17
10	20	Tunnel	12	No	1.0E-17	3.5E-18	-17.0	0.2	5.1E-18	1.7E-17

For the models containing only natural fractures there was no significant change in permeability due to the calculated effects of stress changes. It was necessary to calculate the effective permeability on relatively large volumes of the network to ensure connectivity. Smaller volumes were typically disconnected. The change in permeability by inclusion of the stress coupling was in general found to be small although the transmissibility of some parts of the fractures underwent considerable changes due to the stress coupling. Similar results were obtained in calculations for the Stripa Project by HERBERT et al. (1991). Although stress changes around the tunnel may locally increase fracture transmissivity, flowpaths in the natural fracture system are not confined to this zone and so flow is limited by the transmissivity of parts of the fractures that are either undisturbed or even closed by the stress redistribution. This observation confirms the comment of OLSSON & WINBERG (1996) that: "In a general three-dimensional fracture network it is unlikely that fractures would open in such a way that a permeable path opened along a drift." EDZ models developed for the Wellenberg site by VOMVORIS et al. (1997) showed similar results. However this has not yet been confirmed by experimental evidence.

For the models containing damage zone fractures, the effective permeability was highly dependent on length-scale of the damage zone fractures and the flowpath. For the small EDZ fractures, permeabilities were little higher than those for the natural fractures alone when the flow was simulated over length scales of 10 m or more. For the 10 m

long EDZ fractures, the permeability reduced as the length scale over which flow was calculated was increased.

Permeability enhancement factors were calculated for different annuli of the rock around the tunnel for the various models. They are related to a simplified near-field geometry as shown in Figure 5.12. The results are given in Table 5.5. As can be seen, the length of the damage zone fractures has a critical influence on the values of effective permeability. The increased permeability in the zone from 3.85 to 5.55 m (disturbed zone) may be partly due to the model boundary effects and to some interaction between the damage zone fractures and the stress disturbed natural fractures.

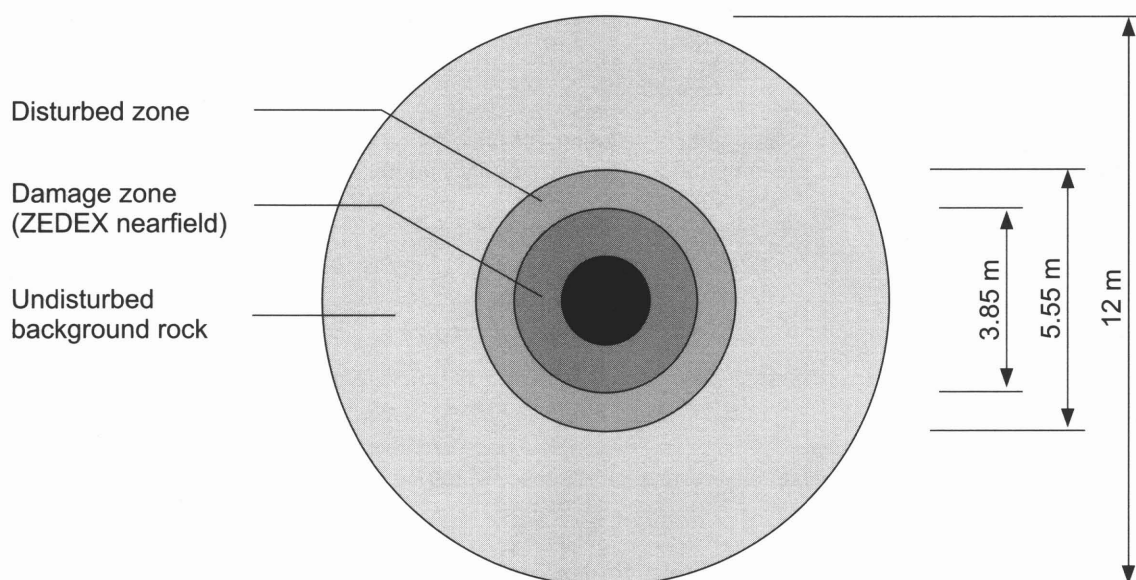


Fig. 5.12: Simplified factor model geometry as might be used in repository scale groundwater flow models.

The results suggest that the effective axial permeability of the rock around the tunnel at the GTS will be controlled by the connectivity of the high permeability features within the damage zone. Where such features are extensive and well connected (compared to the scale of flow - e.g. seal zone length) the results suggest that permeabilities of between 10^{-15} and 10^{-16} m^2 are likely over the first two metres of rock. This is 100 - 1000 times greater than the undisturbed permeability of the rock mass. If the features are considerably smaller than the flow scale, the models predict a lower effective permeability which will be dominated by the micro-scale fracturing in the damage zone. The MMPS results suggest that the micro-scale fracturing would result in a typical permeability of about $3 \cdot 10^{-18}$ m^2 (a factor of three greater than the estimated undisturbed rock permeability).

Table 5.5: Factor model fits to simulate effective permeability for model variant 1

Network Model flow over 10m length*					Factor Model		
Inner radius (m)	Outer radius (m)	Length of model (m)	Geometric mean permeability (m ²)	Arithmetic mean permeability (m ²)	Estimated permeability (m ²)	Factor Model	Factor increase in conductivity
Tunnel	3.85	10	3.9E-16	5.4E-16	5.1E-16	Damage Zone	500
Tunnel	5.55	10	2.4E-16	2.9E-16	2.7E-16	Disturbed Zone	100
Tunnel	12	10	4.3E-17	5.0E-17	5.4E-17	Undisturbed Rock	1
5.55	12	10	1.2E-18	1.4E-18	1E-18		
Network Model flow over 20m length*					Factor Model		
Inner radius (m)	Outer radius (m)	Length of model (m)	Geometric mean permeability (m ²)	Arithmetic mean permeability (m ²)	Estimated permeability (m ²)	Factor Model	Factor increase in conductivity
Tunnel	3.85	20	1.3E-16	1.5E-16	1.5E-16	Damage Zone	150
Tunnel	5.55	20	7.2E-17	8.2E-17	7.6E-17	Disturbed Zone	20
Tunnel	12	20	1.6E-17	1.7E-17	1.6E-17	Undisturbed Rock	1

*For case where damage zone fracture length = 10 m, tensile aperture=100 µm and transmissivity exponent =1

The results discussed above assume that high permeability intervals detected using the MMPS system correspond to damage zone fractures running along the tunnel. If, however, these features are locally channelled and possibly stress-relieved parts of pre-existing fractures that cut across the tunnel rather than run along its length, then effective axial permeabilities will be much lower and comparable to that of the enhanced matrix permeability of $3 \cdot 10^{-18} \text{ m}^2$.

5.4 Issues for further investigation

In order to make estimates of effective permeability of the EDZ it has been necessary to consider several properties of the fracture system that are difficult to characterise and may be highly uncertain. Because of the lack of direct measurements of flow along the EDZ there is considerable uncertainty about the possible permeability of the zone. An alternative methodology would be to measure such flow in order to either validate the detailed models described above or to provide a direct measurement that would obviate the need for such models. Ideally such direct measurements should be integrated with detailed investigations of the EDZ such as those performed at the ZPK / BK and WT / EDZ sites to demonstrate understanding of the EDZ.

A simple experimental design for such measurements has been developed by AECL at the Underground Rock Laboratory (URL) in Pinawa Manitoba and is shown in Figure 5.3. Analysis of the experiment at the URL was particularly simple because of the very low permeability of the host rock, which is due to the sparsity of fractures. A constant

head of water is established in a dam and water is forced beneath the concrete apron and into a measuring system in the slot. The length of the concrete apron can be altered to consider flowpaths of different lengths. Such an experimental set-up is relatively inexpensive and provides a direct measurement of flow through the EDZ. Alternative experiments could use “fans” of boreholes to induce flow through the EDZ. An illustration of one possible experimental geometry is shown in Figure 5.13. An approach similar to this was taken by PUSCH & STANFORS (1992) in the Tunnel Sealing Experiments at Stripa. An advantage of both of these set-ups is that they ensure resaturation of the EDZ, although it may be necessary to consider the potential for degassing effects as suggested by LONG et al. (1992).

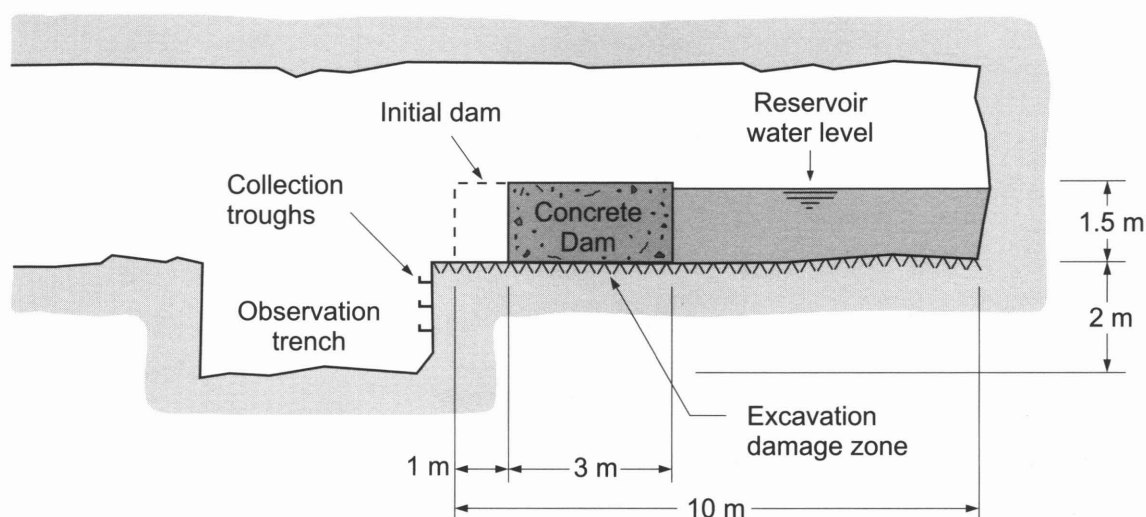


Fig. 5.13: Experimental set-up for Connected Permeability Experiment in the Mine-By Tunnel at AECL Underground Research Laboratory from FROST & EVERITT (1997).

The results and models considered here are relevant only to relatively small tunnels such as those that might be used as access or emplacement tunnels for high-level waste packages. Larger excavations such as emplacement caverns for low- and intermediate level waste would need additional characterisation and consideration. Although the extent of stress concentrations in a homogeneous elastic material scales directly with excavation span, the interaction with discontinuities within the rock will induce scale dependent behaviour. In addition such caverns may require significant support in the form of rock bolts or shotcrete, whose influence would need to be considered. The size of the caverns may also make it difficult to avoid small shear or fracture zones and these may interact with the EDZ.

At several points the influence of saturation on characterisation has been discussed. The reduced sonic velocities observed around tunnels seem to depend significantly on the saturation. Partially saturated conditions may also have been observed during well tests, making them difficult to interpret and increasing uncertainty. For these reasons it is suggested that efforts should be made to ensure saturation and, if possible, lining of the tunnel to allow pore pressures comparable to those expected post-closure to develop prior to hydraulic characterisation.

As discussed previously the issue of time dependence of the disturbed zone is difficult to address from recent excavations and, although PUSCH (1993) has set out an approach to such problems, it may be difficult to develop defensible descriptions of the EDZ development without examination of existing excavations. Pusch's work suggests that logarithmic differences in timescales are needed, potentially requiring investigation of excavations that are tens to hundreds of years old.

6 COMPLEMENTARY STUDIES

The excavation of underground repository facilities and subsequent emplacement of waste will disturb conditions in the tunnel near-field and the environmental conditions will evolve post emplacement. It is therefore necessary to understand these changes, many of which may involve "coupling" between the different environmental conditions (chemical, thermal, mechanical and hydraulic). Development of this understanding requires acquisition of relevant experimental data, development of appropriate models and testing of these models against acquired data. The Tunnel Near-Field Programme as part of the GTS Phase IV, was focused on tunnel near-field investigations. In the CTN project (GTS Phase V) emphasis has been placed on the synthesis of those investigations. As a complementary task, a desk study was initiated to put the GTS investigations into the broader perspective of relevant research work on the tunnel-near-field. This chapter describes the state-of-the-art in terms of modelling of tunnel-near-field processes and relevant experience from other underground laboratories in crystalline rock environments:

- Chapter 6.1 presents a survey of numerical codes available for modelling (i) two-phase flow processes in fractured porous media and (ii) groundwater flow through fracture networks. A brief assessment of the features of the various numerical tools is given.
- Chapter 6.2 presents a survey of tunnel near-field investigations in other underground laboratories situated in crystalline rock formations. A comparison of results from various laboratories is given to highlight the importance of particular processes for different geological settings and at different excavation techniques.

Both code comparison and comparison of experimental results from different underground laboratories are aspects to be considered in the synthesis of geoscientific data as valuable input for performance assessment. Within the framework of the synthesis procedure these surveys may relate to assessment of the spectrum of conceptual models and parameter ranges required as a prerequisite for establishing process models of gas migration, resaturation and axial flow (cf. chapter 2.3). In addition, they supply the needs of PA in a more general way, by building confidence in understanding of geological processes and material properties.

6.1 Numerical models for hydrogeological tunnel near-field investigations

For the understanding and simulation of groundwater and gas flow in the near-field, effects such as density-driven flow, temperature, heat generation and others may have to be considered. It may be possible to treat these effects in an "uncoupled" manner, but phase transitions, mechanical / hydraulic interaction etc., may require a fully coupled approach.

A number of codes are presently available which are appropriate for the specific requirements of performance assessment of repositories in hard rock formations. The mathematical and physical relations describing the various effects relevant to fluid and gas flow in the tunnel near-field, such as two-phase flow, fluid flow and transport, heat transport, phase transitions, gas solubility etc. are combined into conceptual models. Emphasis is given to different aspects of the flow or transport processes within each code, depending on the area of application for which it was developed (e.g. oil or gas production and/or a radioactive waste repository). The conceptual model on which most multiphase flow simulators used in hydrocarbon reservoir engineering and gas

transport in radioactive waste repositories are based is the conventional continuum porous medium two-phase flow model. The basics of this approach are outlined in chapter 4.1.

This model may be inadequate for describing gas and water flow through a network of fractures, if the dimensions of the fractures are large compared with the regions to which average properties are assigned. For the same reason, direct laboratory measurement of relative permeability and saturation functions for real fractured systems would require impracticably large specimen sizes. In such circumstances, alternative models of fluid flow in fracture networks have been developed. These are either a realistic representation of fracture structures and features or they make use of geostatistical distributions of average properties, such as the orientation, frequency and width of the fractures. Such geostatistical models can include observed or hypothesised anisotropy or correlations.

In the following chapters an overview of the features and restrictions of some available two-phase flow simulators will be given to provide information relevant for the selection of adequate codes for specific applications within performance assessment. A description of five continuum two-phase flow models is contained in chapter 6.2.1 and of some fracture network codes in chapter 6.2.2.

6.1.1 Continuum two-phase flow simulators

Several two-phase flow codes are available for modelling the flow of gas and water in fractured porous media. In the following, a description and intercomparison of six codes or code versions will be presented. These codes have either been used in the Grimsel programme or are considered to be the most suitable for modelling phenomena in fractured hard rock. Tables 6.1 and 6.2 at the end of this chapter contain a brief intercomparison of the essential features of the codes. The codes considered are (in alphabetical order):

- CODE_BRIGHT
- ECLIPSE
- MUFTE-ISO
- MUFTE-THERMO
- ROCKFLOW MM
- TOUGH-2

CODE_BRIGHT was developed by Alonso and co-workers at the Technical University of Catalunya, Barcelona (OLIVELLA 1998), originally for saline media. It allows effects resulting from rock convergence and its impact on the porosity and permeability of the salt and solution-dissolution of salt in water to be considered. The code is a finite element model for handling COupled DEformation, BRIne, Gas and Heat Transport. CODE_BRIGHT contains a general formulation of non-isothermal multiphase flow of gas, water or brine through a porous medium. The governing equations are mass balances for each of the components: gas, water and the solid phase. In the case of rock salt, the latter permits consideration of porosity changes as well as dissolution-precipitation processes. Additionally, mechanical and thermodynamic behaviour is considered by means of stress equilibrium and internal energy balance equations. Besides modelling of rock salt and compacted crushed salt, CODE_BRIGHT had been used to

model two phase flow in deformable clays. In this case a saturation-dependent stress-strain relation permits investigation of the influence of clay desaturation.

ECLIPSE is a commercial general-purpose simulator which has a relatively high flexibility due to numerous special modules. ECLIPSE was developed by INTERA/ECL for reservoir engineering applications within the oil industry. The ECLIPSE simulator family provides a suite of tools that permit simulation of reservoir performance from single well models looking at coning up to three-dimensional full-field models. The ECLIPSE simulators use robust numerical techniques and fine convergence controls, aiming to ensure reliable and accurate solutions with minimal material balance errors. All program versions of ECLIPSE contain grid geometry options that allow representations of reservoir morphology including faults, pinchouts and fracture systems. Local grid refinement or coarsening, which allows areas of particular interest to be modelled with a finer grid, is included. The two-phase flow model contains a range of relative permeability and capillary pressure functionalities. Additional packages to assist in building models and graphically analysing the output are also available.

ROCKFLOW is the name of a family of flow and transport codes which have been developed by Zielke and co-workers at the Technical University of Hanover since 1984. It is a finite element program system for simulating two-phase flow and transport processes in fractured porous media (ROCKFLOW 1994). For complex geological structures the flow channels, fractures and the rock matrix have to be considered. To facilitate this the model domain can be decomposed into arbitrarily coupled isoparametric one-dimensional rod elements, two-dimensional quadrilateral planar elements and three-dimensional hexahedral elements. The generation of coupled elements is aided by specific net generators for two- and three-dimensional cases. The output can be visualised with a specially adapted post-processor. ROCKFLOW can be adapted to various problems by means of special program modules. For the simulation of multiphase flow in fractured porous media the MM module is used. This module is described in part 9 of the ROCKFLOW program description (ROCKFLOW 1994). The version of ROCKFLOW used for multiphase problems is therefore known as ROCKFLOW-MM.

MUFTE is a separate development of the ROCKFLOW-MM code which began in 1993 at the Technical University of Stuttgart. The name MUFTE is an acronym of MULTiphase Flow Transport and Energy Model. MUFTE-ISO is the program version for modelling one- and two-phase flow processes in fractured porous media at constant temperature using the pressure-saturation differential equations for one-, two- and three-dimensional models. It was developed by R. Helmig (HELMIG et al. 1994) on the basis of the ROCKFLOW code mentioned above. MUFTE-THERMO is the version capable of modelling one- and two-phase isothermal and non-isothermal flow processes in systems with a gas and a liquid phase in fractured porous media. Air can be dissolved in the liquid phase and the gas phase can take up water vapour. Thermodynamic laws describing gas solubility and evaporation and condensation phase transitions are included in the program. The 1D simulations of tunnel near-field desaturation in the ZPM experiment (GRAEFE 1997) were performed with MUFTE-THERMO (cf chapter 4.4.3).

TOUGH2 (PRUESS 1991) is an improved version of the TOUGH simulator (Transport Of Unsaturated Groundwater and Heat) (PRUESS 1987). It is a three-dimensional numerical model for simulating the coupled transport of water, vapour, non-condensable gas and heat in fractured porous media. Moreover, TOUGH2 offers capabilities and features, including the ability to handle different fluid mixtures (water, water with tracer; water, CO₂; water, air; water, air, with vapour pressure lowering, and water, hydrogen)

(PRUESS et al. 1998). Additional fluid property modules (EOS-Modules) have to be implemented by the user. A considerable number of EOS-Modules are in use, for instance: the T2VOC module for 3-phase/3-component flow of water, air and a single volatile organic compound; or the fluid property module EOS7R for water, air and brine and volatile tracers with radioactive decay. TOUGH2 also has facilities for generating computational grids. TOUGH2 uses an integral finite difference method for spatial discretisation and first-order fully implicit time differencing. A choice of either a sparse direct solver or various preconditioned conjugate gradient algorithms is available for the solution of the linearised equation systems. Thermophysical properties of water are represented by steam table equations. The program provides options for specifying injection or withdrawal of heat and fluids. Double-porosity, dual-permeability and multiple interacting continua (MINC) methods are available for modelling flow in fractured porous media.

Although primarily designed for geothermal reservoir studies and high-level nuclear waste isolation, TOUGH2 can be applied to a wider range of problems of heat and moisture transfer and the drying of porous materials. The TOUGH2 simulator was developed for problems involving strongly heat-driven flow. To describe these phenomena a multi-phase approach to fluid and heat flow is used, which fully accounts for the movement of gaseous and liquid phases, their transport of latent and sensible heat, and phase transitions between liquid and vapour. TOUGH2 takes account of fluid flow in both liquid and gaseous phases occurring under pressure, viscous, and gravity forces according to Darcy's law. Interaction between the phases is represented by means of relative permeability functions. The code includes Klinkenberg effects and binary diffusion in the gas phase, and effects of capillarity and sorption for the liquid phase. Heat transport occurs by means of conduction (thermal conductivity dependent on water saturation), convection, and binary diffusion, which includes both thermal energy and latent heat.

TOUGH2 in combination with the EOS7R fluid property module (water, brine, and air plus volatile tracer with optional radioactive decay chains) has been used in the GTS Phase IV. Here simulations of gas tracer tests performed in a fracture zone have been performed which reproduced the overall breakthrough behaviour observed in the test field experiments (MARSCHALL & CROISÉ 1999).

Various continuum two phase flow simulators had been compared in the European Validation Exercise of Gas Migration Models through geological media (EVEGAS-Project) performed as part of the European Commission's programme on radioactive waste management and storage (MANAI 1995, 1997a, 1997b). Of the simulators described above, CODE_BRIGHT, ECLIPSE and TOUGH2 were included in this project.

Table 6.1 : Comparison of areas of application of various two-phase flow codes

Code	CODE_BRIGHT	ECLIPSE	MUFTE-ISO	MUFTE-THERMO	ROCKFLOW-MM	TOUGH-2
Key reference	OLIVELLA 1998	Schlumberger	HELMIG 1994		ROCKFLOW 1988	PRUESS 1991
max. # of phases and components	3p/3c	3p/2c	2p/1c	2p/2c	2p/1c	3p/3c EOS,T2VOC ⁱ
Arbitrary coupling of 1D-3D elements	n.a.	possible	possible	possible (1D/2D)	possible	no
Heat transport	yes	no	no	yes	possible	yes
Saturation-dependent heat conductivity	n.a.	no	no	yes	no	n.a.
Evaporation & condensation	yes	yes	no	no	no	yes
Gas solubility in liquid phase	yes	yes	no	yes	no	yes
Binary vapour/air diffusional flow	n.a.	yes	no	optional	no	optional
Flow laws	Darcy	Darcy	Darcy	Darcy	Generalised Darcy	Darcy
Consideration of heterogeneities	possible	possible	possible	possible	possible	possible
Consideration of hysteresis ⁱⁱ	no	permeability, capillary pressure	no	no	no	under development
Anisotrop permeability	yes	yes	yes	yes	yes	n.a.
Fracture modelling	n.a.	DPM ⁱⁱⁱ	by element coupling	by element coupling	yes	DPM
Sources	air	air	any ideal gas, any incompressible liquid	air, liquid, heat	any ideal gas, any incompressible liquid	Air, H ₂ , CO ₂
Sorption & radioactive decay	optional	optional	no	no	optional	optional

(n.a. = no information available)

ⁱ EOS: Various TOUGH2 Equation Of State modules available. EOS7R is a fluid property module for water, brine, and air plus volatile tracer with optional radioactive decay chains. T2VOC: module for 3-phase, 3-component flow of water, air and a volatile organic compound.

ⁱⁱ Saturation functions for porous or fractured media usually show a hysteresis. This means that the function values are also dependent on the sign of saturation changes. Hysteresis effects can only be expected for cases where gas or water saturation changes are not monotone.

ⁱⁱⁱ Dual Porosity Model. Extension of the continuum porous medium flow model with the assumption that the porosity of fractured rocks consists of a system of interconnected fracture porosity providing the pathway for flow through the rock, and an impermeable low matrix porosity. Only local fluid exchange between the matrix and the fracture system is assumed. DKM (Double Permeability Model) is an extension of the DPM considering global flow through the matrix.

Table 6.2: Comparison of the numerics, input, output and preprocessing features of various two-phase flow codes

Code	CODE_BRIGHT	ECLIPSE	MUFTE-ISO	MUFTE-THERMO	ROCKFLOW-MM	TOUGH-2
Variables ⁱ	P, S	P(n/w), S(w), T	P, S	P(n/w), S(w), T	P, S	P(w,nw) or f(EOS)
Initial & boundary conditions	Dirichlet Neumann Cauchy	Dirichlet Neumann	Dirichlet f(t) Neumann const.(t)	Dirichlet f(t) Neumann const.(t)	Dirichlet f(t) Neumann f(t)	Dirichlet Neumann?
Discretisation Method	F E (x,y,z)	Finite Difference	Finite Element	Finite Element	Finite Element	Integral F D
Coordinate systems		cartesian or cylindrical	cartesian	cartesian	cartesian	cartesian or cylindrical
Linearisation	Newton	Newton	Newton	Newton	Newton	Newton
Solver	direct or iterative	nested factorisation, iterative	PCG ⁱⁱ	PCG	direct or iterative	direct or PCG (T2CG1)
Mass lumping ⁱⁱⁱ	n.a.	n.a.	optional	optional	optional	n.a.
Upwinding ^{iv}	n.a.	n.a.	optional	optional	optional	yes
Time discretisation ^v	implicit	n.a.	explicit, implicit, Crank-Nicholson	explicit, implicit, Crank-Nicholson	explicit, implicit, Crank-Nicholson	fully implicit
Adaptive Grid ^{vi}	no	no	no	no	yes	no
Restart-Option ^{vii}	n.a.	yes	yes	yes	yes	yes
Preprocessor	n.a.	yes	no	no	partly	n.a.
Grid generator included	n.a.	yes	no	no	yes	no
Free-formatted input data	n.a.	optional	no	no	yes	n.a.
Result visualisation	n.a.	yes GRAF	GNUPLOT, GRAPE	GNUPLOT, GRAPE	any commercial graphics package	n.a.

(n.a. = no information available)

ⁱ P: Pressure, S: Saturation, w: wetting, n/w: non-wetting, F(EOS): dependent on includes EOS-module

ⁱⁱ Preconditioned Conjugate Gradient solver

ⁱⁱⁱ Numerical technique in transport calculations to improve solver performance by concentrating („lumping“) the mass-dependent coefficients at the diagonal elements of the equation system matrix

^{iv} Method to reduce numerical diffusion, dispersion and oscillations often associated with hyperbolic differential equations for convection-dominated flow i.e. for large Peclet-numbers. Fully upwind means that only upstream (or upwind) discretisation nodes are included in the finite differences.

^v For a system $df(x,t)/dt = v(f)$ explicit means that $f(t_0+\Delta t)$ is directly calculated with $v(f)$, whereas implicit with $v(t_0+\frac{1}{2}\Delta t)$ and C/N with $v(t_0+\frac{1}{2}\Delta t)$ require iterative solution.

^{vi} Mesh size may be automatically adapted during calculation

^{vii} Output file of previous calculation can be used as input file for a continuation.

6.1.2 Fracture network and coupled rock mechanical/hydraulic codes

The following section provides a short description of groundwater flow and coupled hydro-mechanical computer codes used in the GTS Near-Field Programme. The ROCKFLOW code will not be discussed here as it is treated more thoroughly in the section on two-phase flow models. It does however contain facilities for modelling of flow through fracture networks.

Discrete fracture network models

The discrete fracture network (DFN) code NAPSAC was used in the GTS programme for modelling flow at the 10 to 50 m scale around tunnels. NAPSAC is a finite element single phase flow model including facilities for steady state flow, transient flow and mass transport (using particle tracking) in networks of fractures (HARTLEY 1998). NAPSAC allows the creation of stochastic models of fracture networks and has been used for studies of flow and transport in networks containing over 100000 fractures. NAPSAC has facilities for stress-dependent fracture transmissivity via coupling to static stress fields imported from rock mechanical models.

Alternative DFN codes that might have been used include FRACMAN (DERSHOWITZ et al. 1998) and FRACAS (BRUEL 1990). FRACMAN has been used extensively in other radioactive waste programmes and has been cross-verified with NAPSAC (SCHWARTZ & LEE 1992). FRACAS has been used in a range of applications including coupled hydromechanical models of flow in a generic geothermal reservoir and simulation of a large scale flow-test in fractured rock as part of the Decovalex II Project (JING et al. 1998).

Continuum groundwater flow models

The CASA equivalent porous medium model was used to perform design calculations for the hydraulic characterisation of the EDZ (KUHLMANN 1995). CASA has also been extensively used in NAGRA's modelling of groundwater flow at the Wellenberg site (NAGRA 1997). Alternative continuum models would include NAMMU (HARTLEY et al. 1996) which has been used extensively in the UK radioactive waste programme (see NIREX 1997) and the d³f code.

d³f has recently been developed, tested, and applied to some field cases (FEIN & SCHNEIDER 1999) and is now available. d³f (distributed density driven flow) was especially developed to model density driven flow through porous media in large and hydrogeologically complex regions. It has been designed to exploit highly efficient numerical methods running on workstation clusters and massive parallel computers.

Distinct element mechanical models

Two distinct element codes were used in the GTS programme. The three-dimensional distinct element model 3DEC was used to develop understanding of the stress field at the GTS site (KONIETZKY 1995). The two-dimensional distinct element model UDEC was used as part of the same study to understand the influence of natural and damage zone fractures on the stress around the WT area tunnel where NAGRA's EDZ experiment was performed. Both UDEC and 3DEC model a „blocky“ rock mass containing fractures. The mechanical behaviour of the rock mass and fractures can be described by a variety of submodels. The Barton-Bandis joint model has also been incorporated

in the version UDEC-BB (CHRYSSANTHAKIS & BARTON 1992). Both UDEC and 3DEC include coupled hydromechanical facilities (DAMJANAC 1996) for the study of fractured media.

Continuum coupled hydromechanics codes

Work in the GTS programme has not used continuum coupled hydromechanics models. The ADINA finite element programme system has been used to study stress and rock failure around tunnels at the GTS (LIEDTKE et al. 1999). However, these models considered only the mechanical responses. ADINA does however have facilities for coupled fluid flow (ADINA-F) and thermal responses (ADINA-T).

NAGRA has used such codes in siting studies for the proposed repository at Wellenberg. The explicit finite difference code FLAC3D has been used to study stress in a heterogeneous medium around a tunnel for EDZ studies (VOMVORIS et al. 1997). In addition larger scale models used the ABACUS code to examine rock mass response to glaciation at Wellenberg (ARISTORENAS & EINSTEIN 1993).

Summary

It can be seen that numerical tools working with either an effective continuum or a fractured medium approach are available to address a range of processes. While no single tool can address all the processes within complex fracture system geometries most problems can be addressed using a mix of the available tools. Problems do however arise with the input requirements of such tools and the need for fracture properties which may be very heterogeneous both within and between individual fractures. Techniques that can be used to "visualise" flowpaths within fracture systems are therefore of special value in providing calibration or validation data for these models.

6.2 Underground rock laboratories

Many countries with nuclear energy programmes, such as Switzerland, Sweden, Finland, Japan, Canada and France have selected or at least are considering, low permeability saturated hard rock formations as host Media for their national radioactive waste repositories. In the course of the site selection or site confirmation process, underground laboratories have been constructed in geological formations similar to that of the planned repository. One major reason for the operation of underground laboratories is the collection of representative data required for performance assessment.

In various underground laboratories, hydrogeological and rock mechanical investigations of the tunnel near-field in crystalline environments have been carried out. As the rock laboratories are situated in different geological settings with different hydrogeological and rock mechanical conditions, a comparison of the results of near-field studies from different laboratories may be ambiguous and needs careful review of the site specific impacts. On the other hand, a synopsis of the results can help to identify the spectra of possible processes and the possible range of near-field parameters. For example these might include:

- the shape and extent of the EDZ under differing stress situations
- the influence of gases dissolved in the groundwater on the development of an unsaturated zone and

- the effective permeability of the rock matrix and the fracture system.

Strictly speaking, the results obtained from investigations in a rock laboratory may have limited applicability as input for the performance assessment of a repository at a different location. However, a comparison of results from various laboratories may be useful in estimating the importance of particular processes. For example, a survey of the EDZ extent measured at different locations, rock conditions and excavation techniques might be used to determine maximum limits. Such a limit might then be used as a realistic assumption in performance assessment.

In this study the following five laboratories in crystalline rock were selected and a compilation of relevant information on near-field investigations was conducted:

- the Grimsel Test Site (GTS)
- the Stripa Mine in central Sweden
- the Äspö Hard Rock Laboratory (HRL) in southern Sweden
- the Underground Research Laboratory (URL) in Manitoba, Canada
- the Kamaishi Mine in north-east Honshu, Japan

These sites cover a wide range of hydrogeological and rock mechanical environments and this selection may thus be representative for the bandwidth of the hydraulic and rock mechanical properties of the near-field and the processes (degassing, desaturation, hydromechanical coupling) to be considered. Table 6.3 gives a condensed summary of relevant information.

Stripa Mine

The Stripa Mine is an old iron mine in central Sweden and was one of the first underground research laboratories for nuclear waste disposal. The depth of the experimental levels is up to 420 m bg. The stress conditions are described by low vertical and anisotropic horizontal stress. As part of the experimental programme, new drifts were excavated using different drill and blast methods (conventional / careful). Experiments related to the tunnel near-field issue are the Buffer Mass Test (BMT), Rock Sealing Test, Validation Drift Inflow Experiment and the Site Characterisation and Validation Experiment (SCV). In BMT, an excavation damage zone of up to 0.75 m was detected and a larger excavation disturbed zone inferred. In the SCV experiment, reduction of groundwater flow towards the tunnel were observed, which some authors have explained by degassing processes (LONG et al. 1992).

Äspö HRL

The Äspö HRL is located in south Sweden close to the town of Oskarshamn. The laboratory was built by SKB to provide an opportunity for research, development and demonstration of waste disposal technologies in a crystalline environment. The laboratory tunnel was excavated from the surface as a spiral down to a depth of 460 m. The HRL started operation in 1995 for an expected duration of 15 to 20 years. Since then a number of research projects -partly with international participation- have been performed (SKB 1998). The ZEDEX (Zone of Excavation Disturbance EXperiment) and Two Phase Flow experiments performed at Äspö are of particular relevance to the work in the CTN programme.

The objective of the ZEDEX experiment is to investigate EDZ with respect to:

- its origin, character, bandwidth of property changes, and dependence on excavation method
- increasing understanding of the hydraulic importance of the EDZ
- testing equipment and methodologies for quantifying the EDZ

As part of the ZEDEX experiment, studies of the extent of the EDZ were conducted for tunnel sections, excavated by drill & blast methods and TBM respectively. The results indicated that the disturbed zone is limited to a distance of less than 2 m from the tunnel surface. The damage zone was less than 0.2 m for the TBM drilled section and up to 0.8 m for the blasted section. In the damage zone an increase in hydraulic conductivity of an order of magnitude was observed.

Subsequent "slotting" of the ZEDEX drifts combined with dye penetration tests clearly showed induced fracture geometries that were in agreement with other estimates of EDZ extent.

The main objectives of the Two-Phase Flow Experiment are the creation of a database for the simulation of two-phase-flow in fractured media and transport of particles in unsaturated rock and the development of 2D and 3D simulation models to calculate gas and particle migration within the near-field. Investigation of degassing effects in the tunnel near-field only minor reductions of flow towards the tunnel, typically by a factor of 2.

URL – Canada

The URL, operated by AECL, is located in Pinawa, Manitoba and was constructed as a research facility for radioactive waste disposal. The layout of the laboratory consists of a vertical shaft with a depth of 443 m below ground and two experiment levels. The host rock is the Lac du Bonnet batholith with very low fracture density. Strong stress anisotropy is observed in the deeper parts of the laboratory with principal stress magnitudes of 60, 45 and 11 MPa. In drill and blast tunnels at approximately 200 m depth the damage zone extends typically to a distance of 0.3 – 0.4 m from the tunnel surface. However a series of "Connected Permeability Tests" suggest that axial flow within the damage zone is limited by the finite extension of blast-induced fractures, resulting in a very poorly connected fracture system (CHANDLER et al. 1996). In the deeper parts of the laboratory the highly anisotropic stresses lead to failure of the tunnel wall and formation of a continuous distinctive "notch" in both the roof and floor. A connected permeability test has shown that the small "failure zone" around this notch is quite permeable and experiments have been performed to investigate excavation of more favourable tunnel geometries that avoid the creation of this failure zone.

Kamaishi Mine

The Kamaishi Mine is an old iron mine in the north-east of the island of Honshu, Japan. Between 1988 and 1998, former PNC conducted a geoscientific research programme to assess the performance of fractured crystalline rock for radioactive waste disposal. The in-situ experiments were carried out in a drift 260 m below ground surface. Groundwater flow at the site was strongly linked to discrete water-conducting features, indicated by high variability of hydraulic conductivity. The results of packer tests gave conductivities between 1E-10 and 1E-7 m/s. Marked anisotropy of hydraulic conductiv-

ity was observed. The principal conductivity directions were consistent with the fracture orientations. A mine-by experiment was conducted to evaluate geomechanical responses of the rock mass to drift excavation. Stress and strain measurements were carried out before and after drift excavation. No damage zones were observed after excavation.

Subsequent experiments performed at approximately 730 m below ground level in an old mine drift (SUGIHARA et al. 1996) identified a zone of increased density of cracks and micro-cracks, reduced P-wave velocity and reduced modulus. The zone extended approximately 0.5 m from the tunnel although zones with reduced moduli were identified up to 1 m from the tunnel.

Comparison with EDZ results from the GTS

The extent of the damage zone observed in most of the laboratories ranges from about 0,3 m to 1 m in depth. The geometry of the damage zone in drill and blast tunnels is commonly related to charging pattern and is typically greater in drift floors. The extent estimated from the BK area is within the observed range. The results from the WT area suggest a larger extent but this may relate to either difficulties in the spalling observed at the site. Results from ZEDEX suggest that, given similar conditions, the damage zone around a TBM drift will be smaller than that from careful drill and blast; however it must be remembered that the WT area is in a much less favourable direction with regard to the expected stresses.

An important observation from the BK area is the apparent dependence of P-wave velocity on saturation. This would suggest that estimates of damage zone extent based on P-wave velocities alone should be treated with caution unless fully saturated conditions have been ensured.

Table 6.3: Comparison of underground laboratories in hard rock formation

	Grimsel Test Site	Stripa Mine	Åspö HRL	URL	Kamaishi Mine
Location	Grimsel Pass, Central Alps, Switzerland	Stripa, central Sweden	Oskarshamn, south Sweden	Whiteshell Laboratories Pinawa, Manitoba Canada	Kamaishi, northeast Honshu, Japan
Start of Operation	1983	Swedish American Cooperat.: 1977-1980 OECD Intern. Stripa Project: 1980-1992	Site investigations: 1988 – 90 Tunnel excavation: 1990 – 94	Monitoring: 1980 onwards Surface Construction: 1982-87 Underground Constr.: 1983-90	Experimental Phase I: 1988-93 Phase II: 1993-98
Depth below ground	450 m (1730m above sea level)	420 m	460 m bottom of shaft	443 m bottom of shaft	260 m (EL 550m drift) 730 m (EL 250m drift)
Total length of openings	1 km	25 km	3600 m	Several kilometres	Approx. 1 km
Host rock type	Grimsel Granodiorite Central Aare Granite	Granite (Stripa granite)	Granite	Granite/Lac du Bonnet batholith	Kurihashi granodiorite
Fracturing	Fracturing associated with K and S conjugate shear zone families. Fracture density varies across site from North to South	Several major fracture zones (100 m – km scale), steeply dipping; minor fractures with variable density / orientation	Variable fracture density with major fracture zone of regional extent	Very low fracture density, especially below major fracture zone	High fracture density with regional fault zones
Excavation method	TBM 3.5 m diameter Drill&blast typical 4 x 4 m square section	drill and blast careful drill and blast	Drill and blast; TBM excavation	Controlled Drill and Blast Line drilling and reaming (Mine-By)	Drill and blast
Extent of disturbed zone	Approximately 0.5 m in drill and blast Some evidence for up to 1.5 m in TBM tunnel at a point where unusual level of spalling occurred	0.75 m in floor, suggestion of deeper disturbed zone from analysis of BMT	< 0.8 m in drill and blast tunnel sections; < 0.2 m in TBM excavated sections	Between 30-40 cm in floor of drill and blast tunnels; no evidence for damage beyond 1 m in Mine-By Experiment	EL550: No damage zone EL250: Increased crack density and reduced velocity zone 0.5-1m around old drift EL250

Table 6.3: Comparison of Underground Laboratories in hard rock formation (cont.)

	Grimsel Test Site	Stripa Mine	Åspö HRL	URL	Kamaishi Mine
Stress situation	Strongly influenced by topography due to mountain location. Typical stress magnitudes within GTS 25-30/12-14/7-10 MPa Maximum stress approximately NW and sub-horizontal	Low vertical stress and anisotropic horizontal stresses. Estimated stress magnitudes at SCVB (385m) level 24.4/16/10 MPa	Estimated stress magnitudes of 32/17/10 MPa (ZEDEX site)	Evidence for stress decoupling across fracture zone, very high stress anisotropy below fracture zone (vertical stress is minimum) Estimated stress magnitudes of 60/45/11 MPa	EL550: 16-30/8/3-6MPa EL250: 21-44/15-27/6-18MPa High σ_1 values may relate to problems with overcoring measurements
Hydraulic properties	Flow focused in discrete shear and fracture zones. Typical background rock conductivity of 10^{-11} m/s. Flow within the shear zones themselves heterogeneous	Flow focused in fracture zones some of regional extent; typical background rock conductivity of 10^{-10} m/s	Flow focused in fracture zones some of regional extent; typical rock conductivity of 10^{-8} m/s	Typically very low conductivity rock $\sim 10^{-13}$ m/s with low fracture density	Flow focused in fracture zones; Hydraulic conductivity $10^{-7} - 10^{-10}$ m/s;
Experiments related to tunnel nearfield investigations	TPF, ZPK, EDZ experiments See chapter 3	Macro Permeability Test Buffer Mass Test Rock Sealing Test Validation drift Inflow Experiment	ZEDEX Degassing and two-phase flow	Monitoring of Shaft Excavation Room 209; Fracture Response Test Mine-By Experiment	Mine-by experiment EL250 EDZ Study
References	NAGRA (1985) NAGRA (1996)	OLSSON (1992), MONSEN et al. (1992), BORGESSON et al. (1992), HODG-KINSON & COOPER (1992)	OLSSON et al. (1996), GELLER & JARSJÖ (1997) EMSLEY et al. (1997)	CHANDLER et al. (1996)	TAKEDA & OSAWA (1993) SUGIHARA et al. (1996) MATSUI et al. (1998)

7 CONCLUSIONS OF THE TUNNEL NEAR-FIELD PROGRAMME

The Tunnel Near-Field Programme Grimsel Investigation Phase IV (1994 - 1996) was initiated as a practically oriented research programme for geoscientific characterisation of the tunnel near-field in a fractured hard rock environment. The programme consisted of four independent experiments focused on the investigation of the excavation disturbed zone around drilled and blasted tunnels (EDZ and ZPK experiments) and on two-phase flow processes in the tunnel near-field (ZPM and TPF experiments). At the end of the Tunnel Near-Field Programme the participating organisations felt the need for a joint interpretation and review of these investigations in the light of performance assessment, integrating the complementary research issues of the different tunnel near-field experiments.

The project "Conclusions of the Tunnel Near-Field (CTN)" was conducted as part of Grimsel Investigation Phase V (1997 - 2002). The emphasis of the CTN project was to develop a comprehensive and systematic methodology for geoscientific characterisation of the tunnel near-field in a fractured hard rock environment as input for scenario analyses of repository system performance. Based on the experience gained in the previous GTS Phase IV experiments, the CTN project addressed the following issues:

- What is the role of the tunnel near-field in performance assessment?
- Which are the key elements in the synthesis procedure, required for converting the field data into valuable deliverables for performance assessment?
- Which are the determining factors for the underground exploration strategy and which site characterisation tools are recommended for geoscientific characterisation of the tunnel near-field?
- How to establish quantitative models for gas migration and post closure repository resaturation?
- How to establish quantitative models for estimating axial flow along sealed tunnel sections and how to estimate groundwater flow enhancement along emplacement caverns?
- Is the experience gained at the GTS comparable with findings derived from other sites?

The role of the tunnel near-field in performance assessment

The tunnel near-field represents the transition from the repository installations to the geosphere. In performance assessment, particular importance is attached to the tunnel near-field, because any repository-induced perturbations, and in particular their evolution with time, will be affected by the rock properties and state conditions in the immediate vicinity of the excavations. In a hard rock formation such as granite, alteration of the rock properties may be largely linked to the effect of *stress redistribution* around the underground openings, creating irreversible rock failure close to the drift wall (*excavation induced fractures*) and, outside this damaged zone, mainly causing reversible changes in hydraulic properties of the *existing network of natural fractures*. Rock creep or chemical alterations of the rock in the tunnel near-field, such as observed in soft rock formations, may be less relevant. In the CTN project, emphasis was placed on the PA issues of migration of waste-generated gas, resaturation of the tunnel near-field after repository closure and the effect of the disturbed zone on groundwater flow.

Synthesis procedure

Geoscientific characterisation of the tunnel near-field in support of performance assessment requires a clear and traceable synthesis procedure to convert the geological databases into a format applicable as input for PA scenario analyses. In this report a synthesis approach is proposed, which consists of two elements: the *geodata set* and the *data flow analysis*. The geodata set consists of a number of tables, aimed at compiling the relevant geoscientific information for performance assessment. Each table is dedicated to a specific PA issue (e.g. "groundwater / gas flow in the tunnel near-field") and contains (i) a brief assessment of important processes and basic assumptions, (ii) the most likely conceptual models and (iii) effective parameters and bandwidths characterising the host rock properties. A generic example of a geodata set on "Groundwater and gas flow in the tunnel near-field" is given in chapter 2.

The data flow analysis represents a technique for structuring the overall synthesis procedure. It aims at determining the key processes of the interpretation and synthesis procedure and to identifying how the field data feed in. Data flow analysis allows the particular relevance of the different sets of field data to the overall procedure to be assessed and, may therefore be applied to refine the site investigation programme and adapt it to the scientific needs of performance assessment. The synthesis procedure can be divided into three different interpretation levels, namely the interpretation of field data, derivation of structural and process models and, finally, development of system models for process simulation.

Exploration concept and equipment developments

When planning the underground exploration of a candidate host rock formation, the exploration concept will be determined by a multitude of factors such as the specific geological conditions of the site, economic and time constraints, waste disposal concept and excavation techniques applied. Based on practical considerations with respect to exploration progress and the specific aims to be achieved, the *exploration procedure* can be divided into different phases (investigations during excavation phases, test phases, long-term monitoring phases). In addition, the investigations can be grouped into categories related to their demands on rock exposure (investigations at the tunnel surface, investigations in boreholes, laboratory tests with drillcore samples). The choice of the *appropriate site characterisation techniques* as part of a particular underground exploration programme must respect these aspects. In chapter 3.5 a comprehensive overview of suitable exploration methods is given which may assist in planning a tunnel near-field investigation programme.

Within the framework of the Tunnel Near-Field Programme, equipment and methodology developments were accomplished for characterisation of the tunnel near-field. Particular emphasis was given to hydraulic characterisation techniques; some of the novel techniques are highlighted in this section. The combined short interval packer and the modular mini packer system represent powerful tools for determination of hydraulic conductivity profiles in radial boreholes with a spatial resolution in the decimetre range. Both systems were successfully applied to delimit the damaged rock zone in the immediate vicinity of the tunnel surface. The slim hole piezometer system was designed for hydraulic head measurements in low permeability matrix zones of the tunnel near-field. The piezometer is characterised by a monitoring interval with very low volume, required for measuring rapid changes in hydraulic head due to changing ventilation conditions in the tunnel. Finally, a novel TDR system (Time-domain reflectometry) was developed for water content measurements in rocks with very low porosity. A special feature of this

method is its ability to measure spatial distributions of water content, such as water content profiles along radial boreholes through the tunnel near-field.

Gas migration and post-closure repository saturation

After closure of a radioactive waste repository, two-phase flow conditions may be expected in the host rock formation originating either from gas generation processes in the backfilled emplacement facilities or from desaturation of the tunnel near-field during the operational phase. Both perturbations are relevant for assessment of repository performance, requiring an appropriate conceptualisation and quantitative description of two-phase flow processes and parameters in the host rock formation.

For modelling two-phase flow processes in fractured hard rock, equivalent porous medium approaches have proved to be an appropriate conceptualisation. It is assumed that gas and liquid flow are governed by viscous, capillary and gravity forces. The properties of the porous medium and of the phases are given as local averages over some representative elementary volume. These two-phase flow properties are expressed by *parametric models*, describing relative permeability and capillary pressure as a function of liquid saturation. The well-known Brooks-Corey and van Genuchten parametric models were successfully applied to characterise on the local scale (scale of the field tests: approx. 1 - 10 m), the two-phase flow properties of the shear zones in the southern part of the GTS. Chapter 4.2 gives a survey of site-specific two-phase flow parametric models and parameter values, representative for matrix and shear zones at the GTS.

Modelling of gas migration through the host rock of a real repository site requires model domains on the site scale (hectometre scale) rather than on the local scale. Assuming a fractured hard rock formation, the complexity of the network of fracture systems represents a limiting factor for quantitative assessment of gas migration processes: to date, the numerical tools do not exist for modelling two-phase flow processes in complex fracture networks. For this reason, *upscaling procedures* are needed to convert the local properties to effective ones which are representative for the site scale. As part of the CTN project, an upscaling approach for two-phase flow properties was developed which ensures consistency with hydraulic fracture network models used for groundwater flow modelling.

Resaturation of the emplacement caverns after repository closure determines the time, when radionuclide migration from the repository to the biosphere is initiated. Evolution of an *unsaturated zone* during the operational phase may impact post closure repository performance in low permeability host rock formations such as salt, clay or crystalline rock with low fracture intensity. Investigations in the Tunnel Near-Field Programme were aimed at obtaining experimental evidence for the evolution of an unsaturated zone around underground excavations and at developing process models of two-phase flow in the tunnel near-field. The field experiments showed the existence of an unsaturated zone in ventilated low permeability tunnel sections. The extent of the unsaturated zone is mainly determined by the humidity and temperature evolution in the tunnel. Desaturation of the tunnel near-field is a reversible process and hysteresis effects were not observed.

Scoping calculations with a numerical two-phase flow simulator indicated that the unsaturated zone around low permeability tunnel sections is restricted to the immediate vicinity of the tunnel surface. Significant desaturation may be expected in a zone of 0.5

- 1.0 m thickness around the tunnel. Assuming constant ventilation conditions, this zone does not grow with time but stays stable in size and magnitude of desaturation.

Axial flow and groundwater flow enhancement

Elevated permeability in the EDZ will facilitate groundwater flow in the annular zones along the tunnel / cavern axis typically having radial extents in the metre scale. Considering the entire repository, the concentration of flow in the near-field will focus groundwater streamlines in the deca- to hectometric range towards or into the EDZ and the total water flow through the repository will be raised. The extents of the EDZ was determined at the GTS for TBM-drilled tunnel sections as well as for sections excavated by drill and blast methods. For both excavation techniques, the thickness of the zone with irreversible rock failure was in the order of a few decimetres (typically 0.3 - 0.5 m). The results of the field tests indicate that the hydraulic properties of the fracture systems in the tunnel near-field are highly variable with fracture transmissibilities (permeability x interval length) ranging from 10^{-19} to 10^{-14} m²·m. The nature of the interconnection between the different features (natural fractures, induced fractures) is difficult to determine, but is decisive for flow enhancement in the axial direction. Within the uncertainty ranges of the field measurements, it was not possible to distinguish between the EDZ around a drill & blast tunnel section and a TBM section, respectively.

Based on detailed hydraulic characterisation of the EDZ, the following conceptual model is suggested for the Grimsel Test Site: The zone of enhanced matrix permeability may be restricted to an annulus of 1 - 2 m thickness with an enhancement factor of 10 (intrinsic permeability of the undisturbed rock matrix approximately $3E-19$ m²). Induced fractures have been created within the first 0.3 m of the tunnel wall. The damage zone containing these induced fractures and also natural fractures which may have reopened due to stress distribution, is confined to the first 0.5 - 2 m. Outside this zone, there is no evidence of permeable fractures.

Analytical and numerical models were established and generic simulations of axial flow through the EDZ were conducted. Sensitivity analyses were based on the above mentioned conceptual model of the EDZ. Changes in fracture transmissivity due to pore pressure changes and stress redistribution were taken into account. The results of the numerical calculations suggest that the effective axial permeability of the rock around the tunnel at the GTS will be controlled by the connectivity of the high permeability features within the damage zone. If the features are extensive and well connected (compared to the length of the seal zone), permeability is 100 - 1000 times greater than permeability in the undisturbed rock matrix. In the case of low connectivity, the simulations suggest permeability enhancement of a factor of 3.

Comparison of GTS investigations with experience from other sites

The CTN project, representing a synthesis of previous field investigations at the GTS, is strongly related to the particular geological conditions of the site. For this reason, as a complementary task, a desk study was initiated to put the GTS investigations into the broader perspective of relevant research work on the tunnel near-field. The desk study consisted of a survey of numerical codes for modelling groundwater flow and two-phase flow processes in fractured media. In addition, an intercomparison was given between tunnel near-field investigations in different underground laboratories situated in crystalline rock formations.

Both code comparison and comparison of experimental results from different underground laboratories are aspects to be considered in the synthesis of geoscientific data as valuable input for performance assessment. In the synthesis procedure these surveys may relate to the assessment of the spectrum of conceptual models and parameter ranges, required as a prerequisite for establishing the process models of gas migration, resaturation and axial flow. In addition, they feed into the needs of PA in a more general way, by building confidence in understanding of geological processes and material properties.

8 REFERENCES

- ALHEID H.-J., M. KNECHT, J.-Y. BOISSON, F. HOMAND-ETIENNE, PEPA, S. (1999): Comparison of in-situ hydraulic and seismic measurements in the excavation damaged zone of underground drifts, Proceedings of the ICRM, Paris.
- ARISTORENAS, G.H., EINSTEIN, H.H. (1993): Numerical Investigation of Underpressures occurring at Wellenberg. NAGRA Internal Report; Nagra, Wettingen, Switzerland.
- BAERTSCHI, P., ALEXANDER, W.R., DOLLINGER, H. (1991): Grimsel Test Site - Uranium Migration in Crystalline Rock: Capillary Solution Transport in the Granite of the Grimsel Test Site, Switzerland. - Nagra Technical Report NTB 90-15; Nagra, Baden, Switzerland.
- BARTON, N., BAKHTAR, K. (1987): Description and modeling of rock joints for the hydrothermal mechanical design of nuclear waste vaults. AECL Technical Report TR 418, AECL Whiteshell Nuclear Research Establishment, Canada.
- BENGTSSON, A., GRUNDFELT, B., MARKSTROM, A., RASMUSON, A. (1991): Impact from the disturbed zone on nuclide migration – a radioactive waste repository study. SKB Technical Report 91-11; SKB, Stockholm, Sweden.
- BÖRGESSON, L., PUSCH, R., FREDRIKSSON, A., HÖKMARK, H., KARNLAND, O., SANDEN, T. (1992): Final report of the Rock Sealing Project – Identification of zones disturbed by blasting and stress release. SKB Stripa Technical Report 92-08; SKB, Stockholm, Sweden.
- BOSSART, P., MAZUREK, M. (1991): Grimsel Test Site - Structural Geology and Water Flow-Paths in the Migration Shear-Zone. - Nagra Technical Report NTB 91-12; Nagra, Wettingen, Switzerland.
- BRÄUER, V., KILGER, B., PAHL, A. (1989): Grimsel Test Site – Engineering geological investigations for the interpretation of rock stress measurements and fracture flow tests. – Nagra Technical Report NTB 88-37E; Nagra, Baden, Switzerland.
- BROOKS, R.H. & COREY, A.T. (1964): Hydraulic properties of porous media, *Hydrol. Pap.*, 3, 1-27, Colo. State Univ., Fort Collins, USA.
- BRUEL, D. (1990): Exploitation de la chaleur des roches chaudes et sèches: Etudes des phénomènes hydrauliques, mécaniques et thermiques au moyen d'un modèle à fractures discrètes. PhD Thesis l'école Nationale Supérieure des Mines de Paris.
- BURDINE, N.T. (1953): Relative permeability calculations from pore-size distribution data, *Trans. Am. Inst. Min. Metall. Pet. Eng.*, 198, 71-78.
- CHANDLER, N.A. (1998): Personal Communication.
- CHANDLER, N.A., KOZAK, E.T., MARTIN, C.D. (1996): Connected pathways in the EDZ and potential for flow along tunnels. Proceedings of EDZ Workshop, September 1996 Winnipeg - International Conference on Deep Disposal of Radioactive Waste.

- CHILÈS, J.P., DE MARSILY, G. (1993): Stochastic models of fracture systems and their use in flow and transport modeling. In "Flow and Contaminant Transport in Fractured Rock - Bear, Tsang & de Marsily (eds)". Academic Press, San Diego.
- CHRYSSANTHAKIS, P., BARTON, N. (1992): Predicting performance of the 62m span ice hockey cavern at Gjøvik. In Fractured and Jointed Rock Masses, Myer, Cook, Goodman and Tsang (eds) Balkema 1995.
- COTTOUR, P., FRIEG, B., ADAMS, J., HOMMAND, F., PEPA, S. (1999): Hydrotesting in the Excavation Disturbed Zone (ED-A). In "Mont Terri Rock Laboratory: Results of the hydrogeological, geochemical and geotechnical experiments performed in 1996 and 1997 - Thury and Bossart (eds)". Geological Report No. 23; Swiss National Hydrogeological and Geological Survey, Bern, Switzerland.
- DAMJANAC, B. (1996): A three-dimensional numerical model of water flow in a fractured rock mass. PhD Thesis University of Minnesota.
- DAVIES, P.B. (1991): Evaluation of the role of threshold pressure in controlling flow of waste generated gas into bedded salt at the Waste Isolation Plant (WIPP). - Sandia report SAND 90-3246.
- DERSHOWITZ, W.S., WALLMAN, P., KINDRED, S. (1991): Discrete Fracture Modelling for the Stripa Site Characterisation and Validation Drift Inflow Predictions. Stripa Project TR 91-16; SKB, Stockholm, Sweden.
- DERSHOWITZ, W., LEE, G., GEIER, J., FOXFORD, T., LAPOINTE, P., THOMAS, A., (1998): FracMan: Interactive Discrete Feature Data Analysis, Geometric Modelling, and Exploration Simulation. User Documentation. Golder Associates Inc., Seattle, WA.
- EMSLEY, S., OLSSON, O., STENBERG, L., ALHEID, J.-H., FALLS, S. (1997): ZEDEX – A study of damage and disturbance from tunnel excavation by blasting and boring. SKB Technical Report 97-30; SKB, Stockholm, Sweden.
- FEIN, E., SCHNEIDER, A. (1999): d³f - Ein Programmpaket zur Modellierung von Dichteströmungen. GRS Report GRS-139; GRS, Braunschweig, Germany.
- FINSTERLE, S. & VOMVORIS, S. (1991): Inflow to Stripa validation drift under two-phase conditions: scoping calculations.- Nagra Internal Report; Nagra, Wetztingen, Switzerland.
- FINSTERLE, S., PRUESS, K. (1993): Design Calculations for a combined ventilation and brine injection experiment at the Grimsel rock laboratory. Nagra Internal Report; Nagra, Wetztingen, Switzerland.
- FINSTERLE, S. (1993): ITOUGH2 User's Guide. Version 2.2, Lawrence Berkeley Laboratory Report LBL-34581, LBL, Berkeley, California.
- FREEZE, G., RUSKAUFF, G., CHRISTIAN-FREAE, T., WEBB, S. (1998): Modeling the Effect of Excavation-Disturbed-Zone Porosity Increase on Groundwater Inflow to an Underground Repository. Proceedings of TOUGH Workshop'98, Karsten Pruess (ed), Lawrence Berkeley National Laboratory, Berkeley, California.

- FRIEG, B., VOMVORIS, S. (1994): Investigation of hydraulic parameters in the saturated and unsaturated zone of the Ventilation Drift. Nagra Technical Report NTB 93-10; Nagra, Wettingen, Switzerland.
- FRIEG, B., MARSCHALL, P., BLÜMLING, P., ALBERT, W., KULL, H., LIEDTKE, L. (1996): The near-field programme and the tomography and boreholes sealing projects. In "Nagra Bulletin No. 27"; Nagra, Wettingen, Switzerland.
- FRIEG, B., BLASER, P. (1999): GTS - The Excavation Disturbed Zone Experiment (EDZ). Nagra Technical Report NTB 98-01; Nagra, Wettingen, Switzerland.
- FRIEG, B., MEIER, E., WYDLER, H. (1999): Experiments in the Unsaturated Zone (UZ). In "Mont Terri Rock Laboratory: Results of the hydrogeological, geochemical and geotechnical experiments performed in 1996 and 1997 - Thury and Bosart (eds)". Geological Report No. 23; Swiss National Hydrogeological and Geological Survey, Bern, Switzerland.
- FROST, L.H., EVERITT, R.A. (1997): Excavation Damage Zone Tracer Experiment in the Floor of the Room 415 Test Tunnel. AECL Report AECL-11640, COG-96-321-1.
- GELLER, J., JARSJÖ, J. (1995): Groundwater degassing: Pilot hole test report. SKB International Cooperation Report 95-03; SKB, Stockholm, Sweden.
- GEMPERLE (1999): GTS / GAM - Hydraulic Testing in GAM98.002 and GAM98.004. Nagra Internal Report; Nagra, Wettingen, Switzerland.
- GIMMI, Th., WYDLER, H., BAER, T., ABPLANALP, H., FLUEHLER, H. (1992): Near field desaturation experiment at the Grimsel test site (FLG). Nagra Internal Report; Nagra, Wettingen, Switzerland.
- GRAEFE, V. (1997): Zweiphasenströmungen von Wasser und Luft in der Umgebung eines Stollens in porösem Hartgestein. GRS - 143; GRS, Braunschweig, Germany.
- GRANT, M.A. (1977): Permeability reduction factors at Wairaki, Paper 77-HT-52, ASME/AICHE Heat Transfer Conference, Utah, USA.
- HARTLEY, L.J. (1998): NAPSAC Technical Summary Document. AEA Technology Report AEA-D&R-0271; AEAT Harwell, UK.
- HARTLEY, L., JACKSON, C.P., WATSON, S.P. (1996): NAMMU (Release 6.3) User Guide. AEA-ES-0138, Release 6.3, Issue 1 1996; AEAT Harwell, UK.
- HAYES, D.J. (1965): The In-situ determination of the complete state of stress in rock: The principles of a proposed technique. National Mechanical Engineering Research Institute, Report MEG 404; Pretoria South Africa.
- HELMIG, R., BRAUN, C., EMMERT, M. (1994): MUFTE - A Numerical Model for Simulation of Multiphase Flow Processes in Porous and Fractured Porous Media. Programmdokumentation (HG 208) Technical Report 94/3, Institut für Wasserbau, Universität Stuttgart, Germany.

- HERBERT, A.W., GALE, J.E., LANYON, G.W., MACLEOD, R. (1991): Modelling for the Stripa Site Characterisation and Validation Drift Inflow: Prediction of Flow Through Fractured Rock. Stripa Technical Report TR 91-35; SKB, Stockholm, Sweden.
- HODGKINSON, D., COOPER, N. (1992): A comparison of measurements and calculations for the Stripa Validation Drift Inflow Experiment. SKB Stripa Technical Report 92-06; SKB, Stockholm, Sweden.
- HONARPOUR, M.M., KOEDERITZ, L., HARVEY, A.H. (1986): Relative Permeability of Petroleum Reservoirs. - Boca Raton, Florida, CRC Press.
- JARSJÖ, J., DESTOUNI, G. (1998): Groundwater degassing in fractured rock - modelling and data comparison. Technical Report TR98-17; SKB, Stockholm, Sweden.
- JING, L., STEPHANSSON, O., TSANG C.-F., KNIGHT, J.L., KAUTSKY, F. (1998): DECOVALEX II - Project Technical Report - Task 1A and 1B. SKI Report 98-39, ISSN 1104-1374. Swedish Nuclear Power Inspectorate, Stockholm, Sweden.
- KELSALL, P.C., CASE, J.B., CHABANNES, C. (1984): Evaluation of excavation induced changes in rock permeability. Int J Rock Mech Min Sci Geomech Abstr. Vol 21, pp121-135; Pergamon London, UK.
- KEUSEN, H.R., GANGUIN, J., SCHULER, P., BULETTI, M. (1989): Grimsel Test Site – Geology. – Nagra Technical Report NTB 87-14E; Nagra, Wettingen, Switzerland.
- KONIETZKY, H. (1995): FLG - Versuch Excavation Disturbed Zone 3D Stress Field and 2D Disturbed Zone Modelling for the Grimsel Test Site. - NAGRA Internal Report; Nagra, Wettingen, Switzerland
- KUHLMANN, U. (1995) FLG: Excavation Disturbed Zone Designrechnungen für diskrete Hydrotests. Nagra Internal Report; Nagra, Wettingen, Switzerland.
- KULL, W., BREWITZ, W., KLARR, K. (1993): Ventilationstest - In-situ-Verfahren zur Permeabilitätsbestimmung im Kristallin. Nagra Technical Report NTB 91-02; Nagra, Wettingen, Switzerland.
- KULL, H., MIEHE, R. (1995): Grimsel Test Site - The influence of Tunnel Ventilation on the Hydraulic Flow Conditions in the Crystalline Rock Zone in the Tunnel Near-Field. - Nagra Technical Report NTB 94-04E; Nagra, Wettingen, Switzerland.
- KULL, H., FLACH, D. & GRAEFE, V. (1999): Untersuchung physikalischer Prozesse und Parameter zum Fluid- und Gastransport im Nahbereich von Endlagern in granitischen Formationen des Felslabors Grimsel Phase 4. Zweiphasenflußbedingungen in einer homogenen granitischen Gesteinsmatrix. GRS Abschlußbericht, Köln, Germany.
- LANDAU, L., LIFSCHITZ, E. (1984). Electrodynamics of Continuous Media. 2nd Edition Pergamon Press.
- LANYON, G. W. (1998): Personal Communication.

- LIEDTKE, L., GÖTSCHENBERG, A., JOBMANN, M., SIEMERING, W. (1994): Grimsel Test Site – Fracture System Flow Test: Experimental and numerical investigations of mass transport in fractured rock. - Nagra Technical Report NTB 94-02E; Nagra, Wettingen, Switzerland.
- LIEDTKE, L., SHAO, H., KULL, H. (1998): Investigation of two-phase flow in fractured rock. Proceedings of Waste Management 98, Tuscon, Arizona; American Nuclear Society, La Grange Park.
- LIEDTKE, L., SHAO, H., SONNKE, J., KNECHT, JOHN, H., ZIMMERMAN, H. (1999): Material transport in fractured rock - Rock characterisation in the near-tunnel zone. - Nagra Technical Report NTB 97-01; Nagra, Wettingen, Switzerland.
- LONG, J.C.S., OLSSON, O., BLACK, J. (1992): Effects of excavation on water inflow to a drift. In Fractured and Jointed Rock Masses Myer LR, Cook NGW, Goodman RE, Tsang C-F (eds). Balkema.
- MAHERS, E.G. (1983): Mass Transfer and Interfacial Phenomena in Oil Recovery. Ph.D.Thesis, London University.
- MAJER, E.L., MYER, L.R., PETERSON, J.E., KARASAKI, K., LONG, J.C.S., MARTEL, S.J., BLÜMLING, P., VOMVORIS, S. (1990): Joint seismic, hydrogeological and geomechanical investigations of a fracture zone in the Grimsel rock laboratory, Switzerland. Nagra Technical Report NTB 90-49; Nagra, Baden, Switzerland.
- MANAI, T. (1995): EVEGAS: European validation exercise of gas migration models through geological media: Phase 1 - Final Report. European Commission Report E.U.R 16639 EN. European Commission. Nuclear Science and Technology. Directorate General, Science Research and Development.
- MANAI, T. (1997a): EVEGAS: European validation exercise of gas migration models through geological media: Phase 2 - Final Report. European Commission Report E.U.R 17556 EN. European Commission. Nuclear Science and Technology. Directorate General, Science Research and Development.
- MANAI, T. (1997b): EVEGAS: European validation exercise of gas migration models through geological media: Phase 3 - Final Report. European Commission Report E.U.R 17557 EN. European Commission. Nuclear Science and Technology. Directorate General, Science Research and Development.
- MARSCHALL, P., CROISÉ, J. (1999): Grimsel Test Site - Determination of two-phase flow properties in shear zones. - Nagra Technical Report NTB 97-06; Nagra, Wettingen, Switzerland.
- MARTEL, J.S., PETERSON, J.E. (1991): Interdisciplinary characterization of fracture systems at the US / BK Site, Grimsel Laboratory, Switzerland. Int. Rock Mech. Min. Sci. & Geomech. Abstr. 28/4.
- MARTIN, C.D., DZIK, E.J., READ, R.S. (1996): Designing an Effective EDZ Cutoff in High Stress Environments. Proceedings of EDZ Workshop September 1996 Winnipeg - International Conference on Deep Geological Disposal of Radioactive Waste.

- SKB (1995): SR 95 - Template for safety reports with descriptive example. SKB Technical Report TR 96-05; SKB, Stockholm, Sweden.
- SUGIHARA, K., MATSUI, H., ISHIJIMA, F., SATO, T. (1996): Study on Excavation disturbance in the Kamaishi Mine. Proceedings of EDZ Workshop September 1996; Winnipeg - International Conference on Deep Geological Disposal of Radioactive Waste.
- TAKEDA, S., OSAWA, H. (1993): Current status and future programme of in-situ experiments of Kamaishi, Japan. International Symposium on In-situ Experiments at Kamaishi, Japan.
- VAN GENUCHTEN, M.T. (1980): A closed-form equation for predicting the hydraulic conductivity of unsaturated soils, *Soil Sci. Soc. Am. J.*, 44, 892-898.
- VOMVORIS, S., FRIEG, B. (1992): GTS – Overview of Nagra field and modeling activities in the Ventilation Drift. Nagra Technical Report, NTB 91-34; Nagra, Wetztingen, Switzerland.
- VOMVORIS, S., ANDREWS, R.W., BLÜMLING, P., MÜLLER, W.H., SCHINDLER, M., TAKEUCHI, K., UMEKI, H., VOBORNY, O., WILSON, W.E. (1993): Northern Switzerland Crystalline Rocks: Preliminary assessment of changes in groundwater flow and their implications on the geo-dataset due to the excavation disturbed zone around a repository tunnel. Nagra Internal Report; Nagra, Wetztingen, Switzerland.
- VOMVORIS, S., BLÜMLING, P., LANYON, G.W., WATSON, C.R. (1997): Excavation Disturbed Zone Assessment of its Hydraulic Properties Based on Surface Investigations. Proceedings of the MRS Meeting Switzerland 1997.